FLOODING OF DELAWARE ROUTE 54 BETWEEN LITTLE ASSAWOMAN AND ASSAWOMAN BAYS DUE TO STORM SURGE AND TIDES

by
Bradley D. Johnson,
Nobuhisa Kobayashi
and
Keith D. Watson

SPONSORED BY
DELAWARE TRANSPORT INSTITUTE

RESEARCH REPORT NO. CACR-94-16
SEPTEMBER, 1994

CENTER FOR APPLIED COASTAL RESEARCH
DEPARTMENT OF CIVIL ENGINEERING
UNIVERSITY OF DELAWARE
NEWARK, DELAWARE
19716

FLOODING OF DELAWARE ROUTE 54 BETWEEN LITTLE ASSAWOMAN AND ASSAWOMAN BAYS DUE TO STORM SURGE AND TIDES

by

BRADLEY D. JOHNSON
NOBUHISA KOBAYSHI
and
KEITH D. WATSON

Department of Civil Engineering
University of Delaware
Newark, Delaware 19716

DELAWARE TRANSPORTATION INSTITUTE
Office of the Vice Provost for Research
University of Delaware
Newark, Delaware 19716

November 1994

The Delaware Transportation Institute is a university-wide multi-disciplinary research unit reporting to the Office of the Vice-Provost for Research, and is co-sponsored by the University of Delaware and the Delaware Department of Transportation.

Delaware Transportation Institute
University of Delaware
Newark, DE 19716
(302)831-1446

ABSTRACT

Flooding of Delaware State Route 54(Roadway) between Little Assawoman and Assawoman Bays due to storm surge and tides propagating through Ocean City Inlet is investigated using an available numerical model for a network of one-dimensional channels. First, the numerical model is evaluated using an analytical solution derived in this study for its capabilities of predicting the propagation, damping, and reflection of incident long(tidal) waves. Second, the numerical model is compared with the small-scale experiment conducted in this study and shown to be capable of predicting the overall free surface variation of converging and diverging flow over an obstacle such as the Roadway. Third, the evaluated numerical model is applied to predict the stillwater elevations at the existing and raised Roadways for storms of 40 and 60 hr durations whose recurrence intervals are 10, 20, 50, 100, and 500 yr. The computed results for these storms indicate that the raised Roadway with a minimum elevation of 5 ft or less above the mean sea level will not increase the essentially horizontal stillwater elevations in the vicinity of the Roadway. The computed peak values and temporal variations of the stillwater elevations at the Roadway for these storms are also presented so that an approximate elevation (for engineering purposes) of the raised Roadway may be determined, improving vehicle passage on the Roadway during storms.

ACKNOWLEDGMENT

This study has been supported by the Delaware Department of Transport through the Delaware Transport Institute. The U.S. Army Corps of Engineers, Philadelphia District and the firm Rummel • Klepper & Kahl provided necessary information for this study.

TABLE OF CONTENTS

1 INTRODUCTION

1.1 Background

Delaware State Route 54, which is simply called the Roadway hereafter, runs between Little Assawoman Bay in Delaware and Assawoman Bay, which are called the North and South Bays, respectively, for brevity. The South Bay is connected to the Atlantic Ocean through the inlet at Ocean City, Maryland as shown in Fig. 1. A relatively narrow connection, called the Ditch, exists between the North and South Bays. The entire area along the Roadway between the North and South Bays is low with an elevation of 2-3 ft. above the mean sea level(the National Geodetic Vertical Datum of 1929). Although the Roadway is supposed to be an evacuation route for the residents along the Roadway and the Atlantic shoreline, even minor storms flood the road, rendering it impassable.

A preliminary hydraulic study was conducted by the second author of this report and is attached in Appendix D. A simple hydraulic analysis has indicated that the flow over the existing roadway is not negligible in comparison to the flow through the Ditch. As a result, roadway improvements alternatives based on discharge considerations such as bridges and culverts will require discharge capacities similar to that of the Ditch.

A more direct way to improve vehicle passage during storms is to raise the elevation of the Roadway with fill and a new pavement. The frequency and duration of no vehicle passage on the raised Roadway during storms needs to be predicted to determine an appropriate elevation of the raised Roadway. One of the major concerns of the residents along the Roadway is whether the raised Roadway would increase the

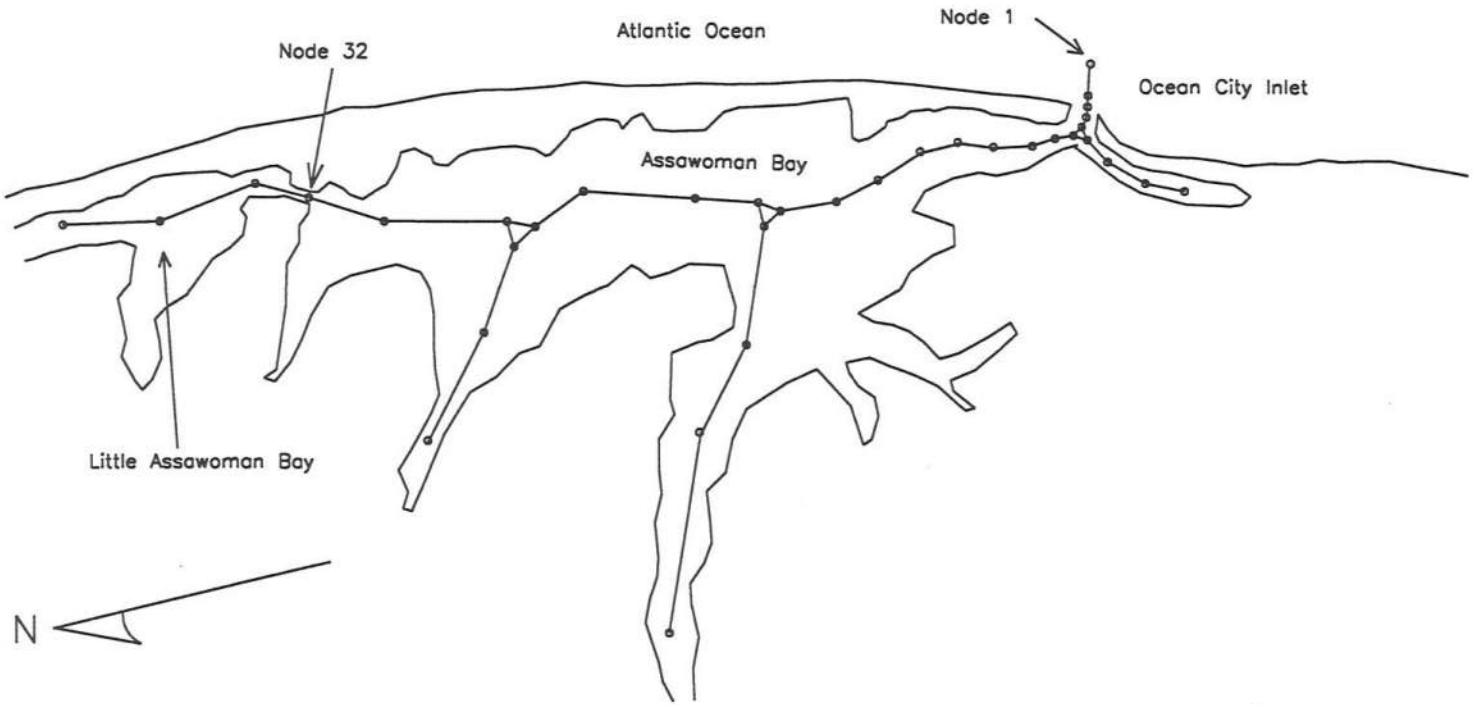

Fig. 1: Flooding of Delaware Route 54 at Node 32 between Little Assawoman Bay and Assawoman Bay due to Storm Surge and Tide through Ocean City Inlet, Maryland.

stillwater elevations during storms in a manner similar to the backwater effect behind a dam in a river. To address these hydraulic problems, the stillwater elevations on the existing and raised Roadways need to be predicted and compared for storms of different recurrence intervals and varied minimum elevations.

The preliminary study based on a simple hydraulic analysis in Appendix D has suggested that the raised Roadway will not increase the peak stillwater elevation but may increase the stillwater elevation slightly before and after the peak of storm surge. To better quantify the effects of the raised Roadway on the stillwater elevations during storms, a numerical model is employed to predict the temporal variations of the stillwater elevations at the existing and raised Roadways.

1.2 Outline of Report

The numerical model adopted in this study is described in Section 2. The governing equations employed in the numerical model are linearized to obtain an analytical solution for an elongated rectangular bay. The analytical solution indicates that tides inside the bay may be regarded as damped standing waves. The analytical and numerical solutions are then compared to examine the accuracy of the numerical solution as well as to gain confidence in the computer program used in this study. Furthermore, an experiment was conducted to calibrate the empirical contraction-expansion coefficient used in the numerical model for the converging and diverging flows over an obstacle such as the Roadway.

The input required for the computation of flooding over the Roadway between the South and North Bays is summarized in Section 3. This relatively small bay system may

be regarded as a network of one-dimensional channels with negligible effects of lateral flow and wind on the bay system. It is noted that the wind effect on the continental shelf is accounted for in the temporal variations of the stillwater elevations at Ocean City Inlet which are specified as input for different storms. In short, the small bay system is driven by the stillwater variations at Ocean City Inlet which are determined by storm surge and tides on the adjacent continental shelf. The temporal variations of the stillwater elevations in the bay system were then computed for different storms. The computed results for the existing Roadway and the raised Roadway with a minimum elevation 3.5, 4.0, 4.5, and 5.0 ft. above the mean sea level have turned out to be practically the same. In agreement with the simple analysis performed in the preliminary study in Appendix D, the raised Roadway will not increase the essentially horizontal stillwater elevation in the vicinity of the Roadway. In other words, the modifications of the Roadway geometry are too small to affect the storm surge and tides which have horizontal length scales much larger than the size of the Roadway.

The summary and conclusions of this study are presented in Section 4. In order to present only the essential results in Section 3, most of the figures related to Section 3 are attached in the following appendices. Appendix A summarizes the cross section geometry and Manning's roughness coefficient specified at each of the 35 nodes shown in Fig. 1. Appendix B lists the temporal variations of the stillwater elevation at Ocean City Inlet for 10 different storms with the recurrence intervals of 10, 20, 50, 100, and 500 yr. and the storm durations of 40 and 60 hr. Appendix C shows the temporal variations of the stillwater elevation at the existing Roadway for the 10 different storms and for spring tides

only. The computed stillwater elevations at the raised Roadway with the minimum elevations of 3.5, 4.0, 4.5, and 5.0 ft. are not shown because they are identical(within the computing accuracy) to those presented in Appendix C. Appendix D presents the report of the preliminary hydraulic study.

A summary of this report is presented at the International Symposium on Waves-Physical and Numerical Modeling by Johnson et al.(1994).

2 NUMERICAL MODEL

The relatively small bay system shown in Fig. 1 may be regarded as a network of one-dimensional channels; and a one-dimensional numerical model for a channel network is adopted in the study. Such numerical models were summarized by French(1985). Amein and Kraus(1991) developed the numerical model called DYNLET for the one-dimensional modeling of the dynamic(time dependent) behavior of tidal flows at inlets. This numerical model is an extended version of the previous model by Amein(1975) and is based on the nonlinear shallow-water equations which are solved using an implicit finite difference technique.

2.1 Governing Equations and Numerical Method.

The one-dimensional time-dependent continuity and momentum equations adopted in this study are as follows:

$$\frac{\partial A}{\partial t}+\frac{\partial Q}{\partial x}=0 \tag{1}$$

$$\frac{\partial Q}{\partial t}+\frac{\partial}{\partial x}\left(\frac{Q^2}{A}\right)=-gA\left[\frac{\partial \eta}{\partial x}+\frac{|Q|Q}{C^2}+\frac{K}{2g}\frac{\partial}{\partial x}\left(\frac{Q}{A}\right)^2\right] \tag{2}$$

$$C=\sum_{n=1}^{M}\frac{\alpha}{n_j}A_j R_j^{2/3} \tag{3}$$

where

t = time
x = distance along the channel
Q = volume flow rate(discharge)
A = cross sectional area
g = gravitational acceleration
η = stillwater elevation above the mean sea level
C = conveyance, related to bottom friction

K = contraction-expansion coefficient, related to head loss due to flow contraction and expansion

To allow for channels of complex geometry, a composite form of Manning's formula is used in (3). For a channel cross section with M subsections of different roughness and depths, the conveyance C is given by (3) with α =1 for SI units and α = 1.49 for English Units. Symbols n_j, A_j, and R_j are the Manning's roughness coefficient, area and hydraulic radius respectively of subsection j. Note: hereafter the Manning's roughness coefficient "n" is simply called the " roughness coefficient".

Eqs. (1) and (2) are the standard continuity and momentum equations for unsteady gradually-varied flow along a single channel except for the last term in (2) which is added to account for head loss due to flow contraction and expansion (e.g., French 1985). The unknown variables in (1) and (2) are the stillwater elevation, η, and the discharge, Q, whereas A, A_j, and R_j can be computed for given η at each cross section. The empirical coefficients in (2) are n_j and K where Amein and Kraus (1991) calibrated these coefficients for Indian River Inlet, Delaware, and Masonboro Inlet, North Carolina. For typical tidal flow in a small elongated bay, the hydrostatic pressure gradient caused by the term, $\partial\eta/\partial x$, in (2) drives the flow from the cross section of large η to the cross section of small η.

To apply (1) and (2) for a network of channels, the mass conservation equation based on Q and the continuity of the stillwater elevation, η, are applied at each junction of the channels (e.g., French 1985). The numerical model DYNLET by Amein and Kraus(1991) solves (1) and (2) with (3) for a network of channels using a weighted four-point implicit finite difference method with appropriate initial and boundary conditions. The finite difference nodes used in the computations for this study are indicated in Fig. 1.

The computations made in this report have been initiated as a cold start in which the stillwater elevation, η, above the mean sea level and the discharge, Q, have been set to be zero at the initial time t = 0. The boundary conditions of zero discharge have been assumed at the landward end nodes with negligible fresh water inflow. The temporal variations of the stillwater elevation at the seaward end node at Ocean City Inlet has been specified as input to drive the flow through the inlet into the bay system shown in Fig.1.

2.2 Comparison with the Analytical Solution.

An approximate analytical solution for an elongated rectangular bay is obtained to gain an insight into the dynamic behavior of tidal flow in an idealized bay. The analytical and numerical solutions are also compared to perform an independent check of DYNLET. Through the use of a simple channel geometry and idealized boundary conditions, an analytical solution can be developed for the linearized equations corresponding to (1) and (2). For a wide rectangular channel of constant width, B, and water depth, d, below the mean sea level, the cross sectional area, A, is given by $A = (d+\eta)B$. For a wide channel with constant roughness coefficient, n, $M = 1$ and $R \cong (d+\eta)$ in (3). There is no flow contraction-expansion in the channel and hence $K = 0$. It is convenient to introduce the average velocity, V, over the cross section given by $V = Q/A$. Under these conditions, (1) and (2) can be shown to reduce to:

$$\frac{\partial \eta}{\partial t} + \frac{\partial}{\partial x}\left[(d+\eta)V\right] = 0 \qquad (4)$$

$$\frac{\partial V}{\partial t}+V\frac{\partial V}{\partial x}=-g\frac{\partial \eta}{\partial x}-\frac{gn^2V|V|}{\alpha^2(d+\eta)^{4/3}} \tag{5}$$

In order to obtain an analytical solution, (4) and (5) are linearized assuming a small amplitude wave for which:

$$(d+\eta)\cong d \quad (d>>\eta)$$

and

$$\frac{\partial V}{\partial t}>>V\frac{\partial V}{\partial x}$$

The bottom friction term is linearized as:

$$\frac{gn^2|V|V}{\alpha^2 d^{\frac{4}{3}}}\cong fV \tag{6}$$

where the parameter, f, will be estimated after the analytical solution is obtained. After these simplifications, the linearized equations corresponding to (4) and (5) are expressed as:

$$\frac{\partial \eta}{\partial t}+d\frac{\partial V}{\partial x}=0 \tag{7}$$

$$\frac{\partial V}{\partial t}=-g\frac{\partial \eta}{\partial x}-fV \tag{8}$$

The linearized equations (7) and (8) can now be solved for a rectangular bay of length L as shown in Fig. 2. The incident long(tidal) wave at $x = 0$ is characterized by its amplitude, A_i, and its period , T ,where the angular frequency ω is given by $\omega = T/2\pi$. The no flux boundary condition of $V = 0$ at $x = L$ is imposed at the end of the bay. The initial time $t = 0$ is chosen such that η at $x = 0$ is zero at $t = 0$.

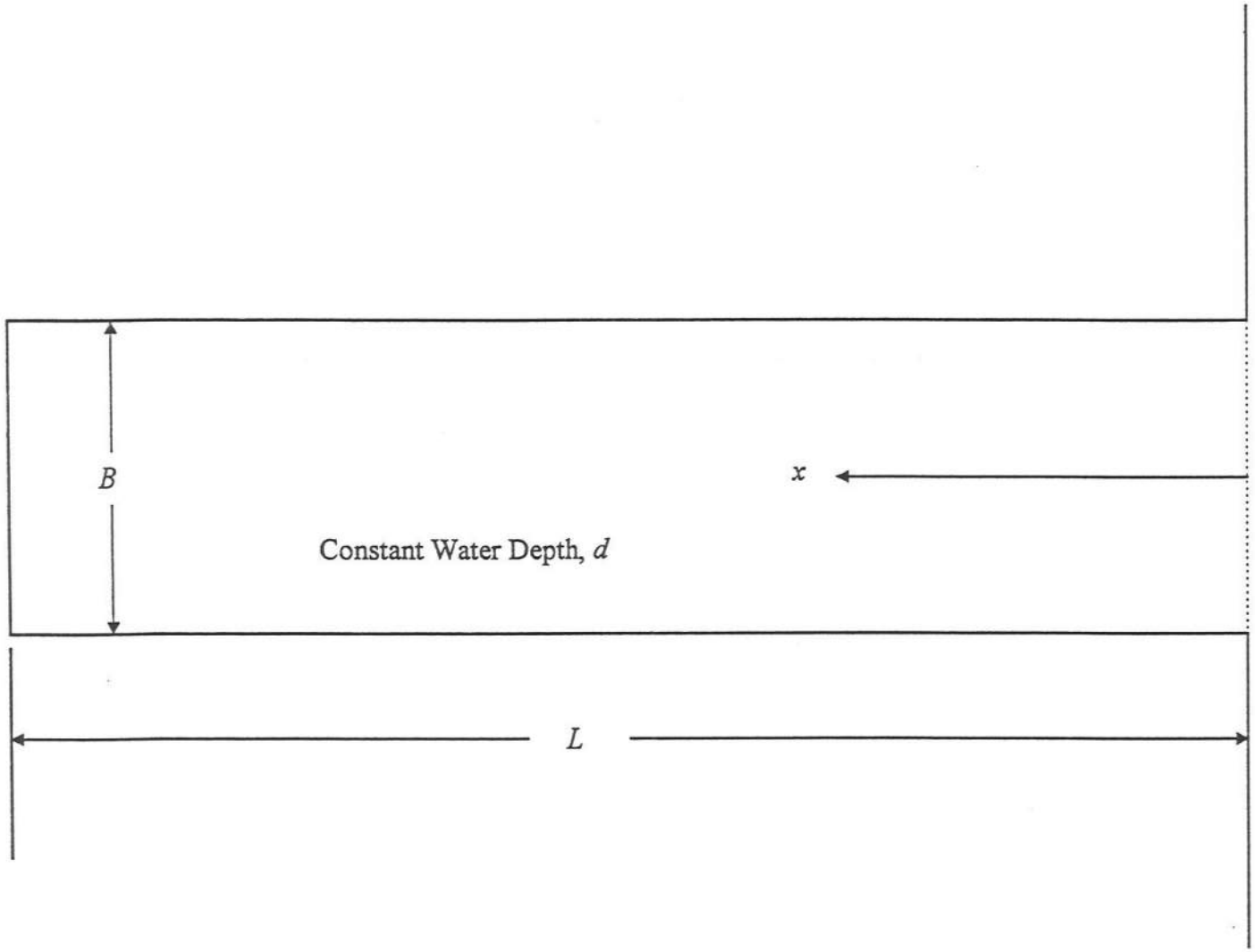

Fig. 2: Analytical Solution for Rectangular Bay.

It is convenient to introduce the following dimensionless variables and parameters indicated by the superscript star:

$$\eta^* = \frac{\eta}{A_i}; \qquad V^* = \frac{V}{A_i\sqrt{\frac{g}{d}}}; \qquad t^* = \omega\, t \tag{9a}$$

$$x^* = \frac{\omega\, x}{\sqrt{gd}}; \qquad L^* = \frac{\omega\, L}{\sqrt{gd}}; \qquad f^* = \frac{f}{2\omega} \tag{9b}$$

The analytical solution for this linearized and normalized problem can be shown to be written as:

$$\begin{aligned}\eta^*(t^*,x^*) = {} & \exp(-f^*x^*)\cos(t^* - t_0^* - x^*) + \\ & \exp\left[-f^*(2L^* - x^*)\right]\cos\left[t^* - t_0^* - (2L^* - x^*)\right]\end{aligned} \tag{10}$$

$$\begin{aligned}V^*(t^*,x^*) = {} & \exp(-f^*x^*)\cos(t^* - t_0^* - x^* + f^*) - \\ & \exp\left[-f^*(2L^* - x^*)\right]\cos\left[t^* - t_0^* - (2L^* - x^*) + f^*\right]\end{aligned} \tag{11}$$

in which the assumption of week damping, that is, $f^* << 1$ with f^* being defined in (9b) is made to simplify the expressions of η^* and V^*. The normalized time shift t_0^* is calculated such that η^* at $x^* = 0$ is zero at $t^* = 0$. This time shift facilitates the comparison between the analytical and numerical solutions where the initial conditions of the numerical solution corresponds to no wave action in the region $0 \le x^* \le L^*$ at $t^* = 0$.

The first and second terms on the right hand sides of (10) and (11) correspond to the damped incident waves propagating toward the end of the bay and the damped waves reflected from $x^* = L^*$ propagating toward the mouth of the bay. Eq. (11) satisfies the no flux boundary condition of $V^* = 0$ at $x^* = L^*$. This boundary condition results in the perfect reflection of the damped incident wave at $x^* = L^*$. The degree of damping due to

bottom friction is determined by the dimensionless parameter, $f^* = f/(2\omega)$. The dimensional parameter, f, introduced in (6) is estimated by a standard linearization method in which the time averaged value of the square of the error involved in the approximate equation (6) is minimized with respect to f (e.g., Mei 1989). The parameter, f, associated with damping due to bottom friction may hence be described as:

$$f = \frac{8}{3\pi}\frac{gn^2}{\alpha^2 d^{1/3}} A_i \sqrt{\frac{g}{d}} \tag{12}$$

The normalized free surface elevation, η^*, given by (10) is evaluated at the mouth (x^*=0) and the end (x^*=L) of the bay:

$$\eta^*(t^*, x^* = 0) = \cos(t^* - t_0^*) + \exp(-2f^*L^*)\cos(t^* - t_0^* - 2L^*) \tag{13}$$

$$\eta^*(t^*, x^* = L^*) = 2\exp(-f^*L^*)\cos(t^* - t_0^* - L^*) \tag{14}$$

For the numerical computation using DYNLET, (13) is used as the seaward boundary condition.

An example computation is made using:

Gravitational acceleration: $g = 32.2$ ft/s^2
Roughness coefficient: $n = 0.02$
English units: $\alpha = 1.49$
Water depth: $d = 10$ ft
Tidal period: $T = 12.4$ hr
Tidal amplitude: $A_i = 0.5$ ft
Bay length: $L = 70{,}000$ ft

The values of n, d, T, and L are typical for the bay system shown in Fig. 1. The tidal height of $A_i = 0.5$ ft is selected so that the normalized damping parameter, $f^* = f/(2\omega)$, is equal to $f^* = 0.73$ and the assumption of $f^* << 1$ used to obtain (10) and (11) may still be acceptable.

Fig. 3 shows the normalized free surface elevation, $\eta^* = \eta / A_i$, at the mouth of the bay given by (13) which has been specified as input to the numerical model DYNLET. The output from DYNLET must necessarily be the same as the specified input. For this example $2L^* = 1.1$ and $\exp(-2f^*L^*) = 0.45$ in (13). As a result, the effect of the reflected wave on the free surface elevation at the mouth is not negligible. The phase speed of the tide is given by $\sqrt{gd} = 17.9$ (ft/s) in this example. The travel time from the mouth to the end of the bay is equal to $L/\sqrt{gd} = 1.1$ hr. The travel time in the bay system shown in Fig. 1 is small in comparison to the tidal period.

Fig. 4 shows the normalized free surface elevation, $\eta^* = \eta / A_i$, at the end $(x=L)$ of the bay given by (14) in comparison to that from the numerical model DYNLET. Fifteen nodes have been used for the comparison with node 15 located at $x = L$. The analytical solution based on the linearized equations (7) and (8) slightly underestimates the crest and trough of the free surface oscillations computed by the numerical method which is based on the nonlinear equations (4) and (5). The analytical and numerical free surface oscillations are essentially in phase in Fig. 4, indicating that the numerical model predicts the phase speed well. The degree of agreement in Fig. 4 is encouraging and we may apply the numerical model with some confidence.

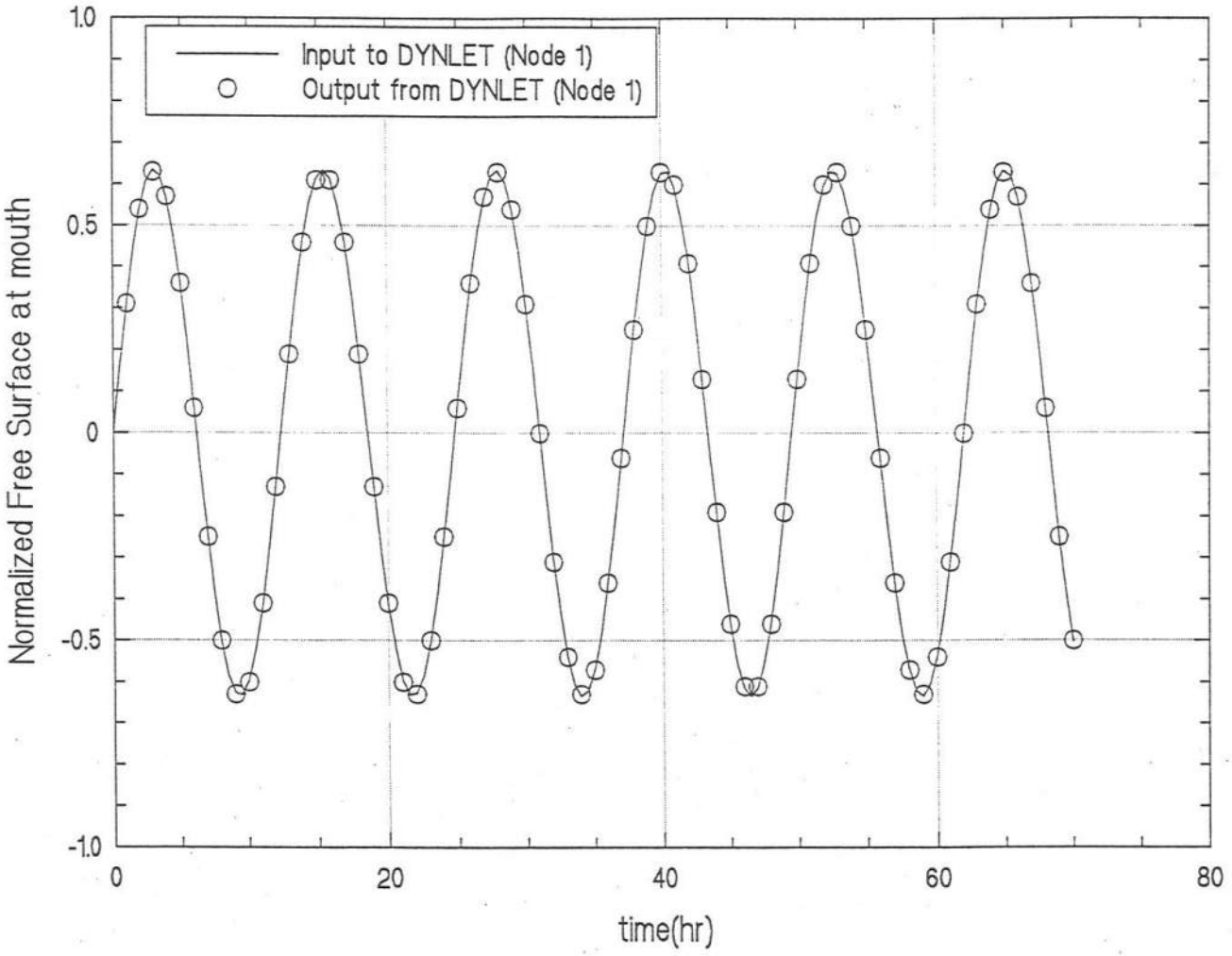

Fig. 3: Normalized Free Surface Elevation, η^*, at $x^* = 0$ as a Function of Time, t (hr), Specified as Input to DYNLET and Obtained as Output from DYNLET.

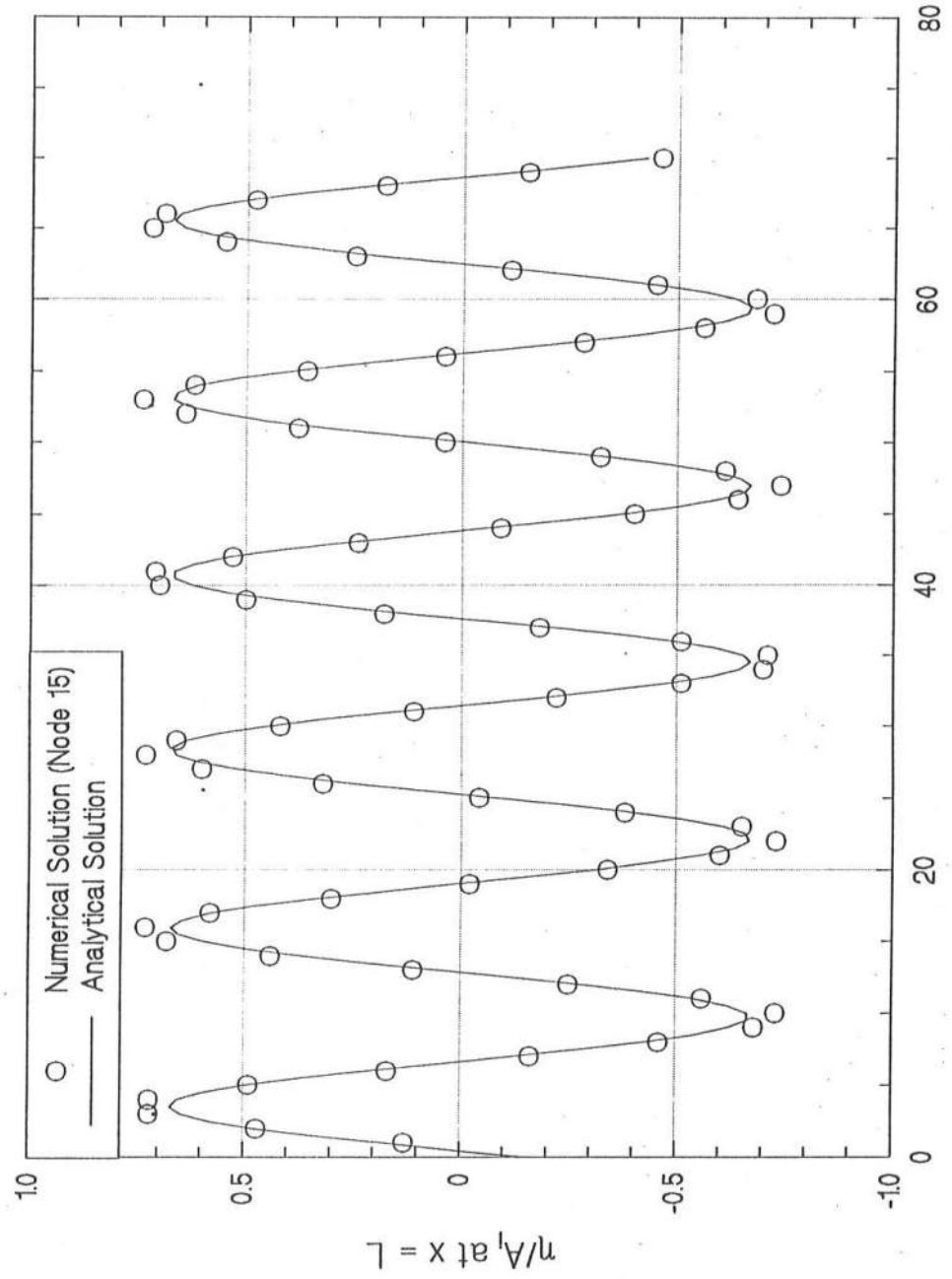

Fig. 4: Comparison of Approximate Anaytical and Numerical Free Surface Elevation, η^*, at $x^* = L^*$ as a Function of Time, t (hr).

2.2 Comparison with Experiment

In order to assess whether the numerical model based on (1) and (2) with a constant value of the empirical contraction-expansion coefficient, K, can predict the converging and diverging flows over an obstacle such as the Roadway, a steady flow experiment was conducted in a horizontal flume, which was 5 m long, 7.6 cm wide and 25 cm high. The bottom and sides of the flume are very smooth unlike natural channels. An available triangular obstacle was used in the experiment. The obstacle was 5 cm high and 37.5 cm long at its base. The side slopes were 1:1.8 and 1:5.7. Three tests were conducted: no obstacle in the flume; the steeper 1:1.8 slope of the obstacle facing upstream; and the steeper slope of the obstacle facing downstream. The bottom of the flume turned out to be somewhat irregular and could not be used as the datum; therefore a horizontal stillwater level of approximately 8 cm depth in the flume was used as the horizontal datum. At 28 horizontal locations within the fully developed flow region, a point gage was used to measure the steady free surface and bottom elevations relative to the datum. The errors of the elevation measurements were estimated to be 0.01 cm. The measured free surface and bottom elevations for the three tests are shown in Fig. 5 where the horizontal coordinate $x = 0$ is located at a distance of 2.2 m from the flume entrance. The relatively small free surface variations are enlarged in Fig. 5 to discern the water level increase upstream of the triangular obstacle and the water level dip in the vicinity of the obstacle crest. The discharge measured by a flow meter was $Q = 1.0$ *l/s* for the three tests.

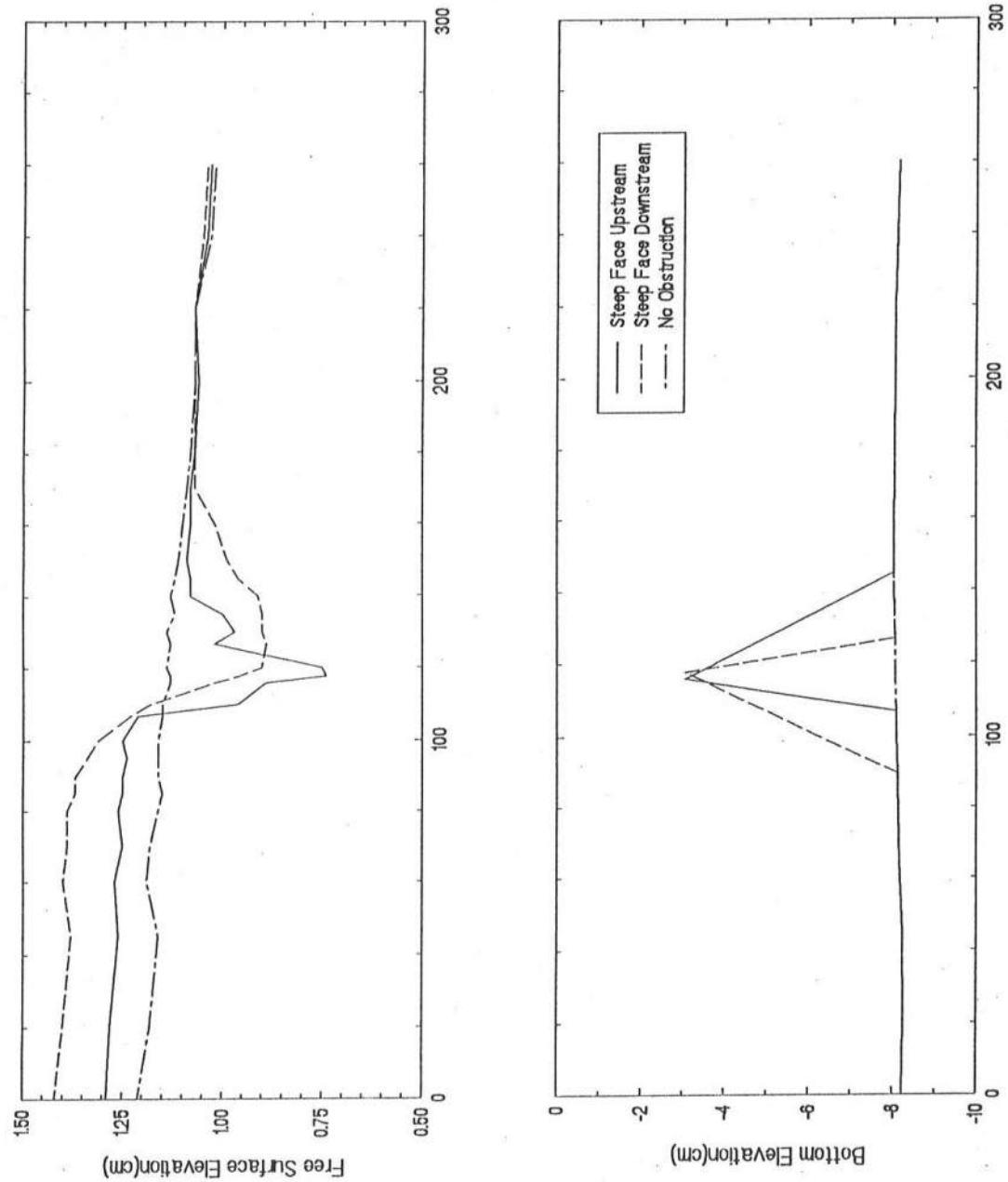

Fig. 5: Measured Free Surface and Bottom Elevations for Three Tests

For the numerical computation, the measured steady free surface elevations at x = 0 and x = 260 cm are specified as the upstream and downstream boundary conditions. The measured steady free surface elevations and discharge in the computation domain are specified as the initial conditions of the time-dependent numerical model so as to obtain the steady flow solution corresponding to the specified boundary conditions in an efficient manner. The computed and measured steady free surface elevations and discharge are compared to assess the degree of the agreement.

The test with no obstacle in the flume was used to estimate the value of the roughness coefficient, n, in this specific experiment so as to separate the frictional effect from the effect of the flow contraction and expansion. Fig. 6 shows the computed and measured free surface variations for this test with $K=0$. However, the computed flow is independent of K because the channel is prismatic in the absence of the obstacle.

The computed free surface variations for n = 0.01, 0.005 and 0.003 are very similar to that shown in Fig. 6 for n = 0.002 partly because the measured free surface elevations at x = 0 and x = 260 cm are specified as the boundary conditions. The computed discharge, however, does vary considerably with different values of the roughness coefficient, n. The following table summarizes the computed steady discharge as a function of the roughness coefficient.

Roughness Coefficient n	Flow Rate Q (l/s)
0.01	0.23
0.005	0.45
0.003	0.79
0.002	1.07

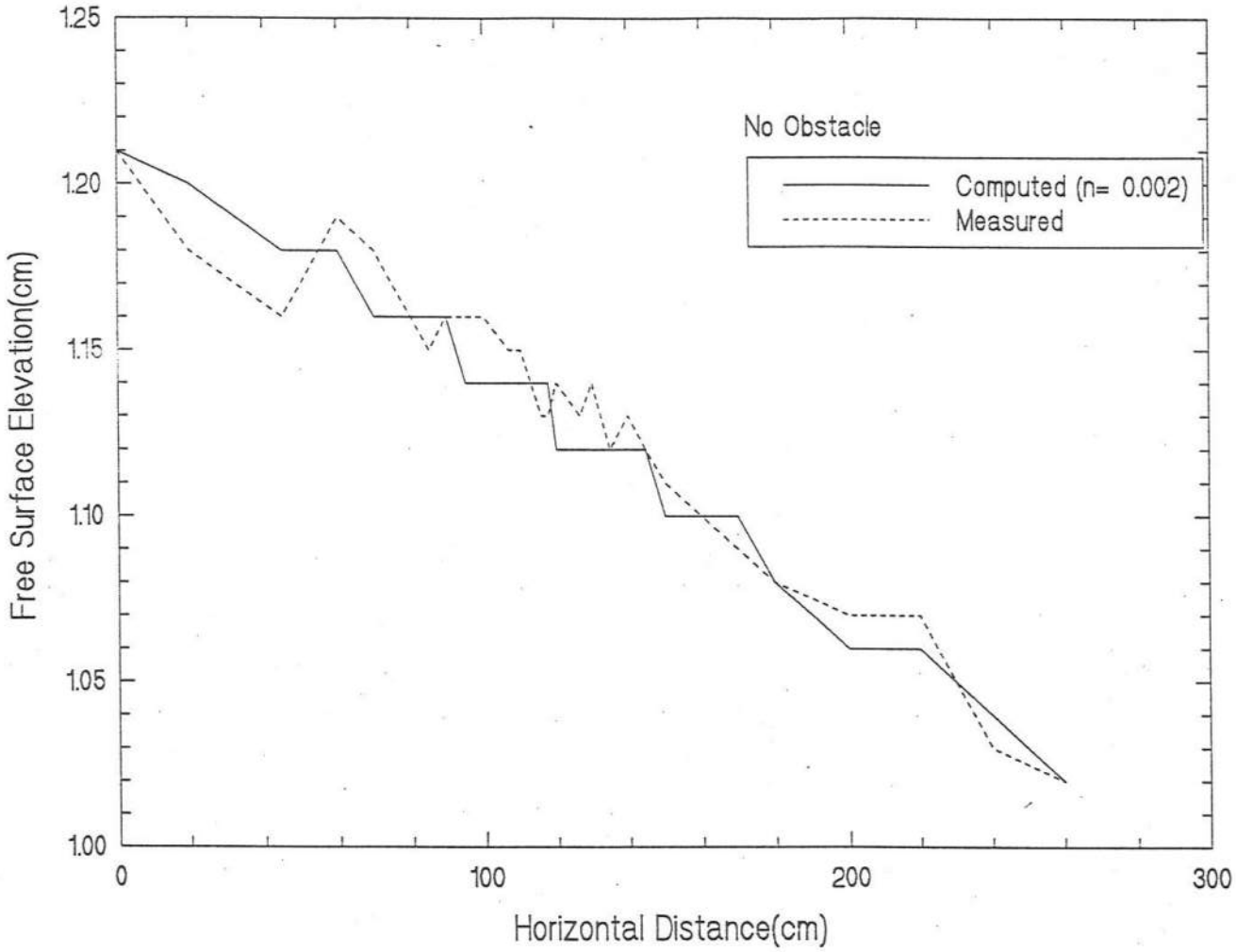

Fig. 6: Measured and Computed Free Surface Elevations of Test with no Obstacle

Recalling that the measured flow rate Q = 1.0 *l/s*, the roughness coefficient n = 0.002 was used in the remaining two tests to calibrate the contraction-expansion coefficient, K. Through the choice of n = 0.002, we have effectively separated the friction effect and are now in the position to calibrate the value of K.

The typical values of $K \cong 0.5$ for both contraction and expansion recommended by Amein and Kraus (1991) may be reasonable for large-scale horizontal contraction and expansion; however, it is not certain whether $K \cong 0.5$ is reasonable for vertical contraction and expansion of the flow such as the Roadway would produce. The computed and measured free surface variations for the tests with the steeper, 1:1.8, slope of the triangular obstacle facing downstream and upstream are shown in Figs. 7 and 8 respectively for K = 0.5. The computed free surface variations and discharge are not very sensitive to K in the vicinity of K = 0.5. The computed discharge for the test shown in Fig. 7 (steep face downstream) as a function of K is as follows:

Contraction-Expansion Coefficient K	Flow Rate Q *(l/s)*
0.6	0.79
0.5	0.85
0.4	0.91

The computed discharge for the test shown in Fig. 8 (steep face upstream) as a function of K is as follows:

Contraction-Expansion Coefficient K	Flow Rate Q *(l/s)*
0.5	0.57
0.4	0.62
0.3	0.62

The computed discharge for these values of K is smaller than the measured discharge 1.0*l/s*.

Figs. 7 and 8 indicate that the constant value of $K = 0.5$ yields reasonable agreement between the computed and measured free surface variations except for the dip in the vicinity of the sharp crest of the triangular obstacle. The free surface dip for an obstacle with a rounded crest may not be as pronounced as those shown in Figs. 7 and 8. In summary, these limited comparisons suggest that $K \cong 0.5$ may be used as a first approximation for predicting the overall free surface variations over an obstacle, although the details of the free surface variations may not be predicted well, and the computed discharge may not be very accurate. It should be noted that the numerical model somewhat overpredicts the free surface elevation on the crest of the obstacle and may be regarded to yield a conservative estimate. The calibration of K for different obstacle shapes and orientations may somewhat improve the agreement between the computed and measured results; but the last term on the right hand side of (2) added to the standard one-dimensional momentum equation may be too simple and crude to describe the detailed converging and diverging flows over an obstacle such as the Roadway.

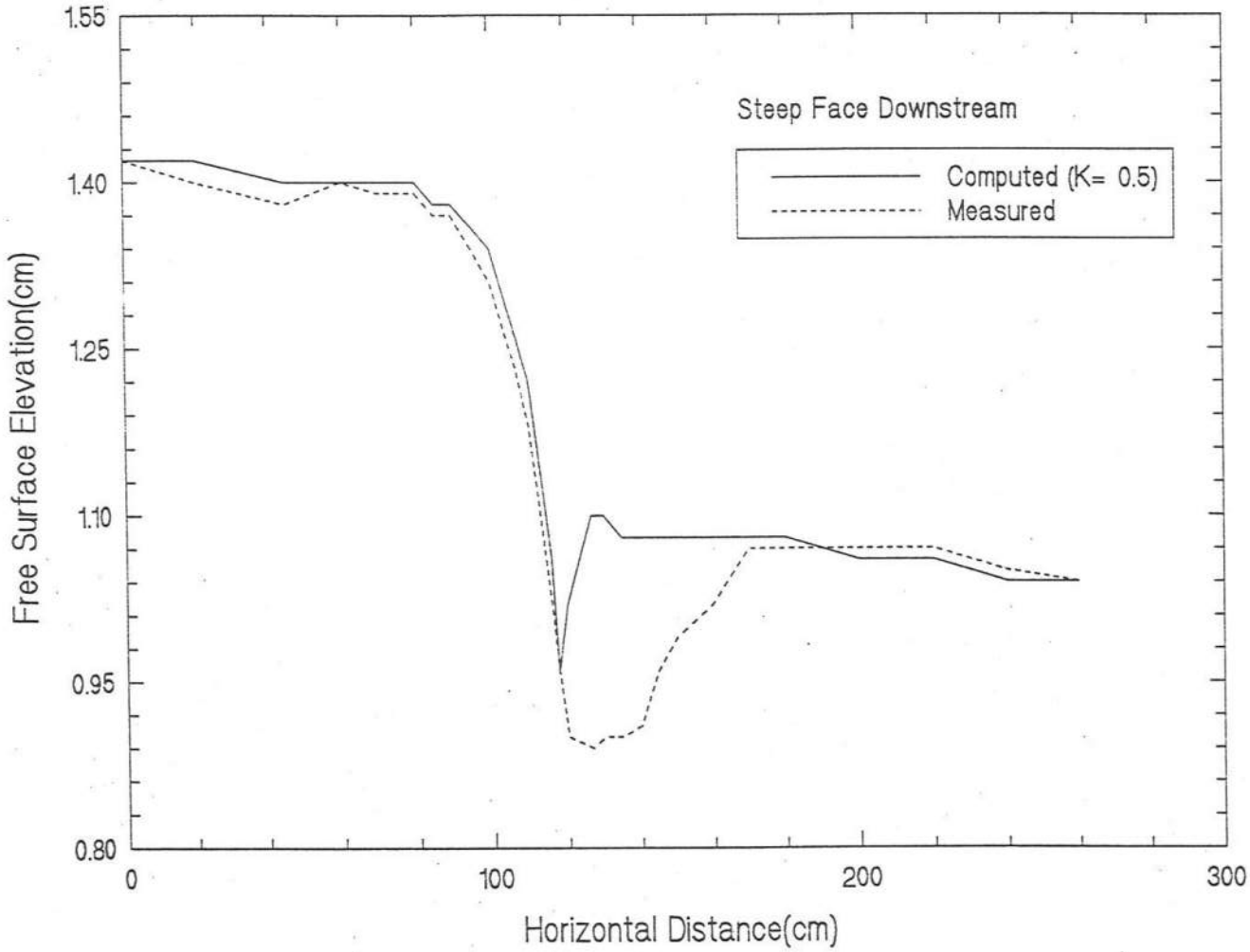

Fig. 7: Measured and Computed Free Surface Elevations of Test with Steep Face Downstream

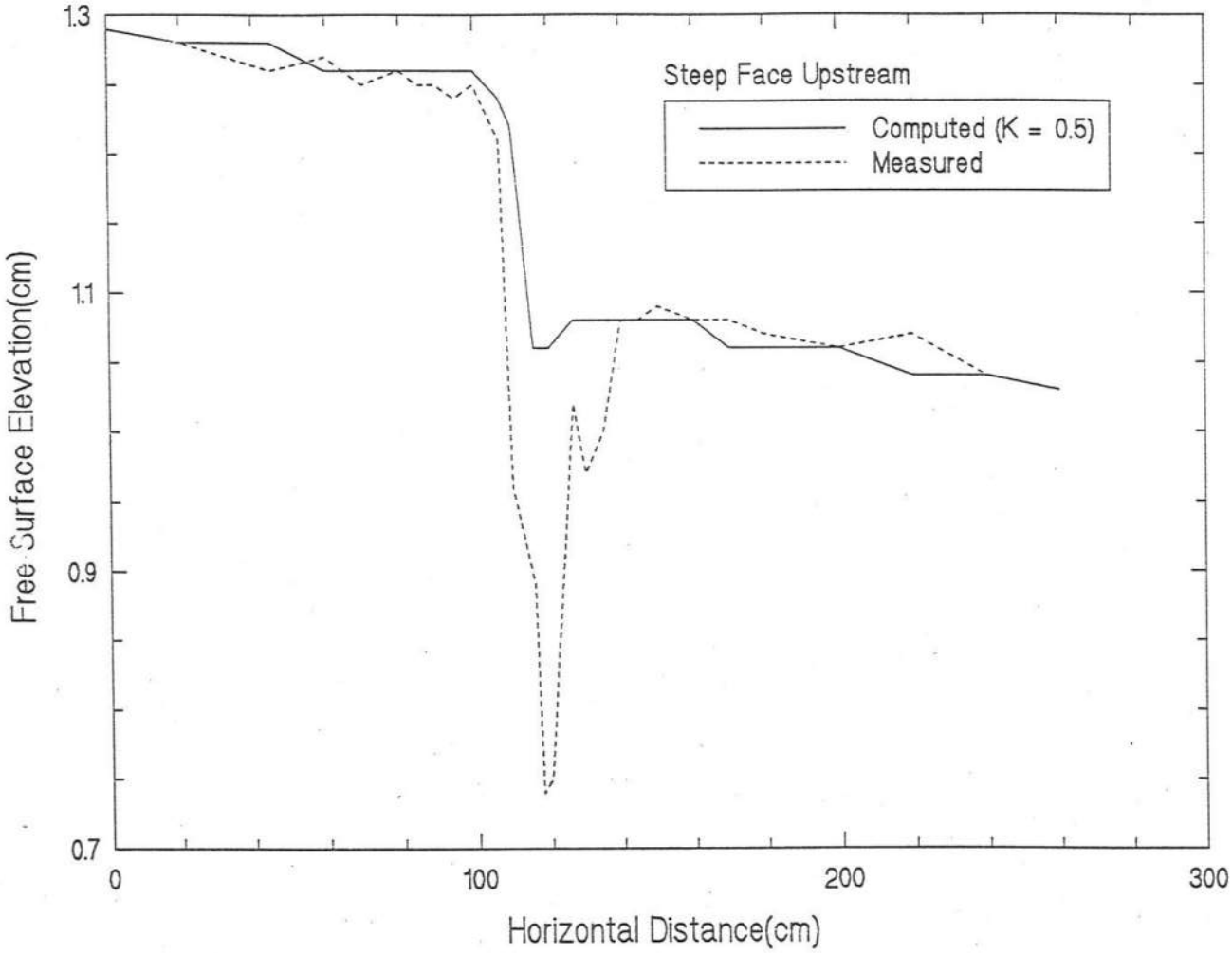

Fig. 8: Measured and Computed Free Surface Elevations of Test with Steep Face Upstream

3 INPUT AND COMPUTED RESULTS FOR ROADWAY

The numerical model based on (1) and (2) with $K = 0.5$ is applied to the bay system shown in Fig. 1. The network of relatively small channels is represented by 35 cross sections, 7 channels and 3 junctions. The length between node 1 and the North Bay is approximately 71,000 ft (22,000 m). The Roadway is located at node 32; the stillwater elevations at the Roadway are therefore given by the elevations at node 32. The bathymetry at each cross section is specified as input. It is easy to account for the wetting and drying of subsections at each cross section in the one-dimensional model. The values of the roughness coefficient, n_j, for subsections in (3) are taken to be 0.02 for deep areas, 0.025 for shallow areas, and 0.035 for areas covered with vegetation on the basis of the guidelines given by Amein and Kraus(1991). Appendix A shows the cross-section geometry and the roughness coefficient specified at each of the 35 nodes. The boundary conditions of zero discharge is assumed at the landward end nodes where fresh water inflow is negligible. At node 1, seaward of the Ocean City Inlet, the temporal variation of the stillwater elevation, η, is specified as input. Section 3.1 explains the development of the hydrographs used in this study.

3.1 Synthetic Hydrographs at Ocean City Inlet

In the numerical simulations, the temporal variation of the water surface elevation, η, at the Atlantic Ocean boundary is specified as input. Because in the computational domain the free surface elevation is not known a priori, the computation is initiated with a

zero free surface displacement. Therefore, a few periods of the spring tide alone precede the storm surge to minimize the effect of the initial transients on the computed results during the storm surge. Storm hydrographs were developed for storms of 10, 20, 50, 100, and 500 year recurrence intervals. Each hydrograph is the superposition of a semi-diurnal spring tide and an idealized storm surge for given recurrence interval and duration. The stage or stillwater elevation, $\eta(t)$, above mean sea level(MSL) in feet is expressed as:

$$\eta(t) = \eta_{st}(t) + \eta_{surge} \tag{15}$$

where

t = time in hours beginning at $t = 0$ for the duration $0 \le t \le 95$ hours
$\eta_{st}(t)$ = semi-diurnal spring tide hydrograph
η_{surge} = idealized storm surge hydrograph for given recurrence interval

The spring tides at Ocean City Inlet were measured from the fishing pier in February, 1992 during the Perigean tide. The peak tidal elevation was 2.57 ft above MSL. Fig. 9 shows the measured spring tide hydrograph, $\eta_{st}(t)$, where the time, t, in hours in this figure is shifted such that $\eta_{st} = 2.57$ ft at t = 55 hr.

On the other hand, the idealized storm surge elevation, η_{surge}, is assumed to be approximated by:

$$\eta_{surge} = A\cos\left(\pi\frac{t-55}{T_{surge}}\right) \qquad \text{for} \quad \left(55-\frac{T_{surge}}{2}\right) \le t \le \left(55+\frac{T_{surge}}{2}\right) \tag{16a}$$

$$\eta_{surge} = 0 \text{ otherwise} \tag{16b}$$

where

T_{surge} = storm surge duration which is taken to be 40 or 60 hr.
A = maximum storm surge elevation occurring at t = 55 hr.

Eq. (16a) together with (15) and Fig. 9 assumes that the maximum surge elevation occurs at the same time as the peak spring tide. This assumption may somewhat

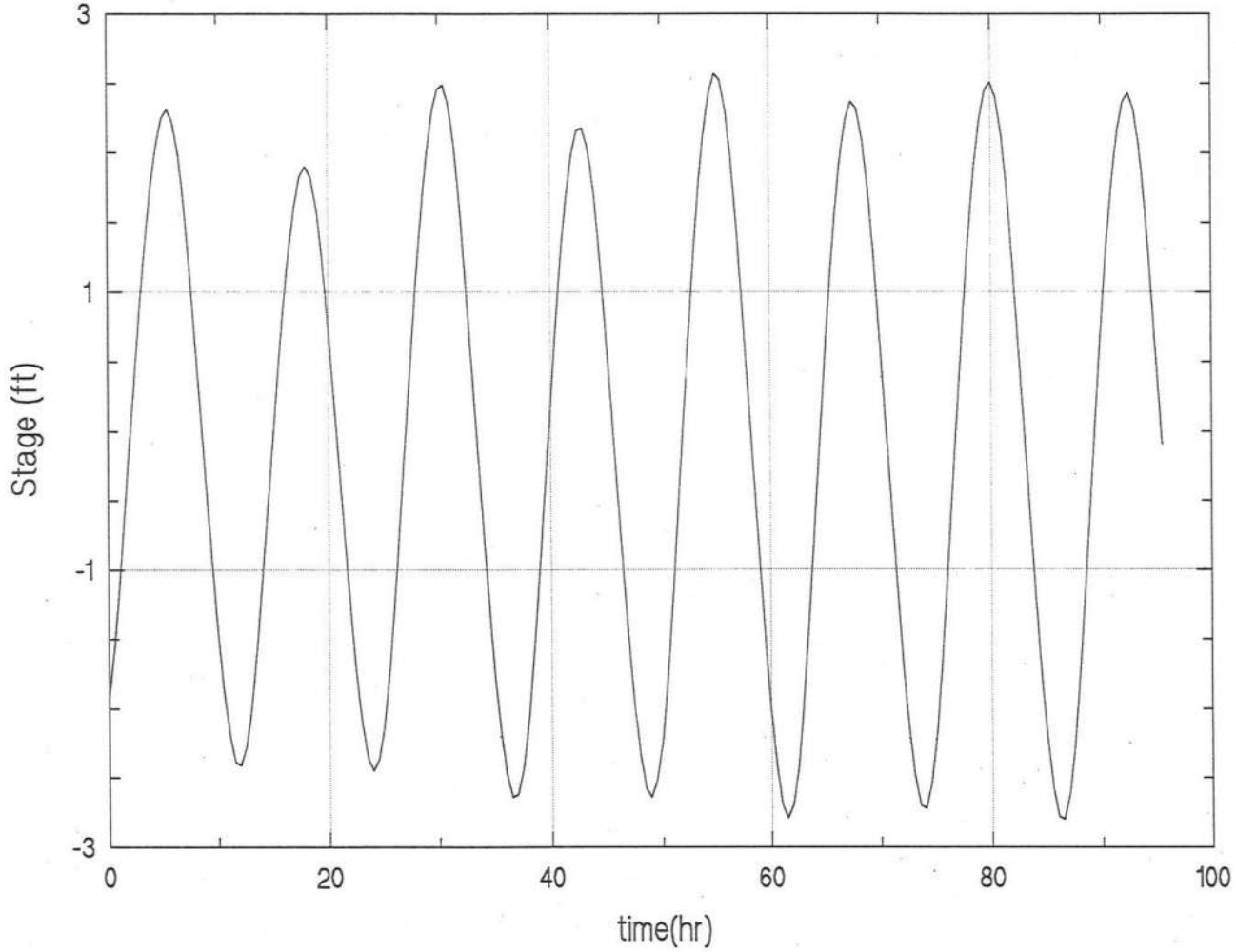

Fig. 9: Spring Tide Hydrograph Used in the Study

overestimate the combined maximum stage due to the storm surge and tide. Under this assumption, the peak stillwater elevation, η_{peak}, due to the storm surge and the spring tide is given by

$$\eta_{peak} = (2.57 + A) \quad \text{in feet} \tag{17}$$

from which the maximum storm surge elevation, A, may be estimated using available data on η_{peak}. Fig. 10 shows the idealized storm surge based on (16) with T_{surge} = 40 hr. and A = 4.83 ft.

A relationship between the peak stillwater elevation, η_{peak}, and the recurrence interval, T_r, may be developed in the following manner. The U.S. Army Corps of Engineers has suggested the following recurrence intervals and corresponding peak stillwater elevations at Ocean City Inlet based on available data analyzed by Ho et al.(1976):

Recurrence Interval T_r (yr.)	Peak Stillwater Elevations At Ocean City Inlet η_{peak} (ft)
10	5.9
50	7.4
100	8.1
500	10.2

In order to interpolate a peak stillwater elevation for a recurrence interval of 20 years, the above tabulated values may be assumed to follow the Gumble distribution(e.g. Benjamin and Cornell 1970) which can be written as:

$$y = -\ln\left[\ln\left(\frac{T_r}{T_r - 1}\right)\right] = a\ \eta_{peak} - b \tag{18}$$

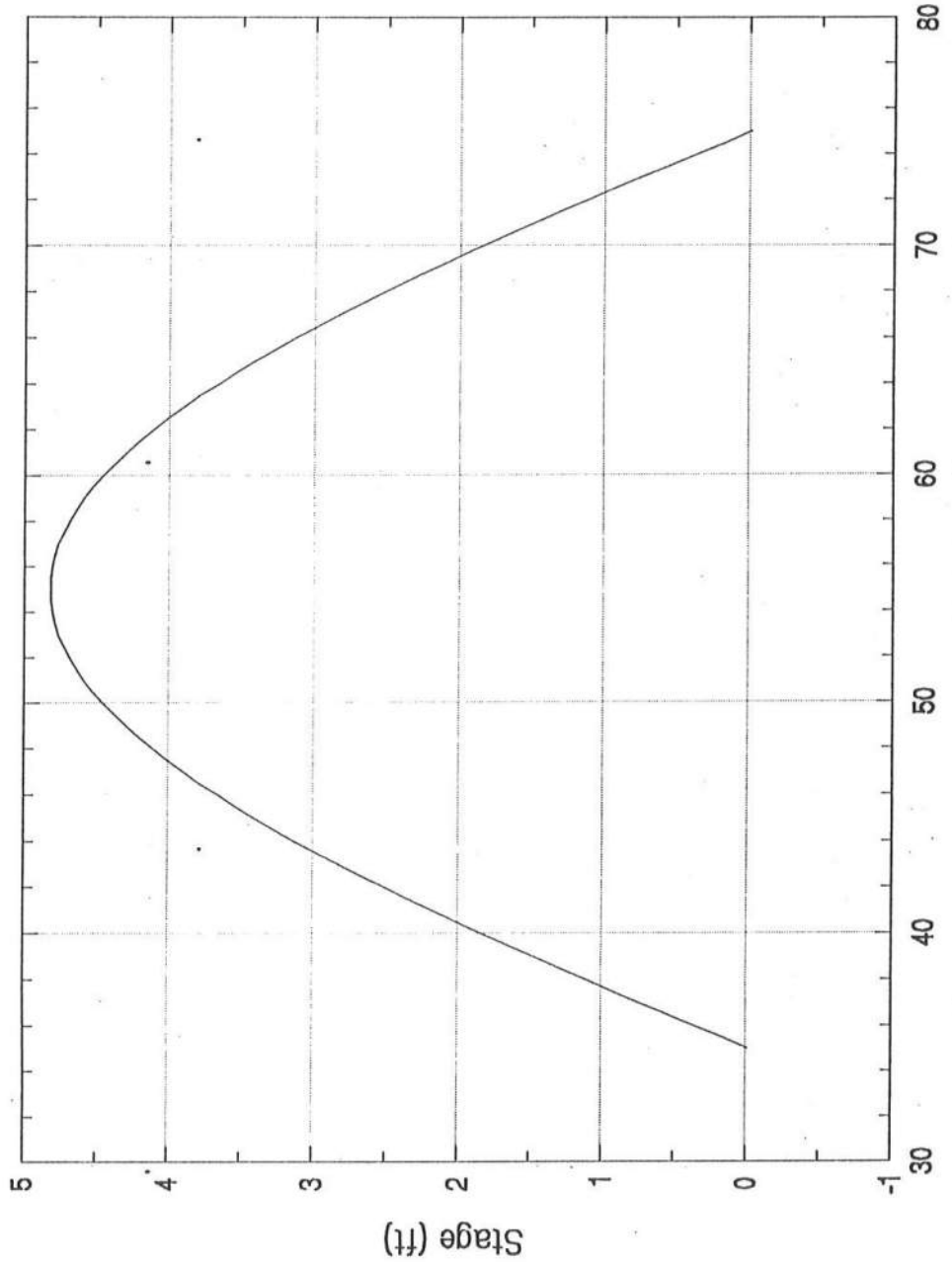

Fig. 10: Idealized Storm Surge with 40 hr Duration and 4.83 ft Maximum Surge

where a and b are estimated by a linear regression analysis. Fig. 11 shows that $a = 0.914$ and $b = 2.98$. For $T_r = 20$ yr., Eq. (18) with $a = 0.914$ and $b = 2.98$ yields $y = 2.97$ and $\eta_{peak} = 6.51$ ft.

Finally, the maximum surge elevation, A, for the specified recurrence interval is computed using (17) as summarized below:

Recurrence Interval T_r (yr)	Peak Stillwater Elevation at Ocean City Inlet η_{peak} (ft)	Maximum Surge Elevation A(ft)
10	5.9	3.33
20	6.51	3.94
50	7.4	4.83
100	8.1	5.53
500	10.2	7.63

The synthetic hydrographs calculated using (15) and (16) with the value of A listed above and $T_{surge} = 40$ or 60 hr are tabulated and plotted in Appendix B for each storm as well as for the spring tide alone. For example, Fig. 12 shows the specified temporal variations of the stillwater elevation at node 1 for 50 yr. storm with $T_{surge} = 40$ and 60 hr.

3.2 Existing and Raised Roadways

Five different cross sections at node 32 are examined to represent the existing Roadway and raised Roadways with the minimum elevations of 3.5, 4.0, 4.5 and 5.0 ft. above the mean sea level as shown in Fig. 13. The temporal variation of the stillwater elevation at the Roadway is computed for these 5 raised cross sections at node 32 driven by each of the 10 synthetic hydrographs at node 1. The water depth in the Ditch, shown in Fig. 13, is 6 ft below the mean sea level for each case. It is noted that both sides of the

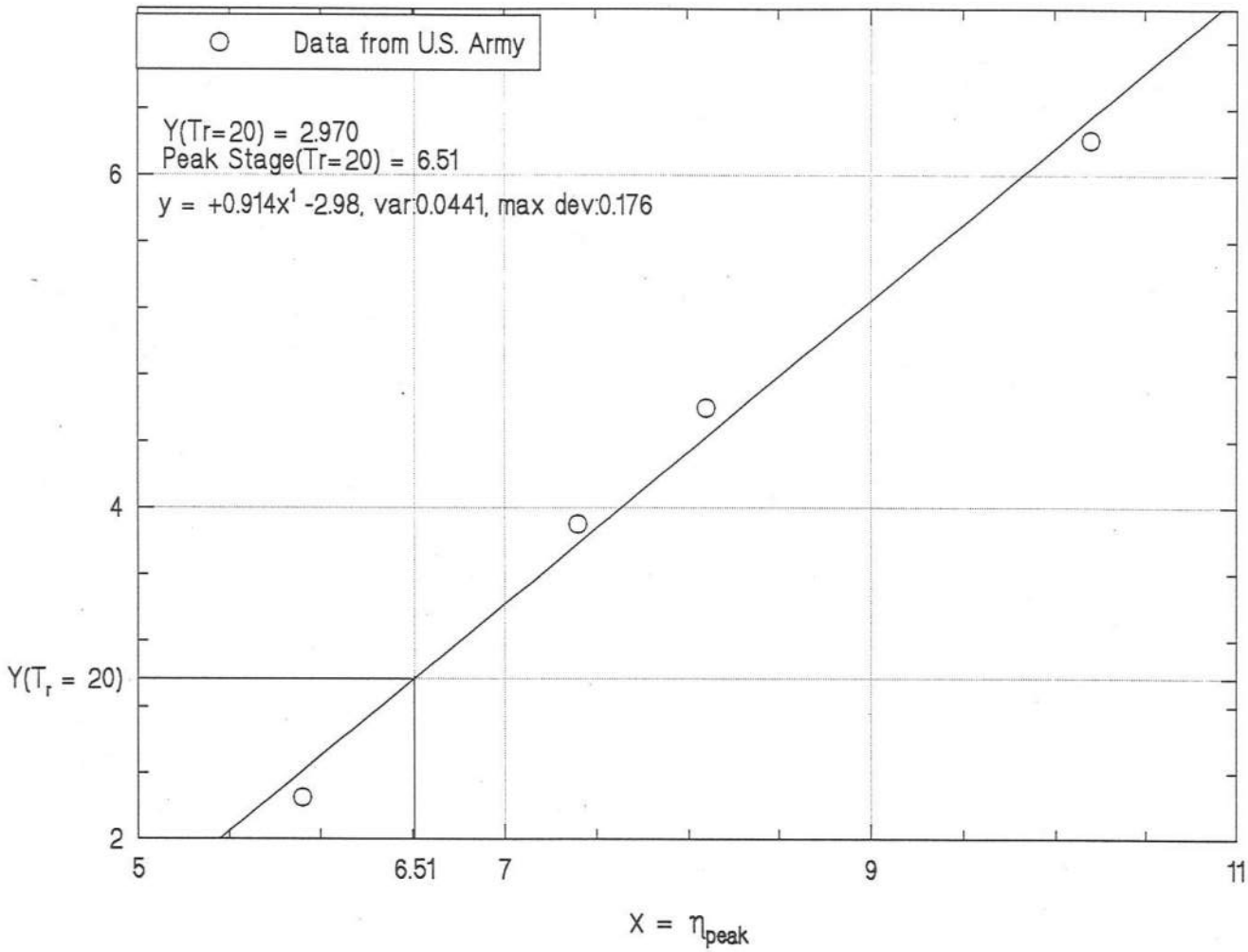

Fig. 11: Linear Regression between $x = \eta_{peak}$ and $y = -ln\{ ln [T_r / (T_r-1)] \}$ with T_r = Recurrence Interval on the Basis of Gumbel Distribution

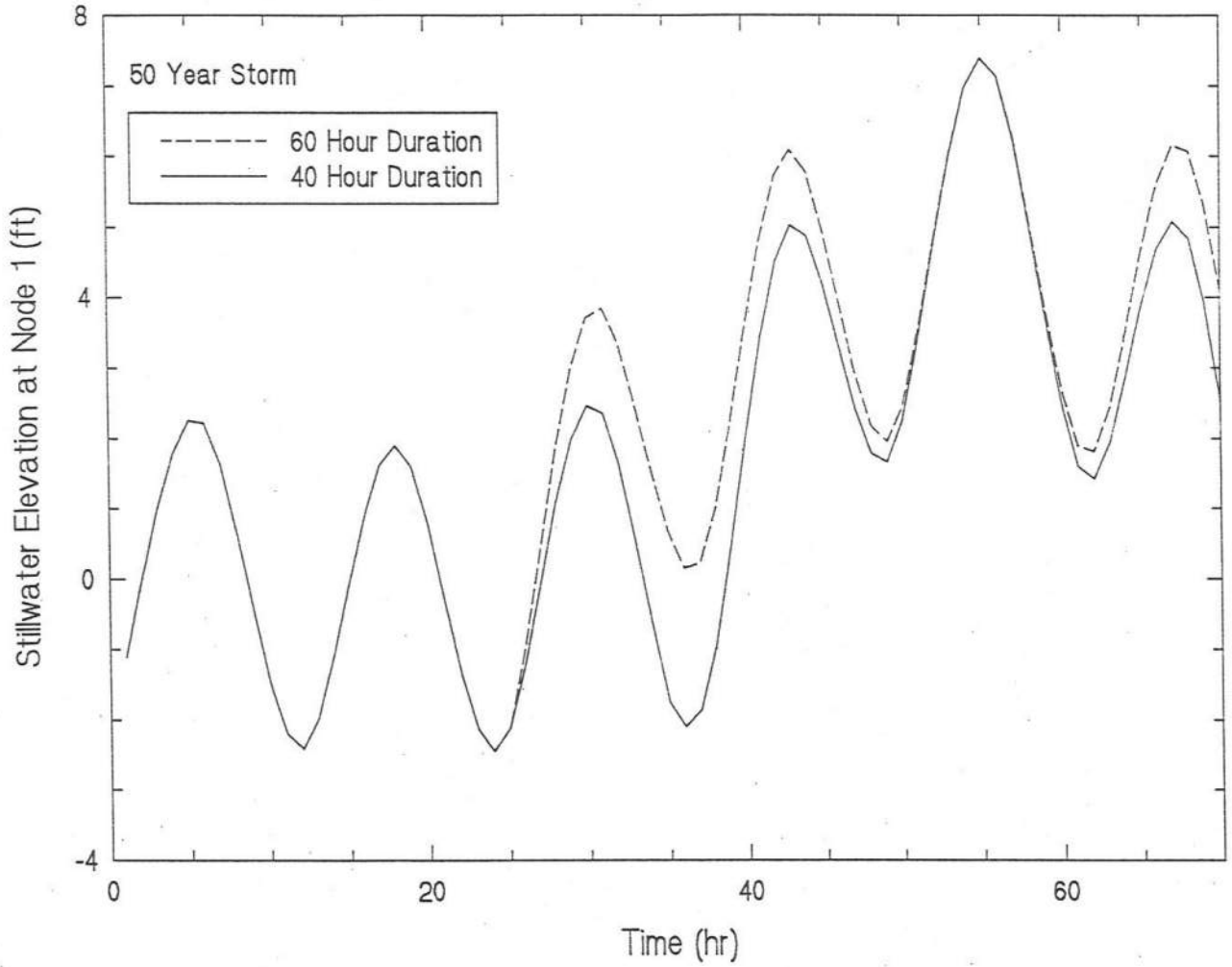

Fig. 12: Specified Temporal Variations of Stillwater Elevation at Node 1 for 50 yr Storm

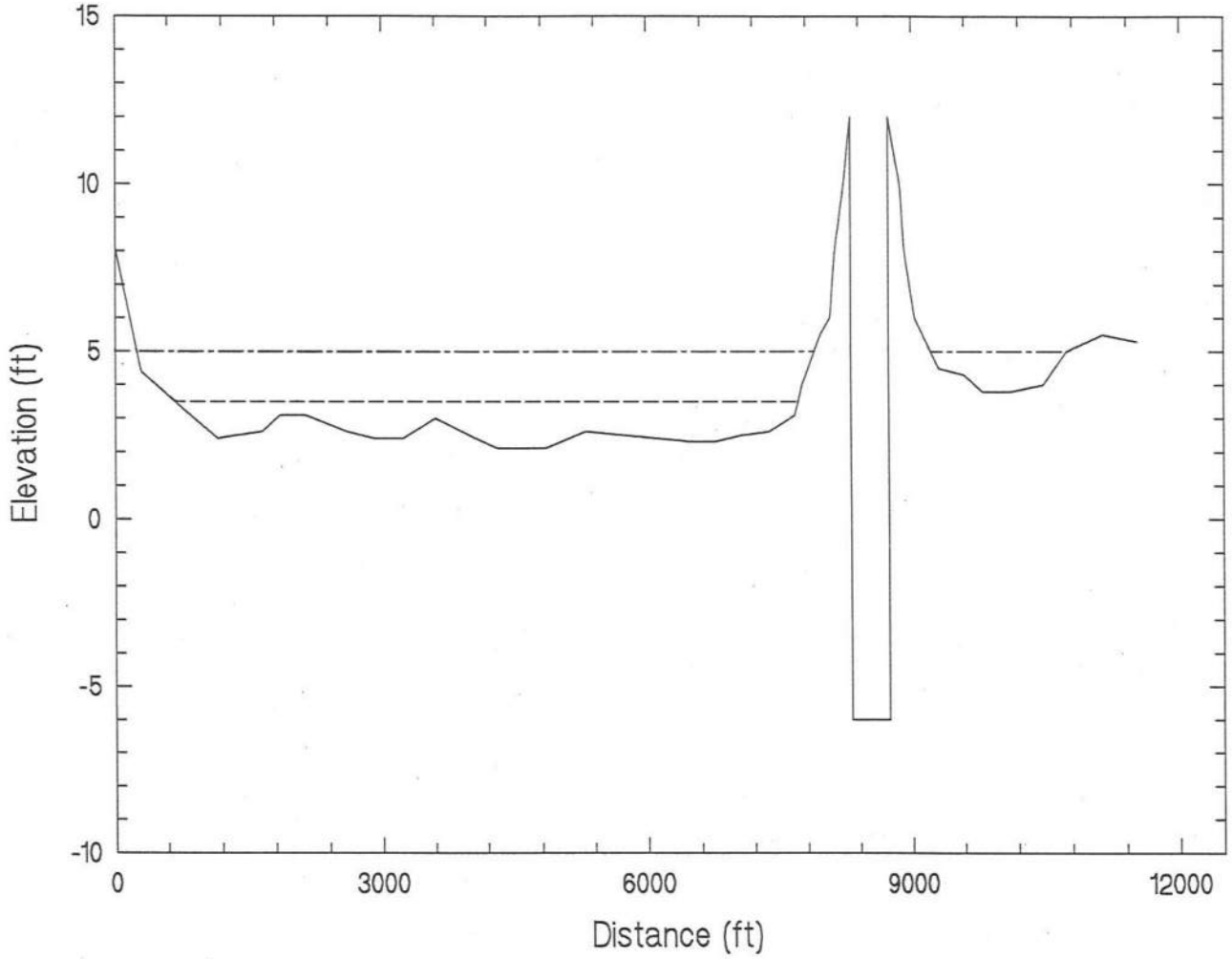

Fig. 13: Existing Cross Section Geometry at Node 32 and Minimum Fill Levels for 3.5 ft and 5.0 ft

Ditch are high because of abutments for the bridge spanning the waterway. The existing cross section geometry and the roughness coefficient at the rest of the nodes are plotted in Appendix A.

3.3 Summary of Computed Results

Appendix C contains plots of the temporal variations of the stillwater elevation at node 32 vs. time for the existing Roadway and for the raised Roadways for the minimum elevations of 3.5-5.0 ft. as explained in the following. Fig. 14 shows the computed temporal variations of the stillwater elevation at the Roadway for storms of 50 yr recurrence interval and durations of 40 and 60 hr. A total of 11 different hydrographs at node 1 have been used and are plotted along with the stillwater elevations at node 32 in Appendix C.

The computed peak stillwater elevations at node 32(the Roadway) for each hydrograph with the existing Roadway as well as the Roadway raised to a minimum of 3.5, 4.0, 4.5, and 5.0 feet are summarized in Table 1. It is readily apparent that the peak stillwater elevations are practically the same for the five different cross sections at node 32 for all of the 11 hydrographs at Ocean City Inlet. In addition, the temporal variations of the stillwater elevations are also essentially the same for the existing and raised Roadways. This is because the stillwater elevation in the vicinity of the Roadway is essentially horizontal for storm surge and tides whose horizontal length scale is much larger than the length of the flooded Roadway. On the other hand, the computed results indicate that for the storm with the same peak stillwater elevation at node 1, the increase of the storm

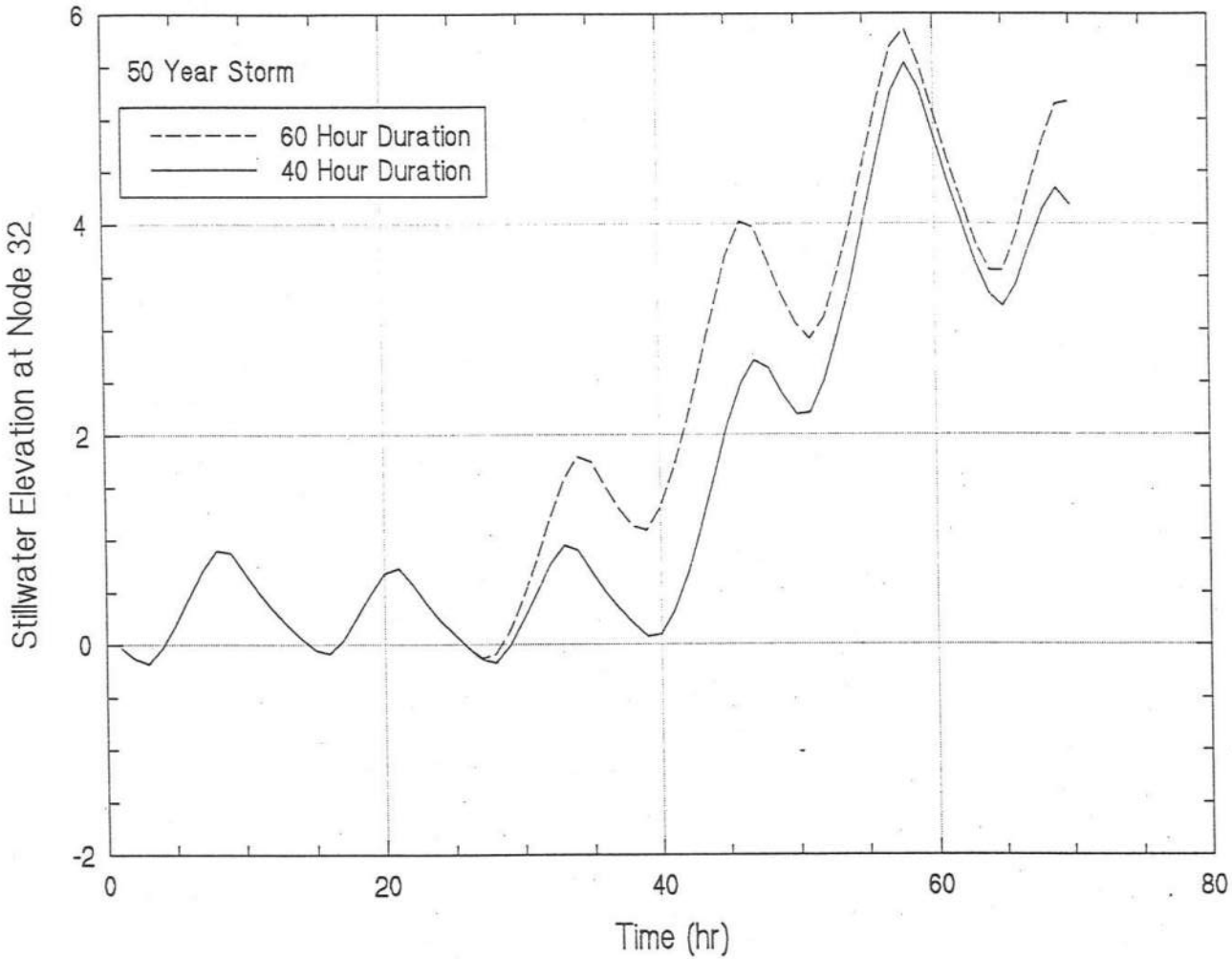

Fig. 14: Computed Temporal Variations of Stillwater Elevation at Node 32 for 50 yr Storm

Table 1: Computed Peak Stillwater Elevations at Existing and Raised Roadways

Storm	spring tides	10 yr. 40 hr	10 yr. 60 hr	20 yr. 40 hr	20 yr. 60 hr	50 yr. 40 hr	50 yr. 60 hr	100 yr. 40 hr	100 yr. 60 hr	500 yr. 40 hr	500 yr. 60 hr
Existing Geometry	0.99	3.93	4.20	4.54	4.83	5.49	5.81	6.24	6.56	8.55	8.84
Roadway Raised to Minimum of 3.5 ft.	0.99	3.93	4.20	4.54	4.83	5.49	5.81	6.24	6.56	8.55	8.84
Roadway Raised to Minimum of 4.0 ft.	0.99	3.93	4.20	4.54	4.83	5.49	5.81	6.24	6.56	8.55	8.84
Roadway Raised to Minimum of 4.5 ft.	0.99	3.93	4.20	4.54	4.83	5.49	5.81	6.24	6.56	8.55	8.84
Roadway Raised to Minimum of 5.0 ft.	0.99	3.93	4.20	4.54	4.83	5.49	5.81	6.24	6.56	8.55	8.84

surge duration from 40 hr to 60 hr does result in a slight increase of the stillwater elevation at node 32.

Fig. 15 shows the peak stillwater elevations as a function of the horizontal distance from node 1 along the main channel for the 10, 20, 50 and 100 yr storms with 40 and 60 hr durations. The computed peak stillwater elevations along the main channel are practically the same for the existing Roadway and the Roadways raised to a minimum elevation of 3.5, 4.0, 4.5 and 5.0 ft. The peak stillwater elevations computed for the 500 yr storm are not shown in Fig. 15 because breaching of the barrier island separating the Atlantic Ocean and the Bays may occur during the 500 yr storm and increase the peak stillwater elevations in the Bays. In the absence of breaching of the barrier island, the peak stillwater elevations decrease rapidly in the vicinity of the narrow entrance of Ocean City Inlet and remain almost the same in the South and North Bays for each storm with a specified duration. For the same peak stillwater elevations at node 1, the 60 hr storm surge increases the peak stillwater elevation at node 32 by about 0.3 ft in comparison to the 40 hr storm surge.

There is little historical storm surge data for the Bays. For the 1991 Halloween Storm, the peak elevation recorded at the NOAA tide gage at Ocean City, Maryland was 5.5 ft, while the Delaware Department of Natural Resources and Environmental Control reported a peak elevation of 4.0 ft in the North Bay. The recurrence interval associated with this storm was considered to be about 10 yr. The computed results for the 10 yr storm shown in Fig. 15 are at least qualitatively consistent with this limited data. It should be stated that the computed stillwater elevations may not be very accurate for lack

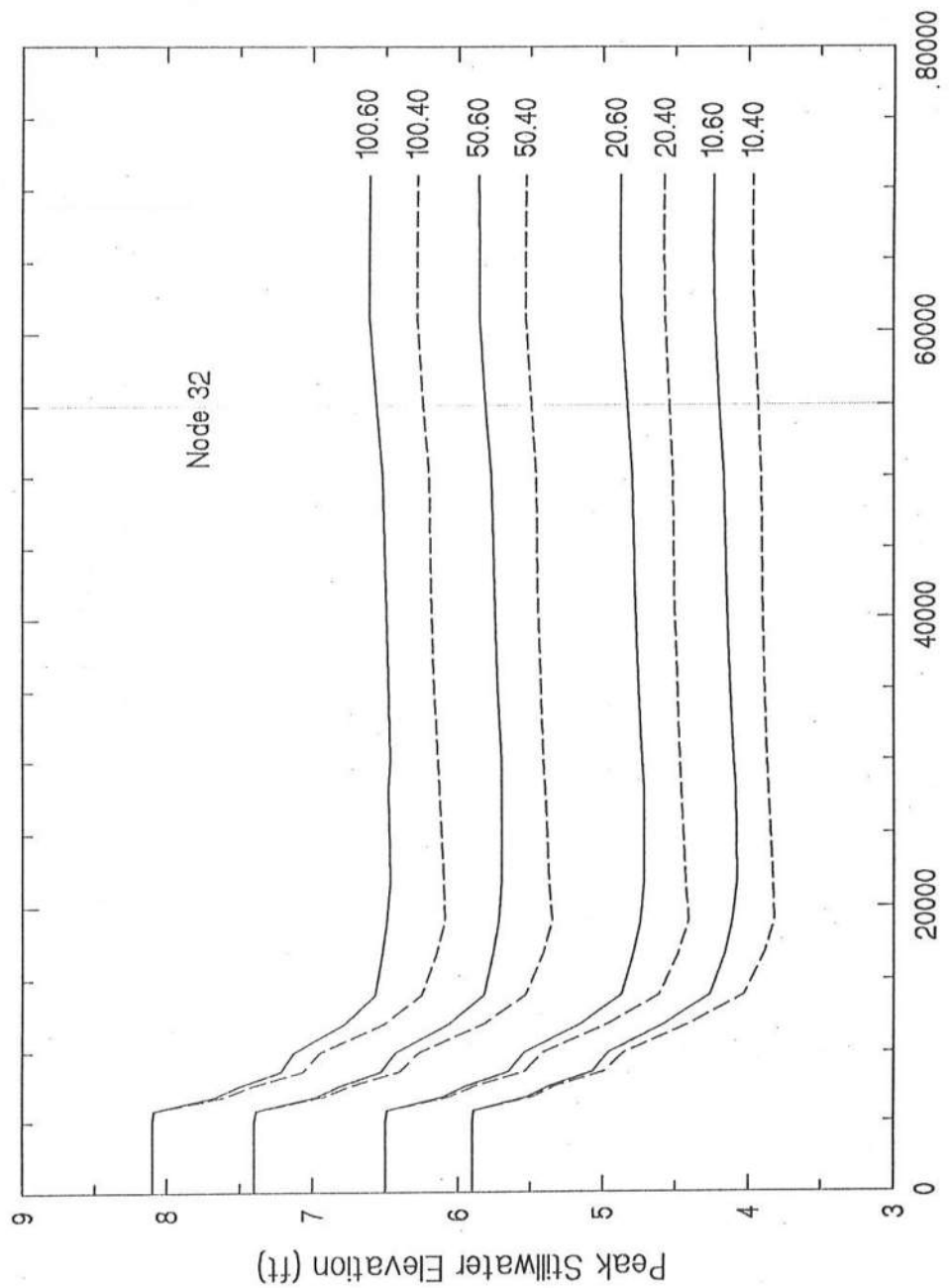

Fig. 15: Peak Stillwater Elevations as a Function of Horizontal Distance along Main Channel from Node 1 for 10, 20, 50, and 100 yr Storm

of calibrations of the empirical coefficients in the numerical model. However, the model can still be used with some degree of confidence to quantify the effect of the raised Roadway on the stillwater elevation in the vicinity of the Roadway.

In summary, the stillwater elevations at node 32 are computed to be essentially unchanged by the raising of the roadway to a minimum of up to 5.0 ft. The relation between the peak stillwater elevation, η_{peak}, and the recurrence interval, T_r, is depicted in Fig. 16 for the storm durations of 40 and 60 hr. Available data is insufficient to establish the relation between η_{peak} and T_r at the Roadway considering the statistical distribution of the storm duration.

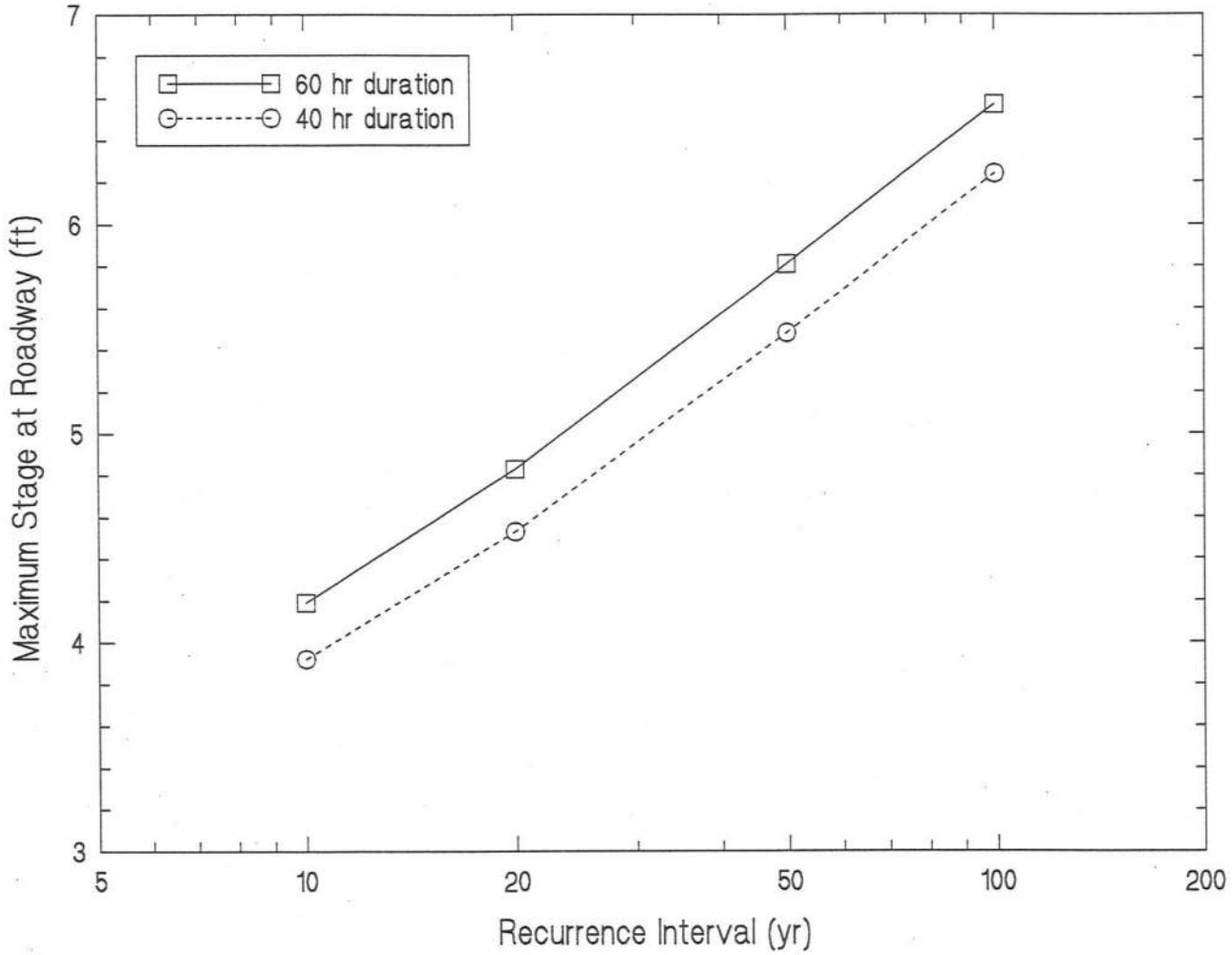

Fig. 16: Relation between Peak Stillwater Elevation at Roadway and Recurrence Interval for Storm Duration of 40 and 60 hr

4 SUMMARY AND CONCLUSIONS

An available numerical model for a network of one-dimensional channels is applied to examine flooding of the Roadway between the Bays due to storm surge and tides through Ocean City Inlet. An analytical solution for an elongated bay is obtained to gain a physical insight into the propagation, damping, and reflection of incident long (tidal) waves in the bay as well as to perform an independent check of the numerical model. A small-scale experiment for steady converging and diverging flow over an obstacle was also conducted to assess the capability of the numerical model based on an empirical contraction-expansion coefficient, K. The numerical model, with $K = 0.5$, is shown to be capable of predicting the overall free surface variation over the obstacle, although the detailed free surface variation and discharge may not be predicted very accurately.

The numerical model with $K = 0.5$ is then applied to predict the stillwater elevations at the existing and raised Roadways for different storms. The computed results indicate that the raised Roadway with a minimum elevation of 5 ft or less above the mean sea level will not increase the essentially horizontal stillwater elevations in the vicinity of the Roadway. This finding confirms the simple analytical results obtained in the preliminary hydraulic study whose report is attached in Appendix D. The computed peak stillwater elevations in the vicinity of the Roadway seem to be consistent with limited available data but need to be verified using more comprehensive and quantitative data. Nevertheless, the numerical model whose empirical coefficients are calibrated using limited data will yield an accurate assessment of the stillwater elevation changes caused by the raised Roadway. In conclusion, The stillwater elevations during storms in the vicinity of the Roadway will remain practically unchanged even if the Roadway is to be raised to a

minimum elevation of 5 ft or less above the mean sea level.

REFERENCES

Amein, M. (1975). "Computation of flow through Masonboro Inlet, NC " Journal of Waterways, Harbors and Coastal Engineering Division, American Society of Civil Engineers, Vol. 1, No. WW1, pp. 93-108.

Amein, M. and Kraus, N. C. (1991). "DYNLET1: Dynamic implicit numerical model of one dimensional tidal flow through inlets" Tech. Rept. CERC-91-10, Coast. Engrg. Res. Ctr., Vicksburg, MI.

Benjamin, J. R. and Cornell, C. A. (1970). Probability, Statistics, and Decision for Civil Engineers, McGraw-Hill, New York, NY.

French, R. H. (1985). Open-Channel Hydraulics, McGraw-Hill, New York, NY.

Ho, F. P., Tracey, R. J., Myers, V.A. and Foat, N.S. (1976). "Storm tide frequency analysis for the open coast of Virginia, Maryland and Delaware," NOAA Tech. Memo. NWS HYDRO-32, NOAA, NWS, Office of Hydrology, U.S. Dept. of Commerece, Silver Spring, MD.

Johnson, B. D., Kobayashi, N. and Watson, K. D. (1994). "Flooding of roadway between bays due to storm surge and tide." International Symposium on Waves-Physical and Numerical Modeling, Vancouver, Canada (in press).

Mei, C. C. (1989). The Applied Dynamics of Ocean Surface Waves, World Scientific, Teaneck, NJ.

Appendix A

Cross-section Geometry and Roughness Coefficient at Each of 35 Nodes.

The bottom elevation(solid line) below the mean sea level (the National Geodetic Vertical Datum of 1929) and the value of the roughness coefficient, n, (dashed line) are plotted as a function of the horizontal distance perpendicular to the channel alignment at each of the 35 cross sections used in the computations. The figure for cross section No. J is shown on page A-(J+1) where J = 1, 2, ..., 35. The bottom elevation for cross section No. 32 plotted on page A-33 corresponds to the existing Roadway.

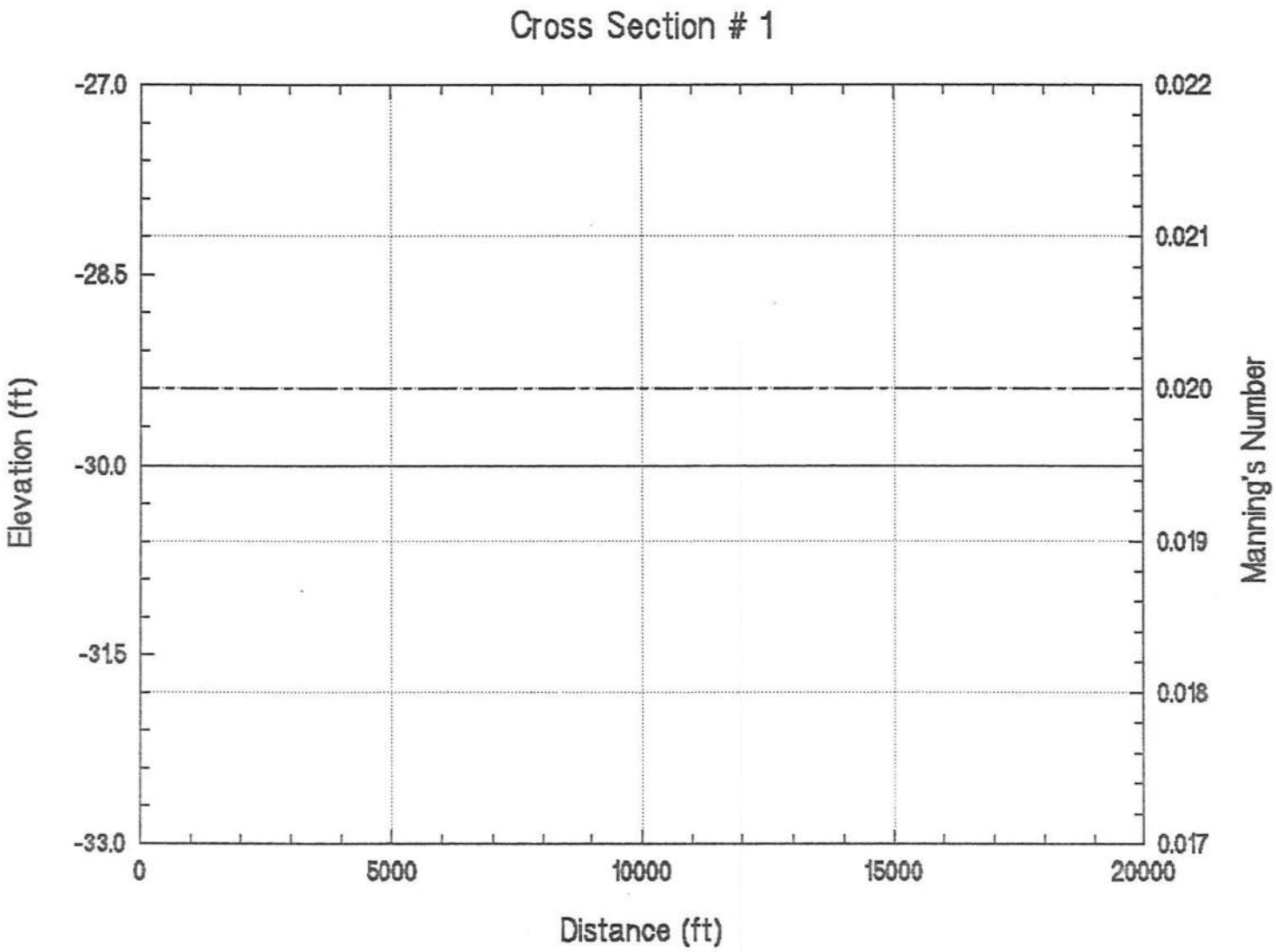
Cross Section # 1
-27.0
-28.5
-30.0
-31.5
-33.0
Elevation (ft)
0.022
0.021
0.020
0.019
0.018
0.017
Manning's Number
0
5000
10000
15000
20000
Distance (ft)

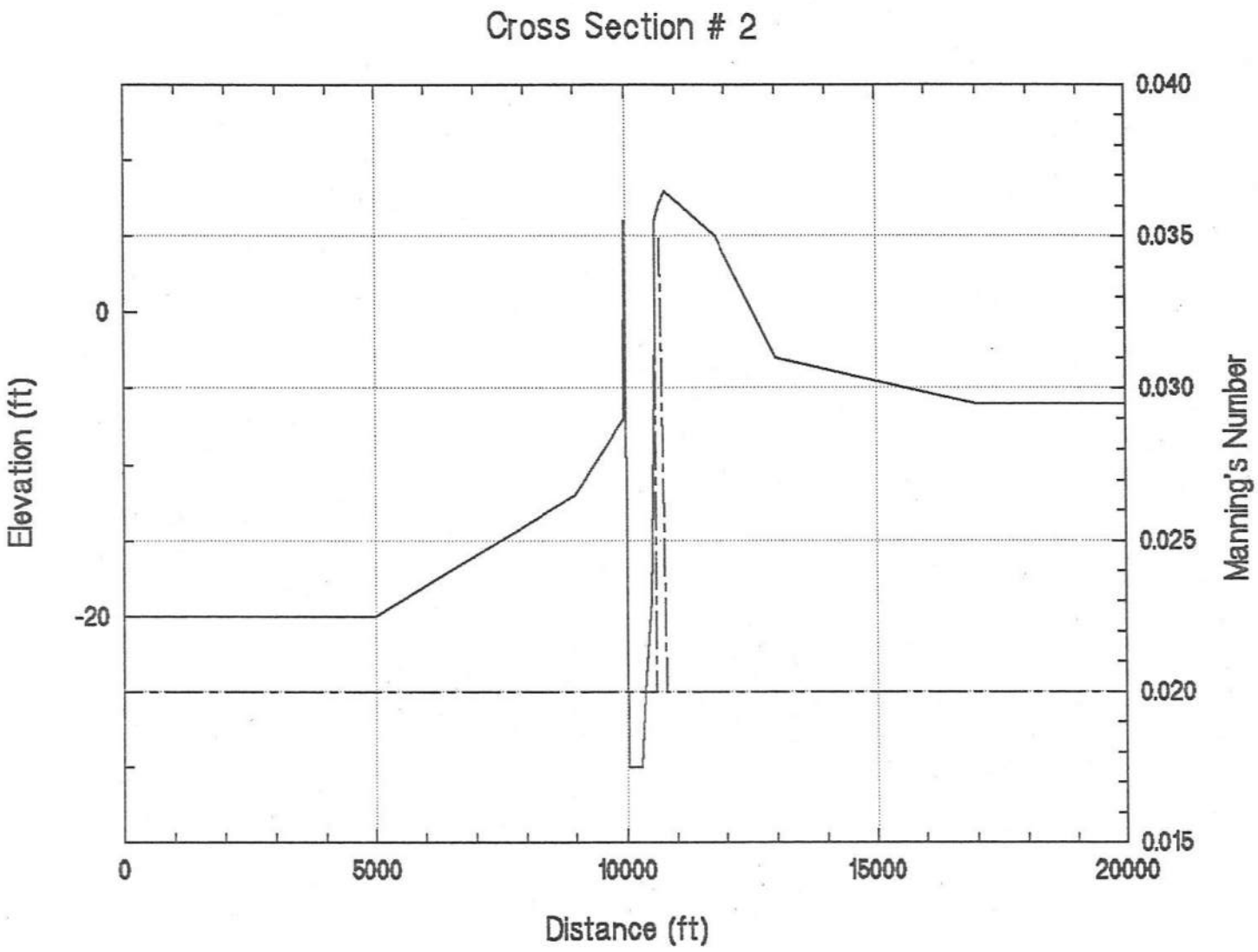
Cross Section # 2
Elevation (ft)
0
-20
0
5000
10000
15000
20000
Distance (ft)
0.040
0.035
0.030
0.025
0.020
0.015
Manning's Number

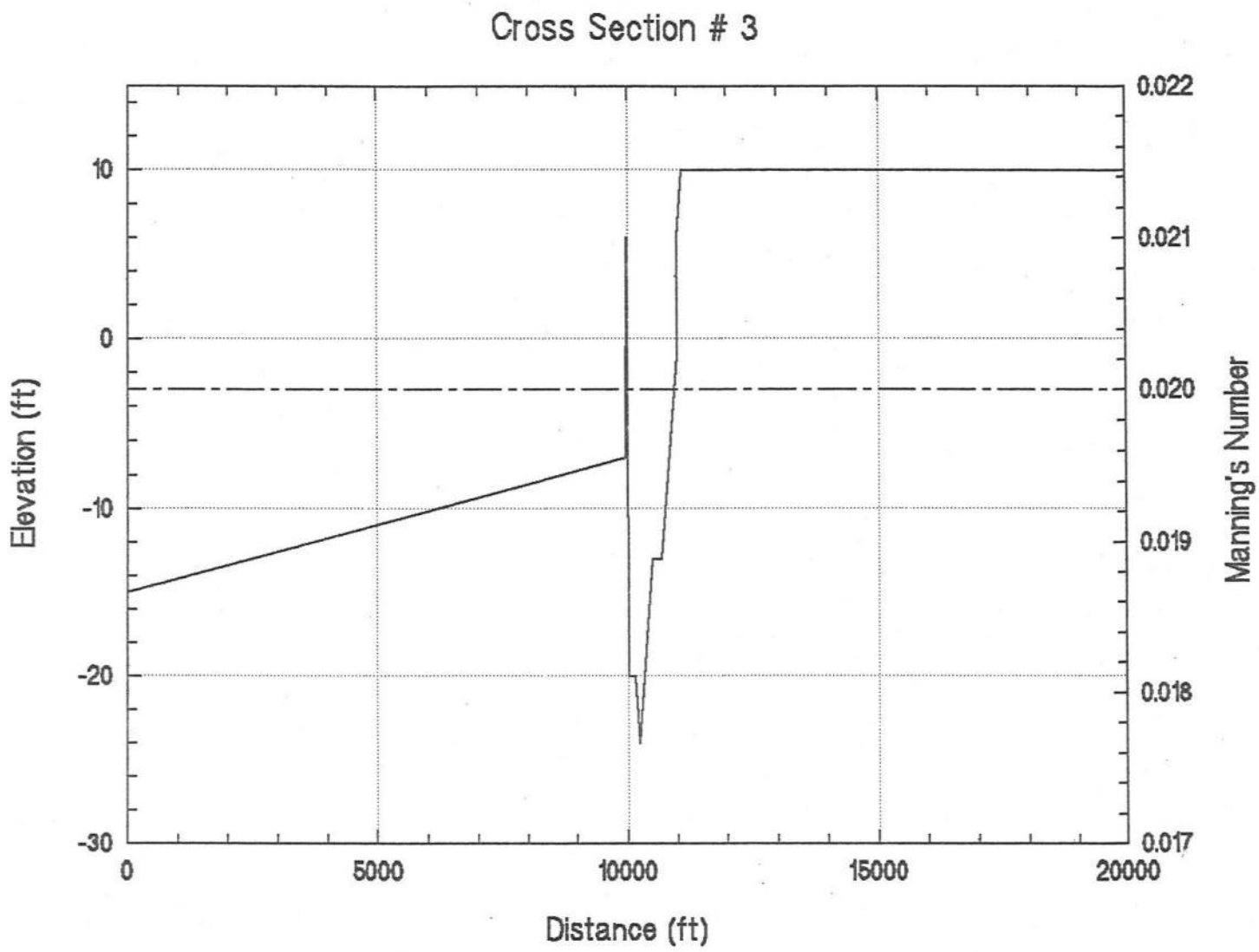
Cross Section # 3
Elevation (ft)
10
0
-10
-20
-30
0
5000
10000
15000
20000
Distance (ft)
0.022
0.021
0.020
0.019
0.018
0.017
Manning's Number

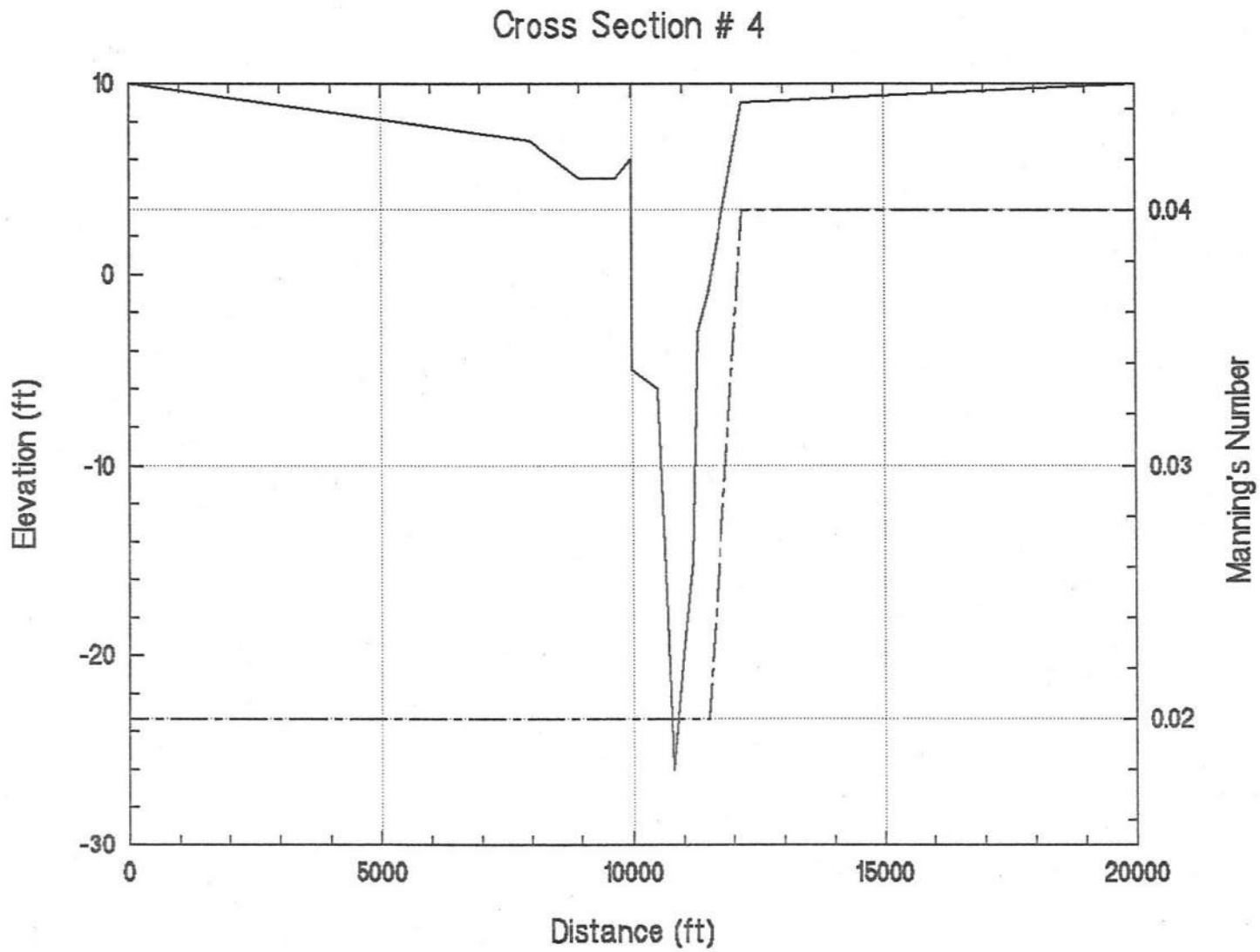
Cross Section # 4
Elevation (ft)
Manning's Number
Distance (ft)
10
0
-10
-20
-30
0
5000
10000
15000
20000
0.04
0.03
0.02

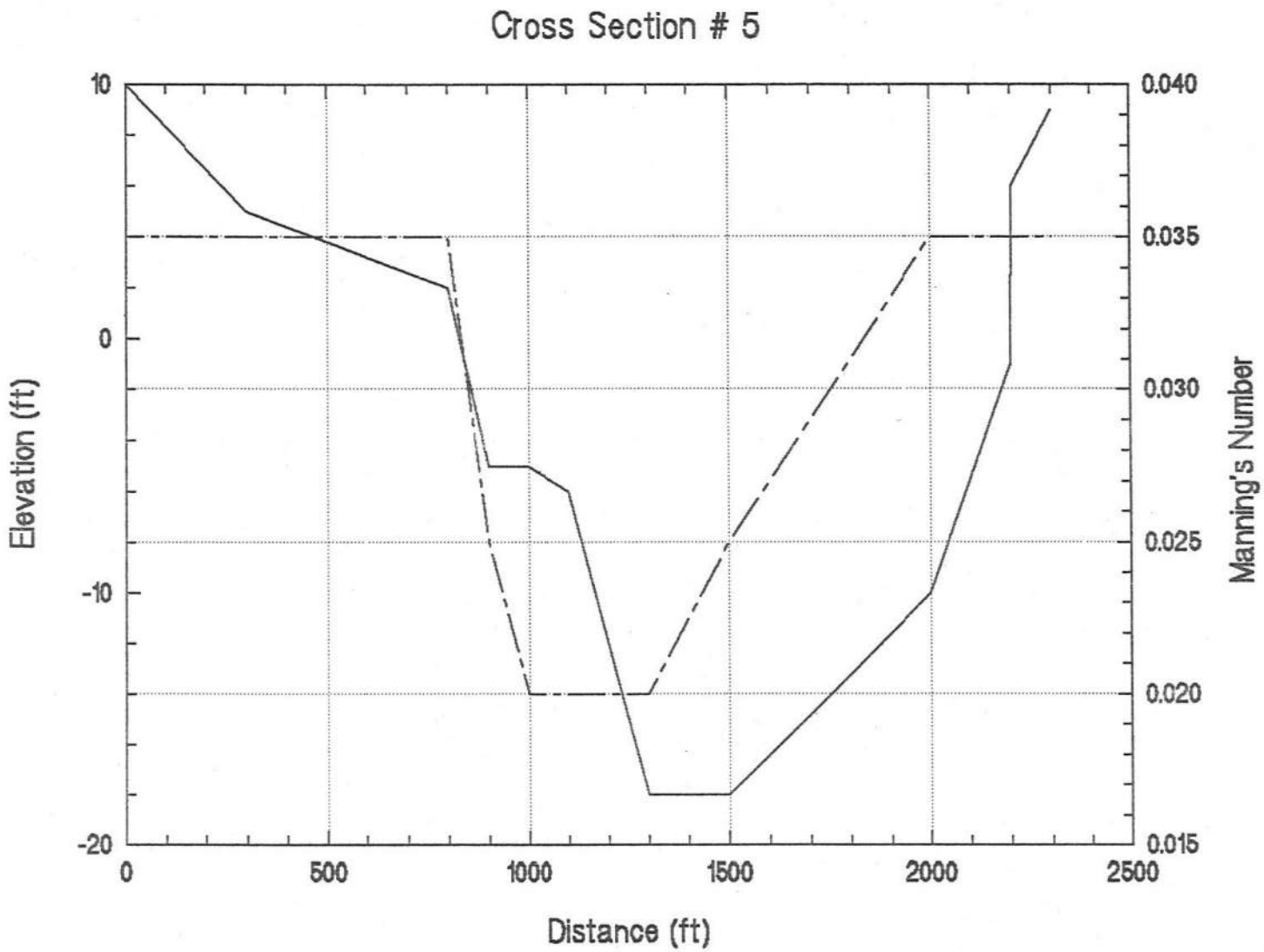
Cross Section # 5
Elevation (ft)
Manning's Number
Distance (ft)
10
0
-10
-20
0.040
0.035
0.030
0.025
0.020
0.015
0
500
1000
1500
2000
2500

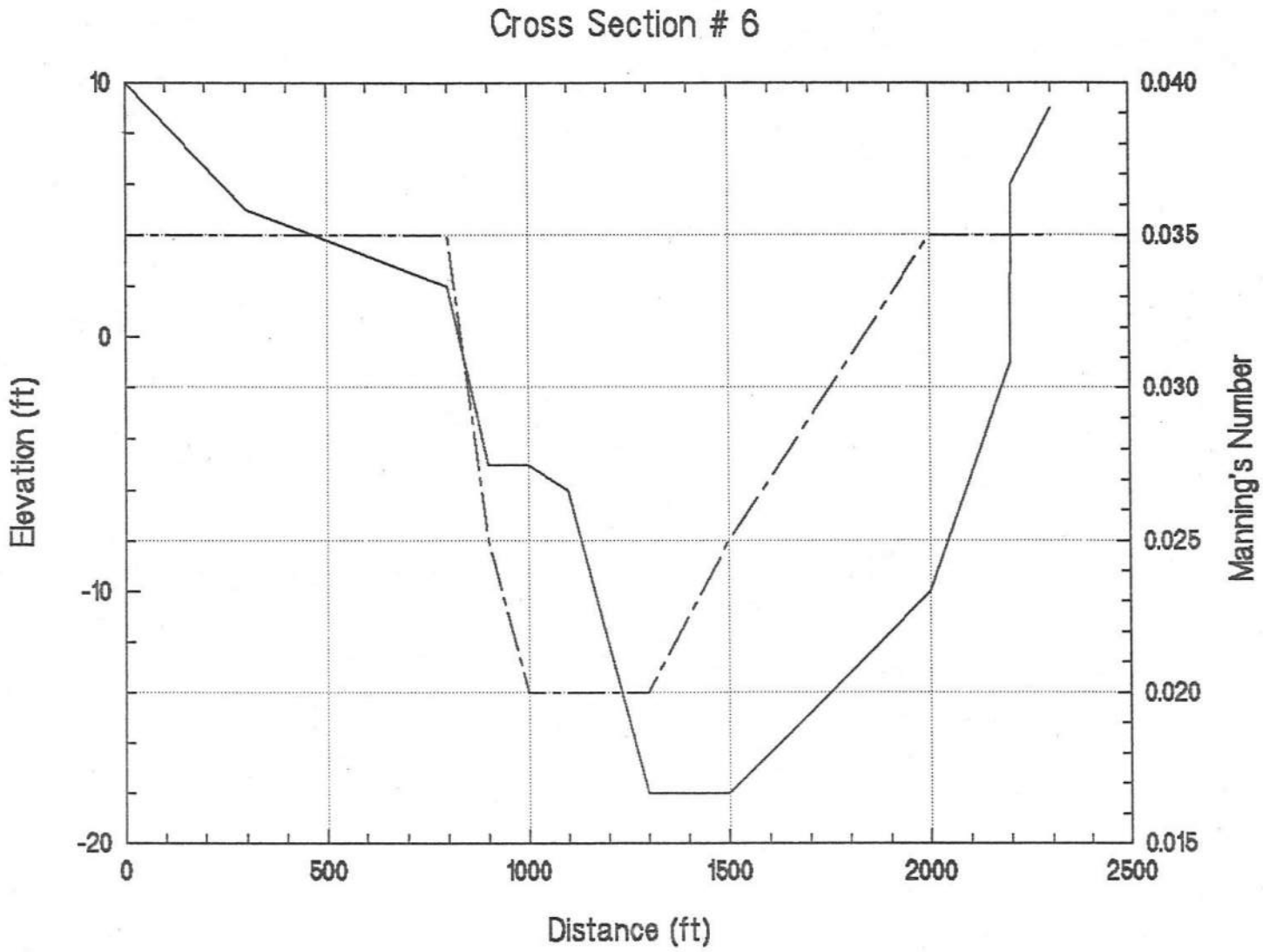
Cross Section # 6
Elevation (ft)
Manning's Number
Distance (ft)
10
0
-10
-20
0.040
0.035
0.030
0.025
0.020
0.015
0
500
1000
1500
2000
2500

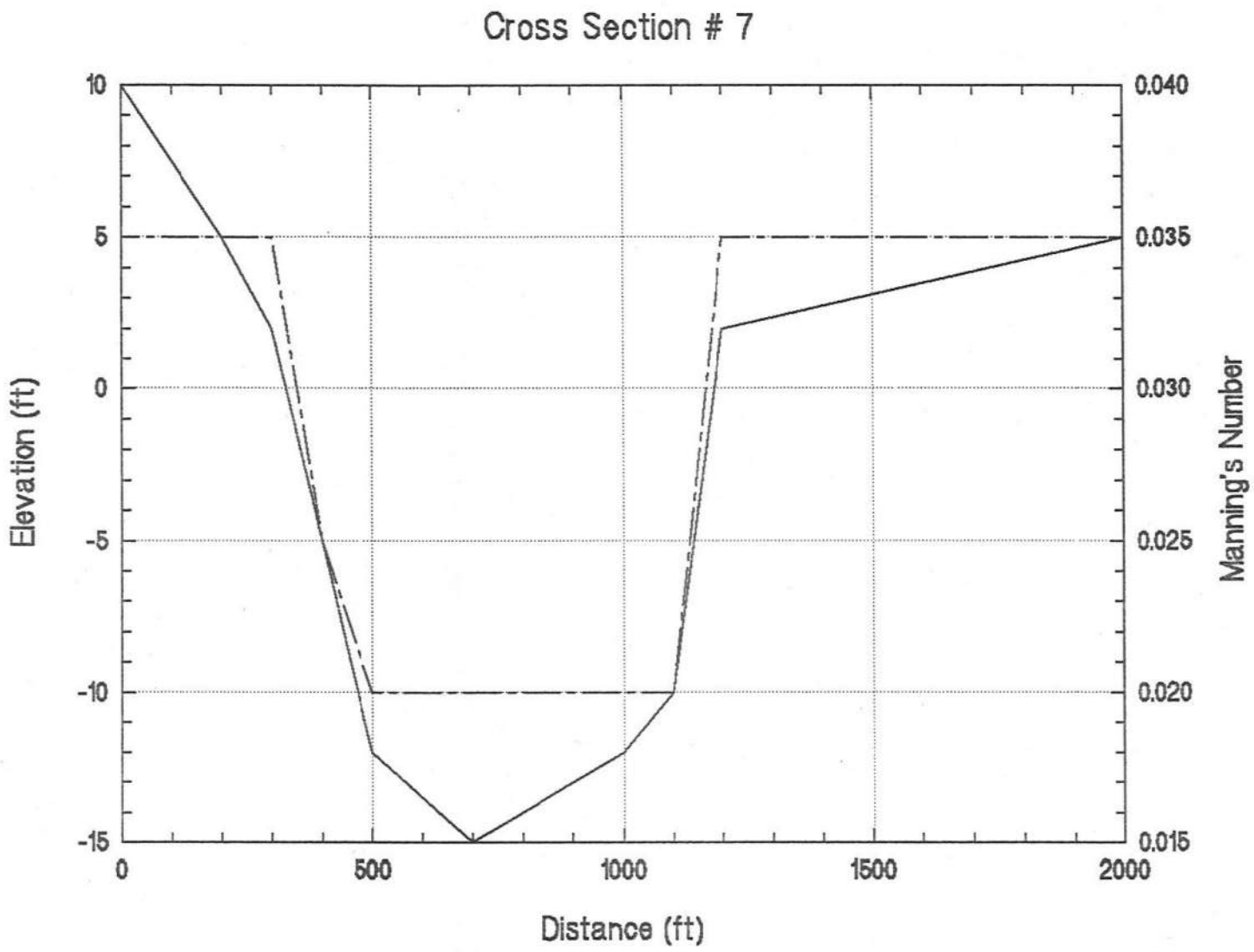
Cross Section # 7
Elevation (ft)
Manning's Number
Distance (ft)
10
5
0
-5
-10
-15
0.040
0.035
0.030
0.025
0.020
0.015
0
500
1000
1500
2000

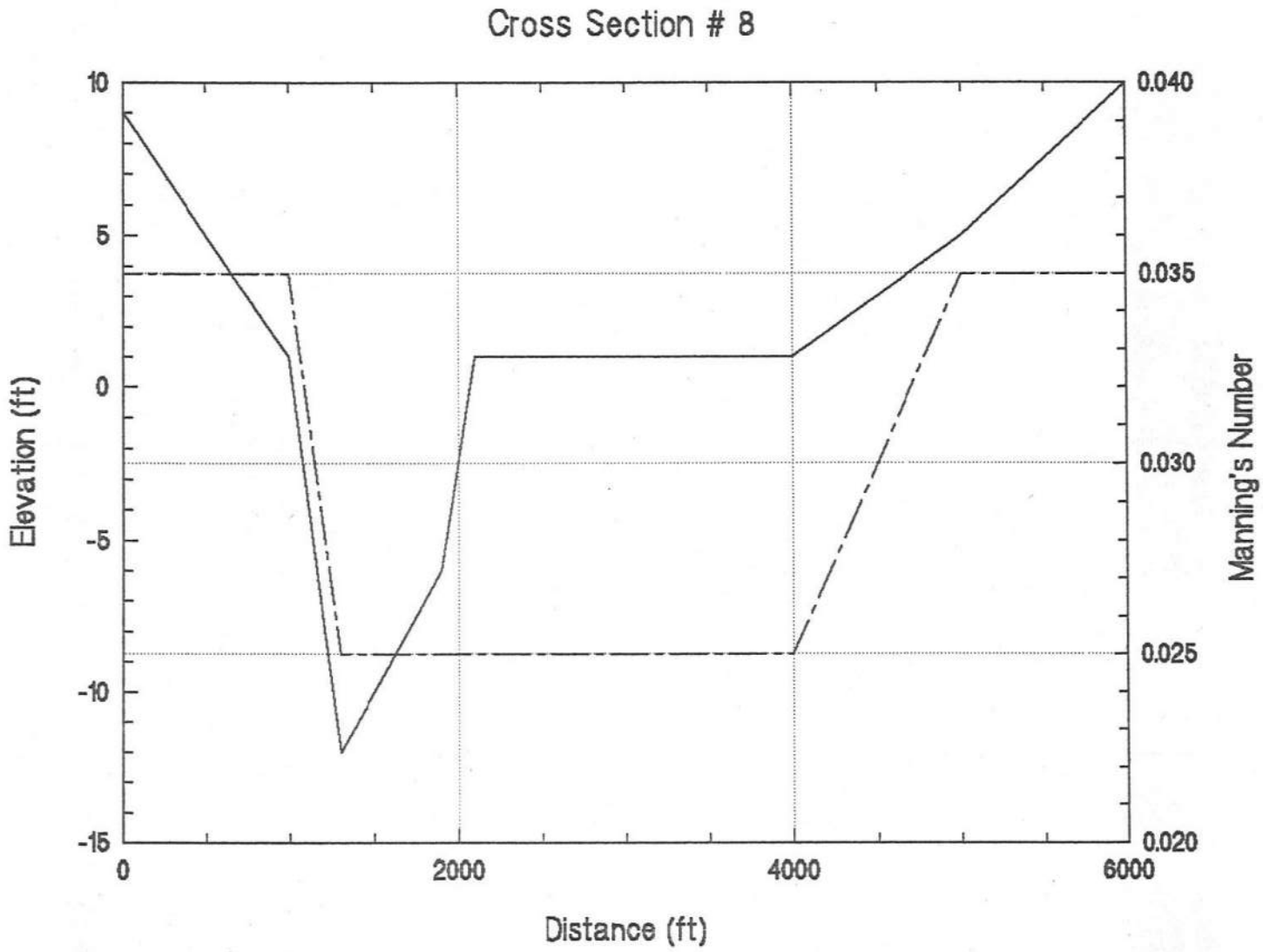
Cross Section # 8
Elevation (ft)
Manning's Number
Distance (ft)
10
5
0
-5
-10
-15
0.040
0.035
0.030
0.025
0.020
0
2000
4000
6000

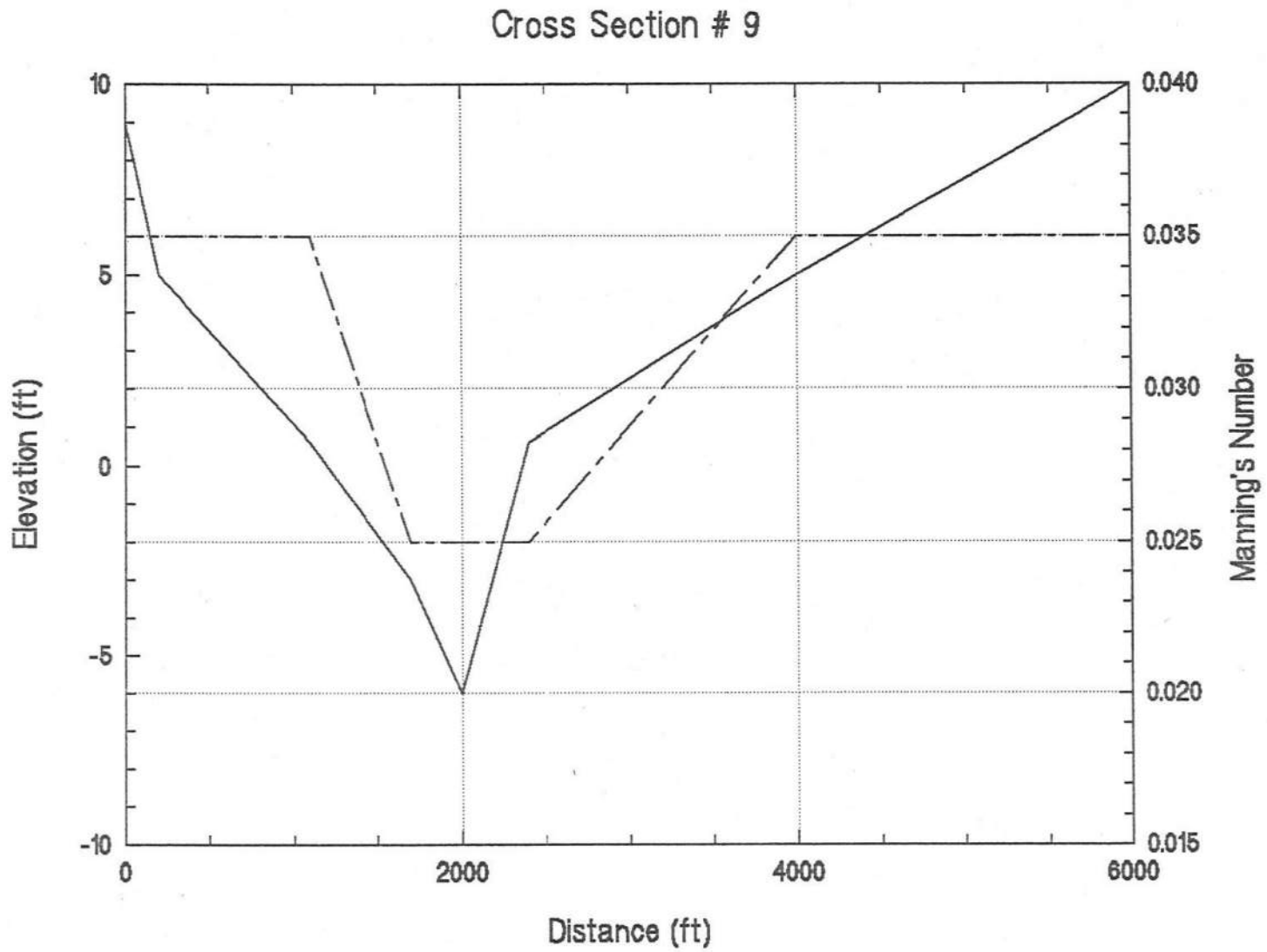
Cross Section # 9
Elevation (ft)
Manning's Number
Distance (ft)
10
5
0
-5
-10
0.040
0.035
0.030
0.025
0.020
0.015
0
2000
4000
6000

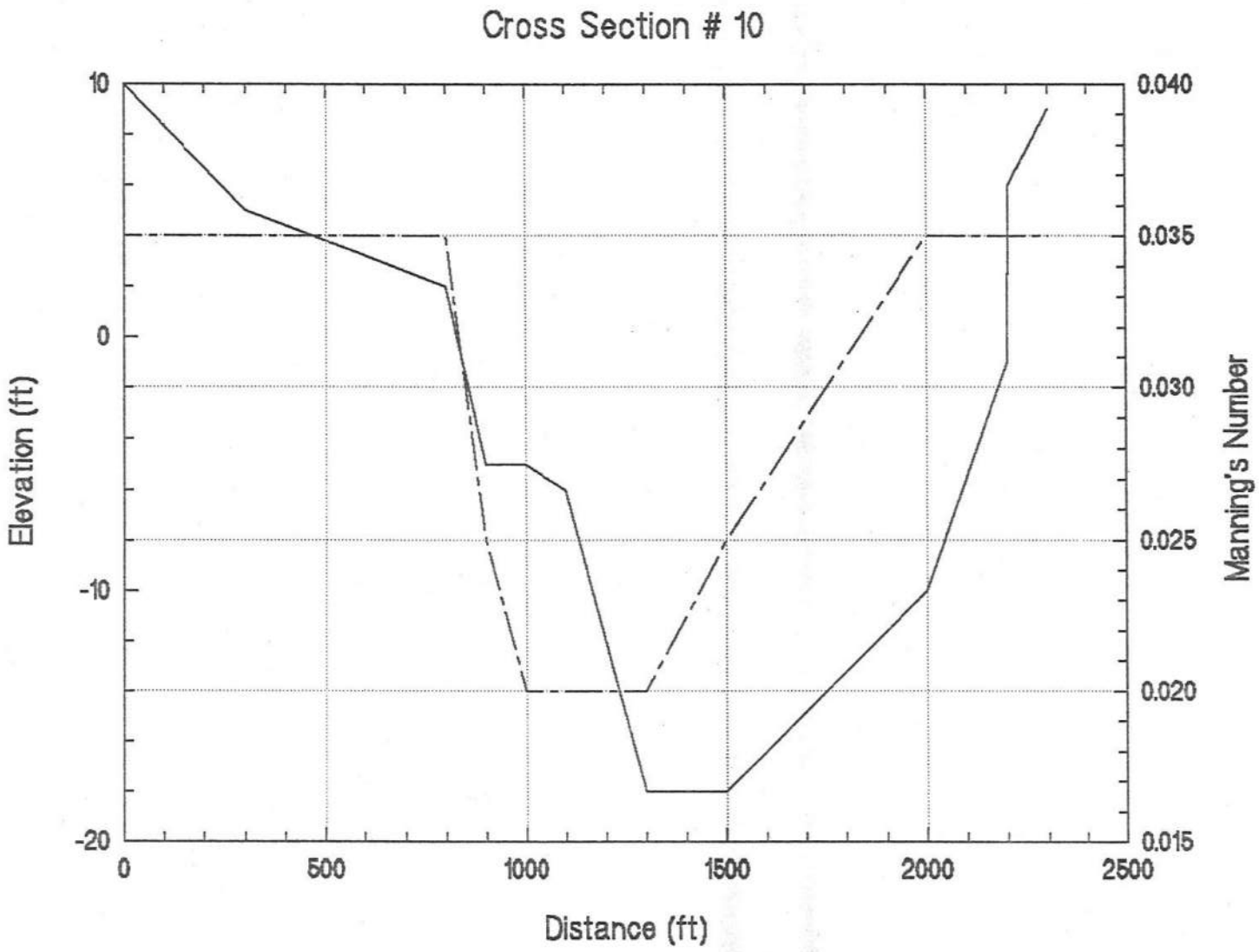
Cross Section # 10
Elevation (ft)
Manning's Number
Distance (ft)
10
0
-10
-20
0.040
0.035
0.030
0.025
0.020
0.015
0
500
1000
1500
2000
2500

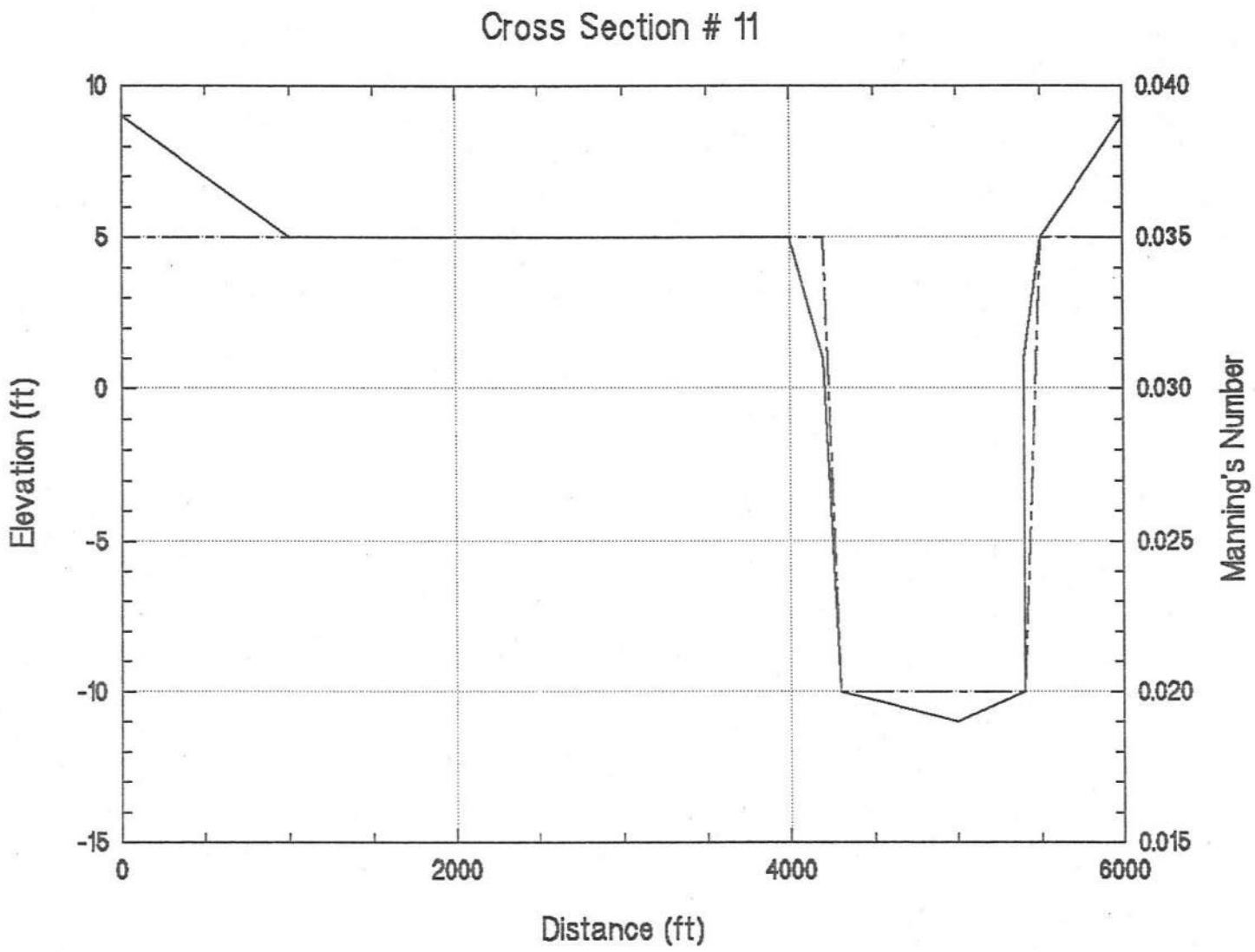
Cross Section # 11
Elevation (ft)
Manning's Number
Distance (ft)
10
5
0
-5
-10
-15
0.040
0.035
0.030
0.025
0.020
0.015
0
2000
4000
6000

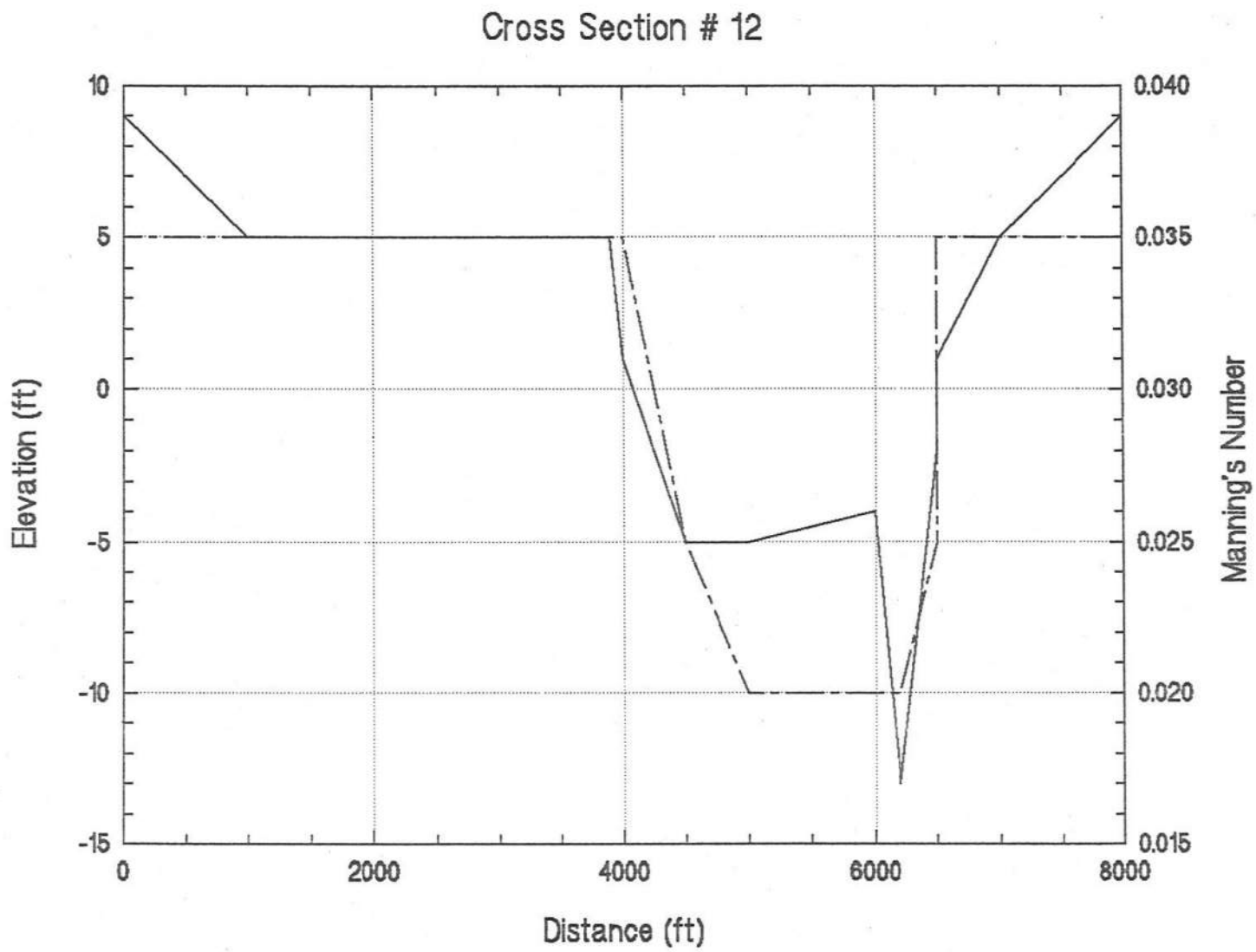
Cross Section # 12
Elevation (ft)
Manning's Number
Distance (ft)
10
5
0
-5
-10
-15
0.040
0.035
0.030
0.025
0.020
0.015
0
2000
4000
6000
8000

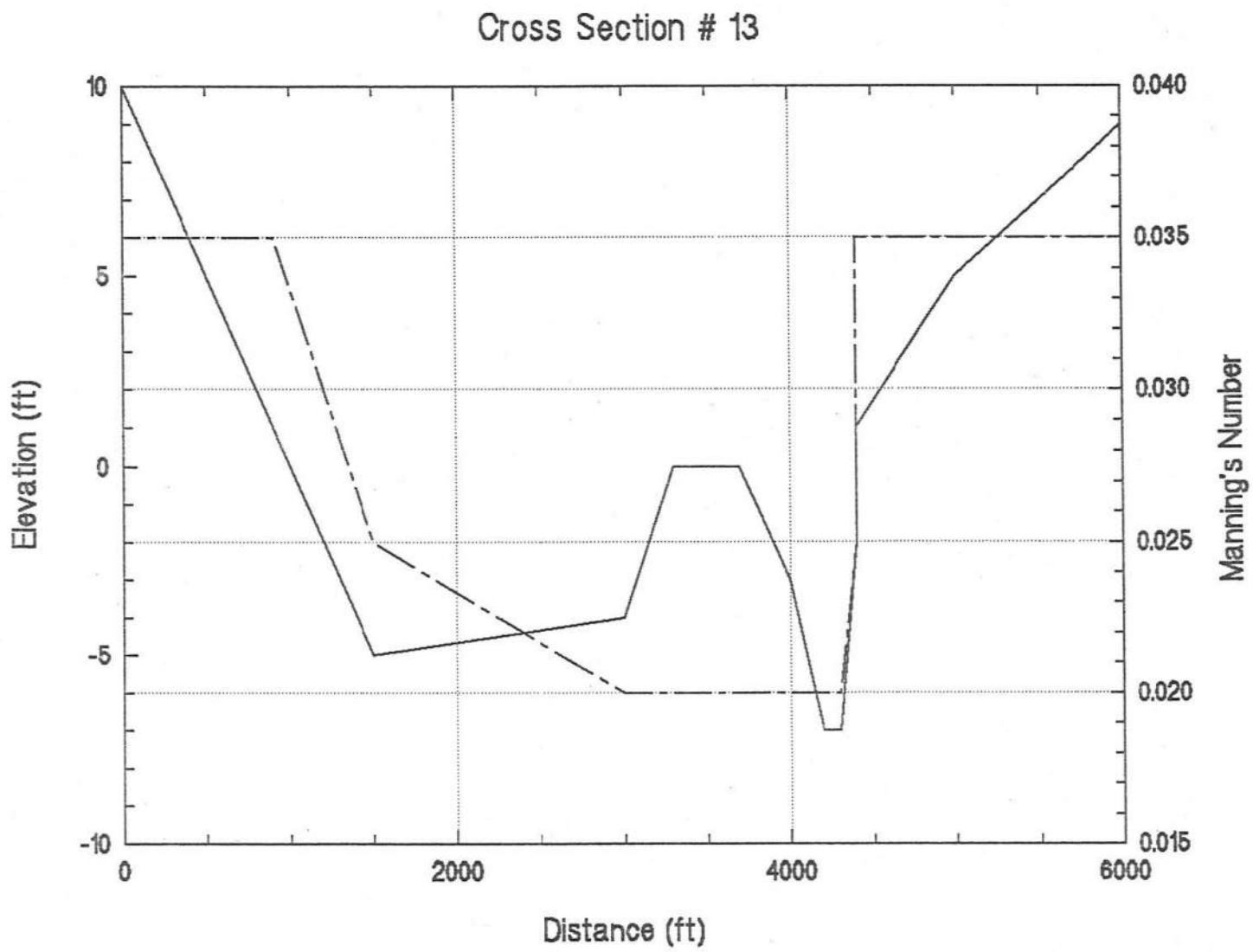
Cross Section # 13
Elevation (ft)
Manning's Number
Distance (ft)
10
5
0
-5
-10
0.040
0.035
0.030
0.025
0.020
0.015
0
2000
4000
6000

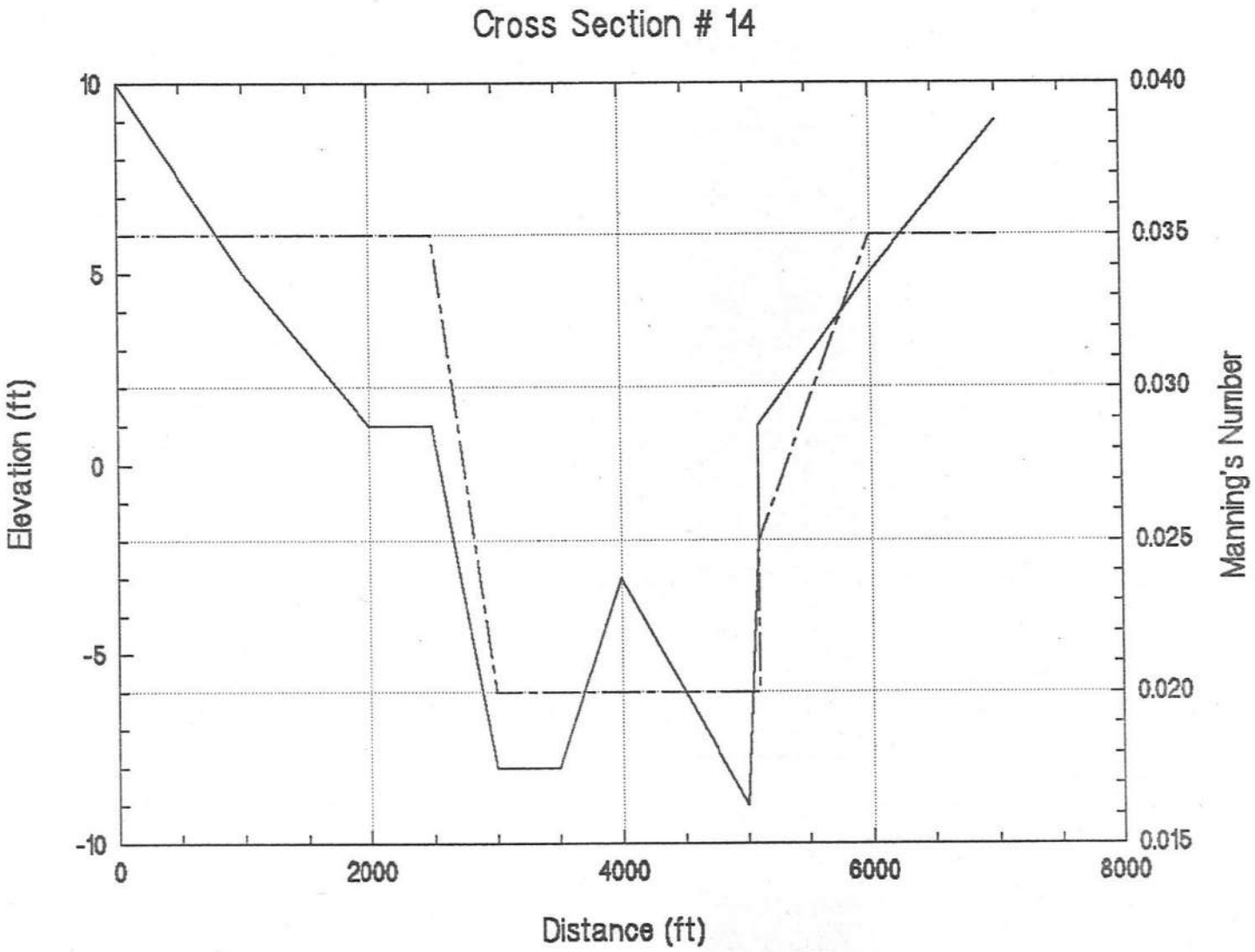
Cross Section # 14
Elevation (ft)
Manning's Number
Distance (ft)
10
5
0
-5
-10
0.040
0.035
0.030
0.025
0.020
0.015
0
2000
4000
6000
8000

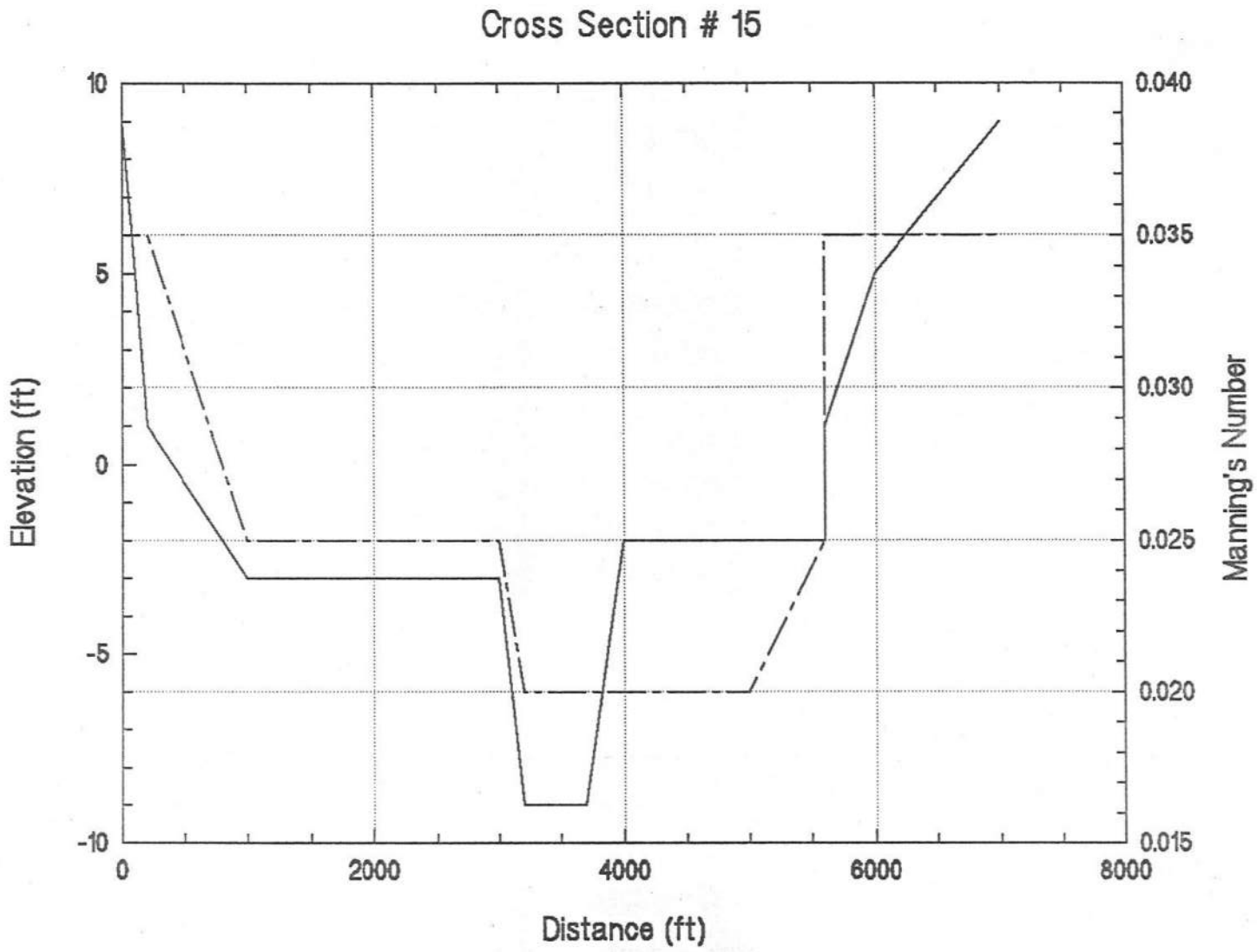
Cross Section # 15
Elevation (ft)
Manning's Number
Distance (ft)
10
5
0
-5
-10
0.040
0.035
0.030
0.025
0.020
0.015
0
2000
4000
6000
8000

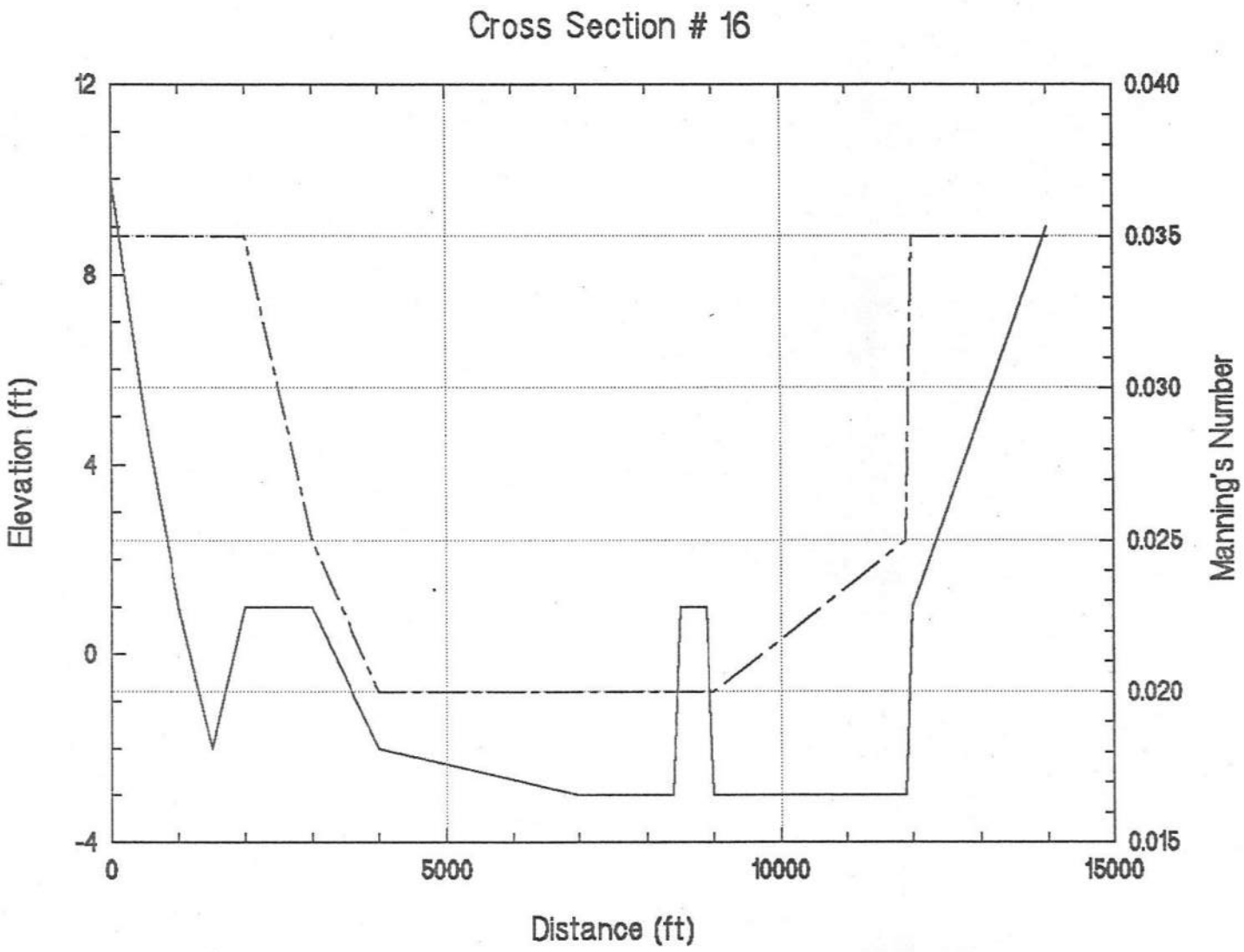
Cross Section # 16
Elevation (ft)
Manning's Number
Distance (ft)
12
8
4
0
-4
0.040
0.035
0.030
0.025
0.020
0.015
0
5000
10000
15000

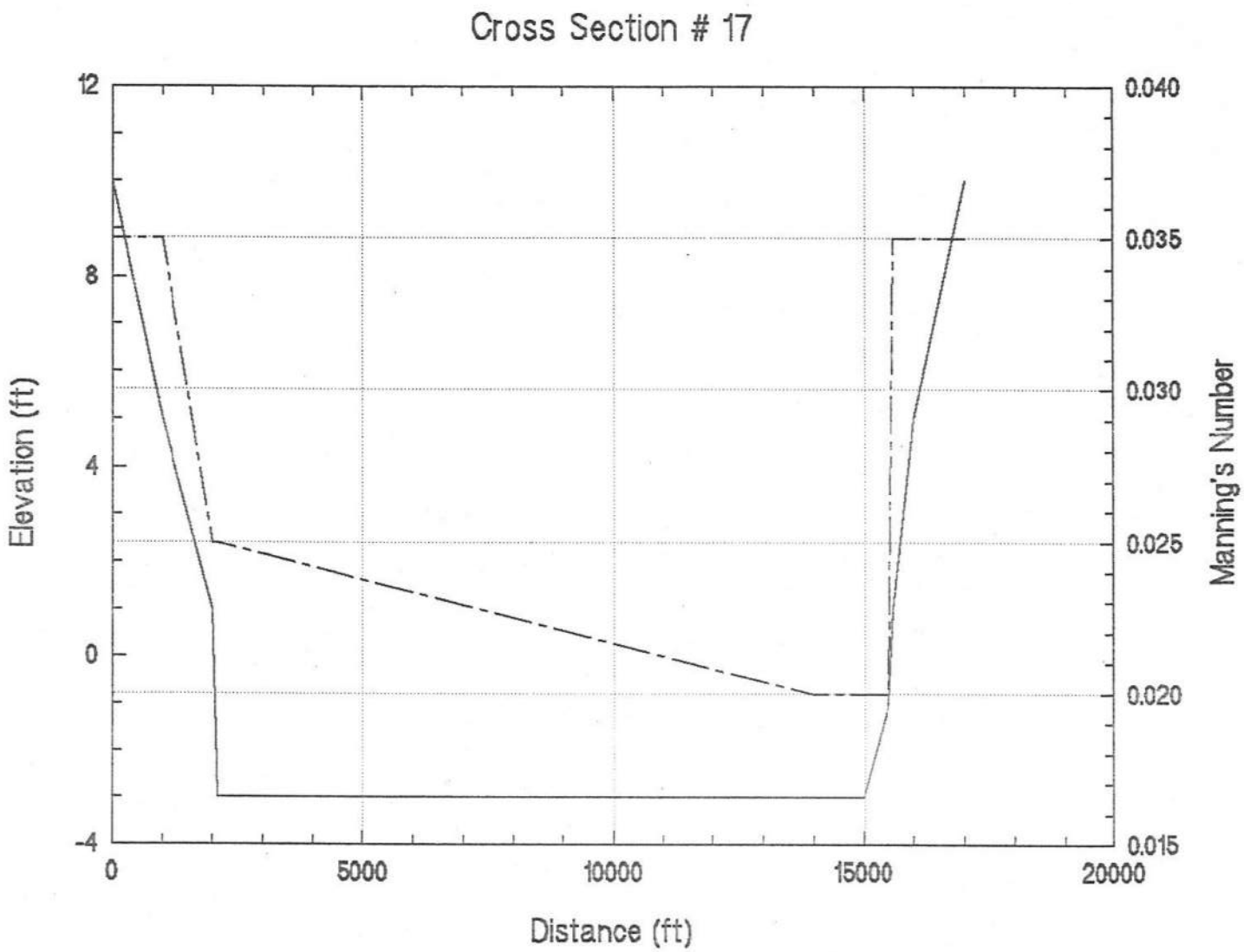
Cross Section # 17
Elevation (ft)
Manning's Number
Distance (ft)
12
8
4
0
-4
0.040
0.035
0.030
0.025
0.020
0.015
0
5000
10000
15000
20000

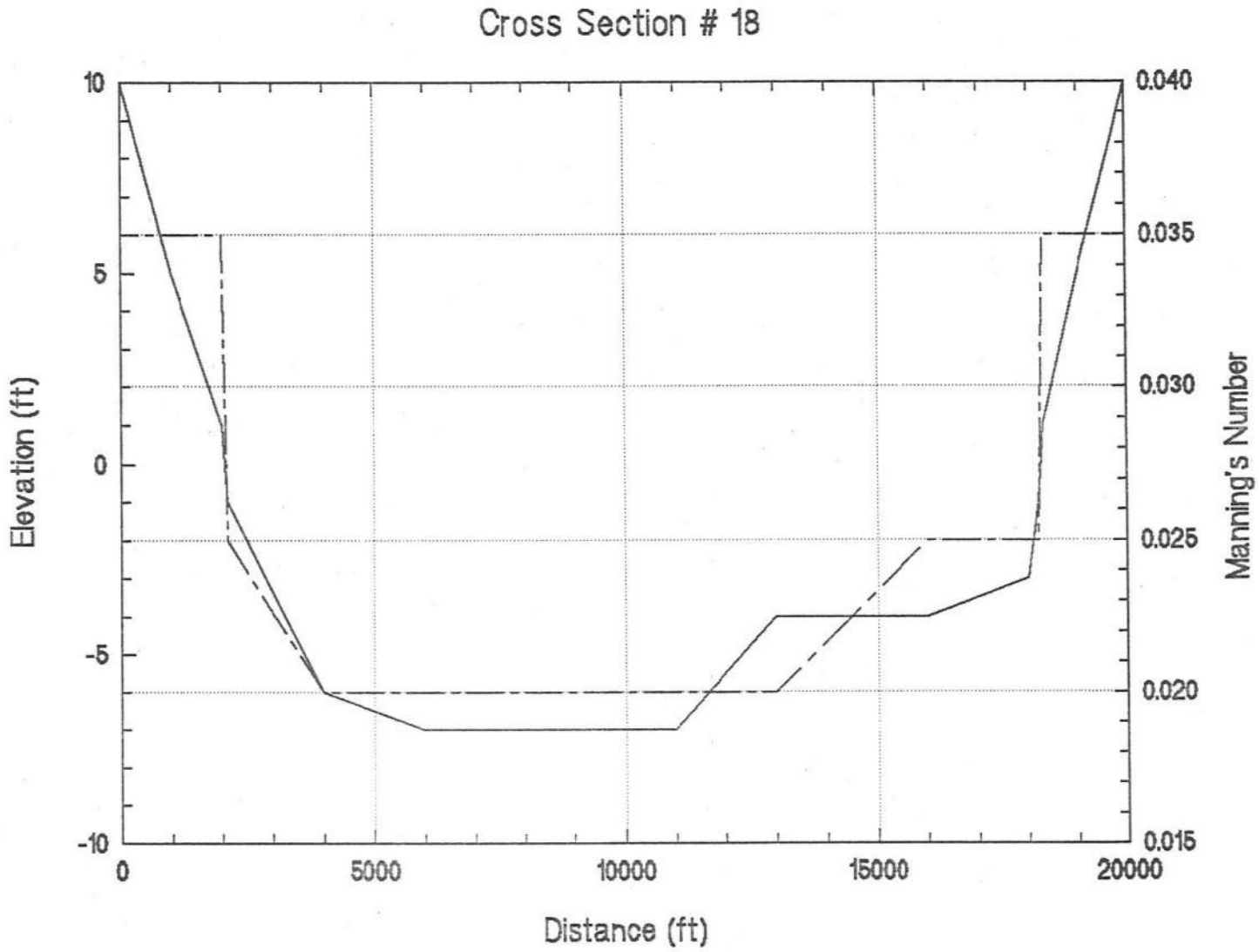
Cross Section # 18
Elevation (ft)
Manning's Number
Distance (ft)
10
5
0
-5
-10
0.040
0.035
0.030
0.025
0.020
0.015
0
5000
10000
15000
20000

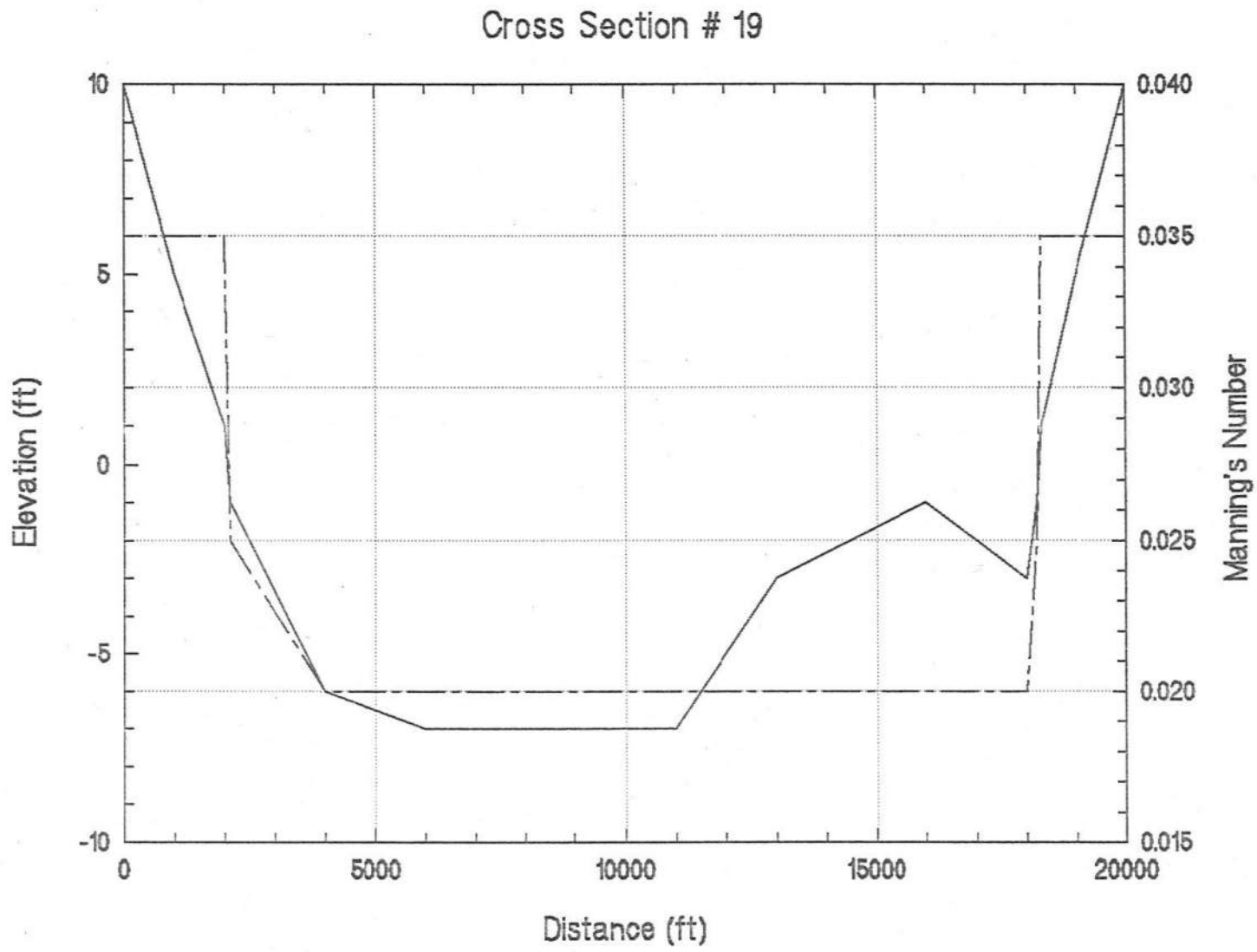
Cross Section # 19
Elevation (ft)
Manning's Number
Distance (ft)
10
5
0
-5
-10
0.040
0.035
0.030
0.025
0.020
0.015
0
5000
10000
15000
20000

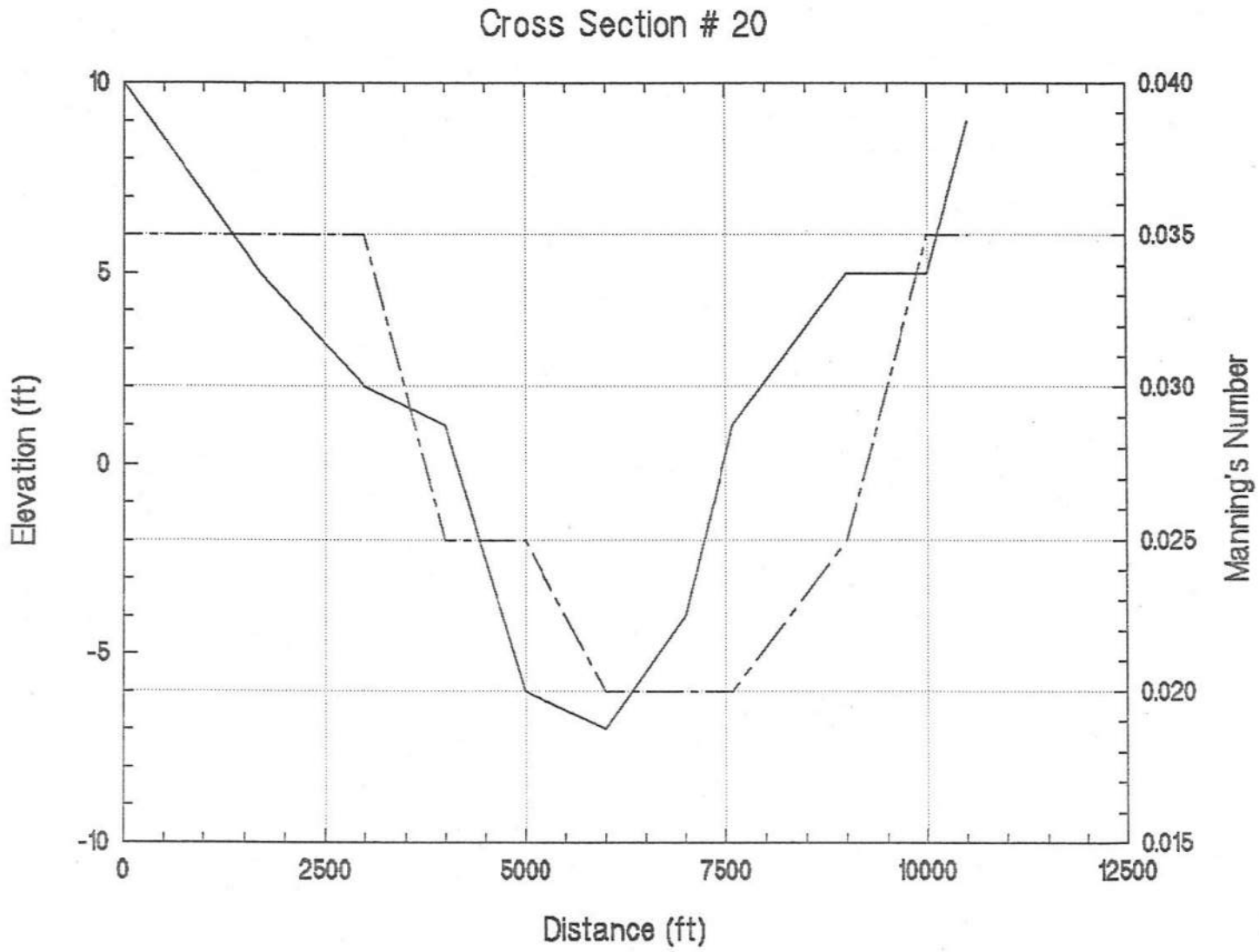
Cross Section # 20
Elevation (ft)
Manning's Number
Distance (ft)
10
5
0
-5
-10
0.040
0.035
0.030
0.025
0.020
0.015
0
2500
5000
7500
10000
12500

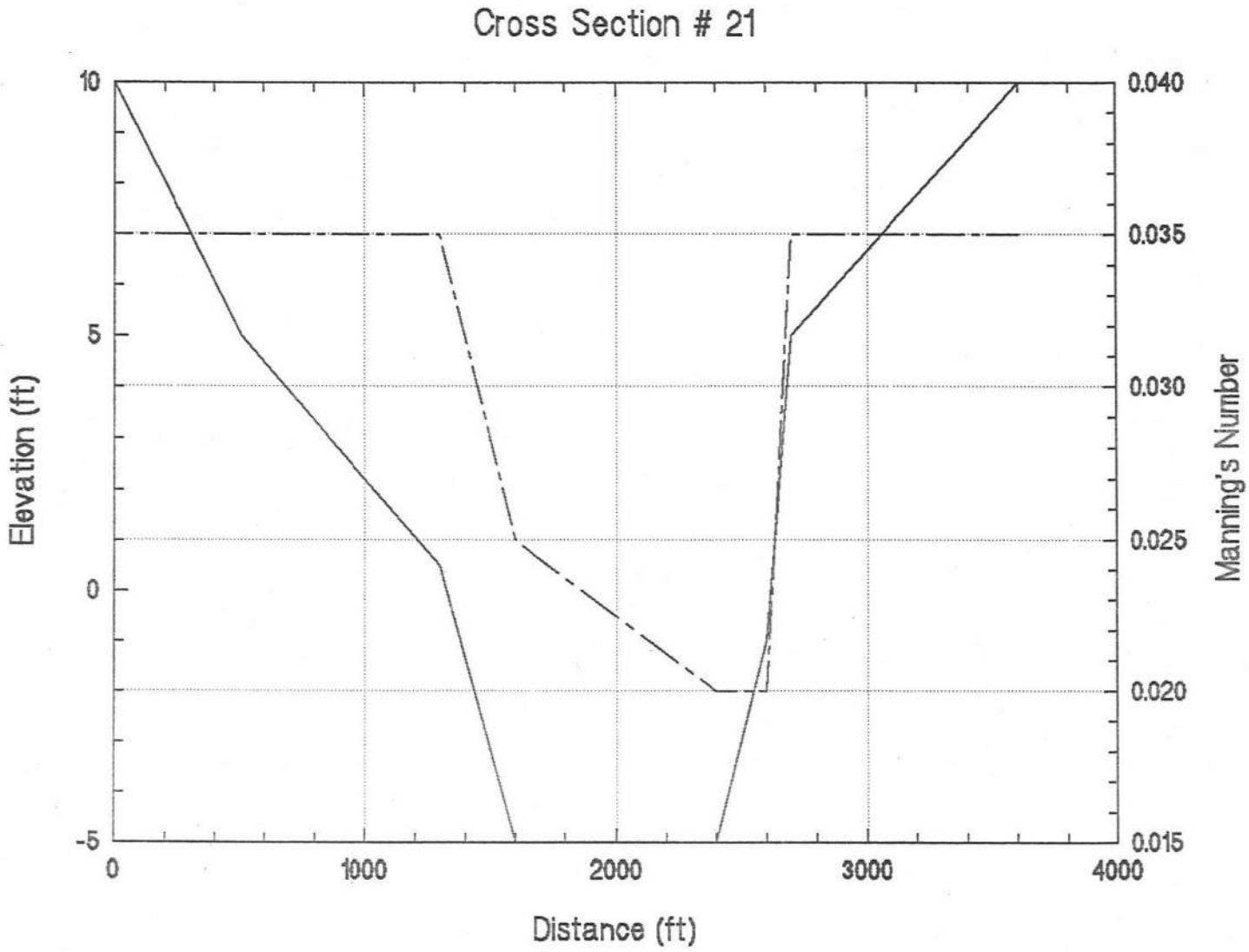
Cross Section # 21
Elevation (ft)
Manning's Number
Distance (ft)
10
5
0
-5
0.040
0.035
0.030
0.025
0.020
0.015
0
1000
2000
3000
4000

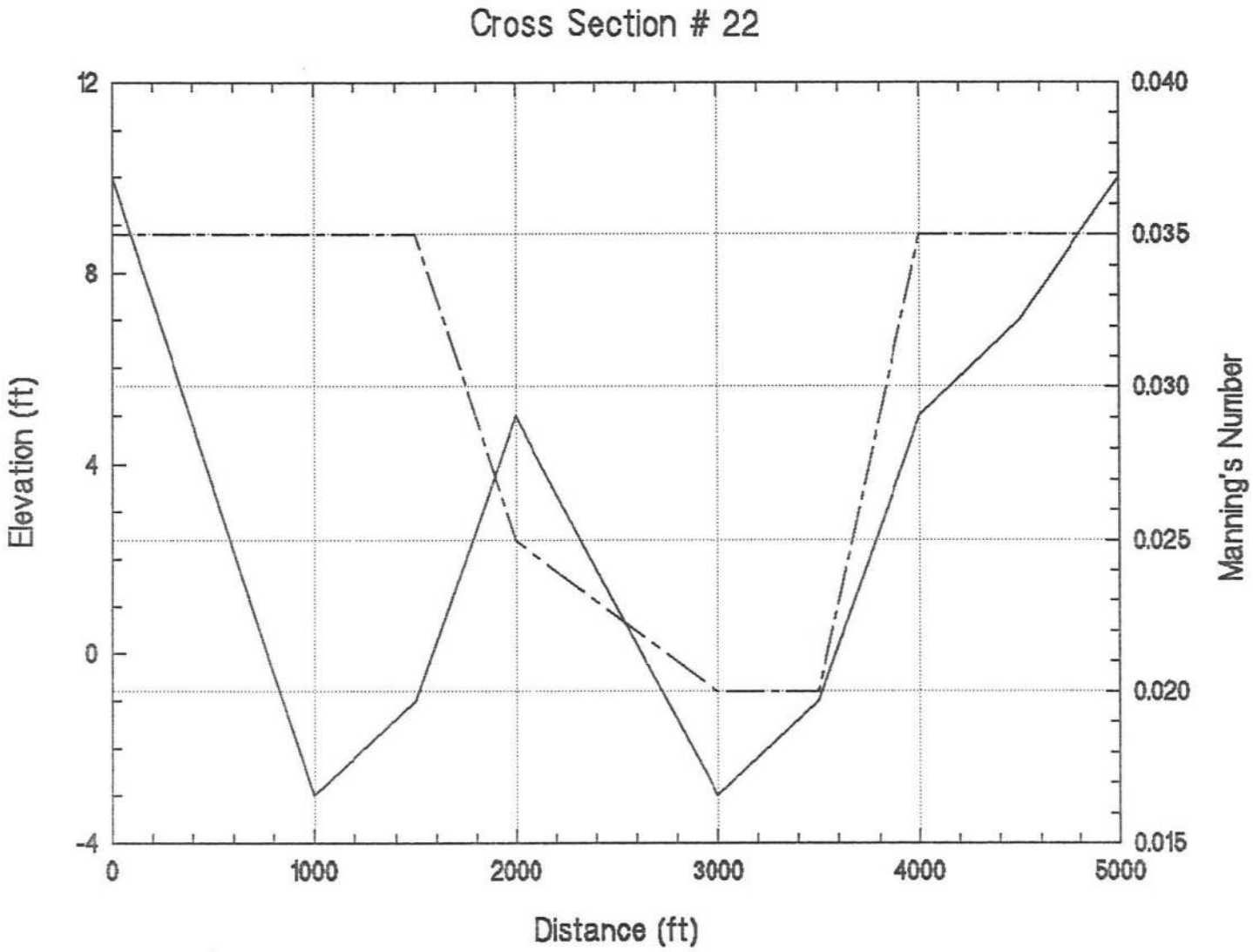
Cross Section # 22
Elevation (ft)
Manning's Number
Distance (ft)
12
8
4
0
-4
0.040
0.035
0.030
0.025
0.020
0.015
0
1000
2000
3000
4000
5000

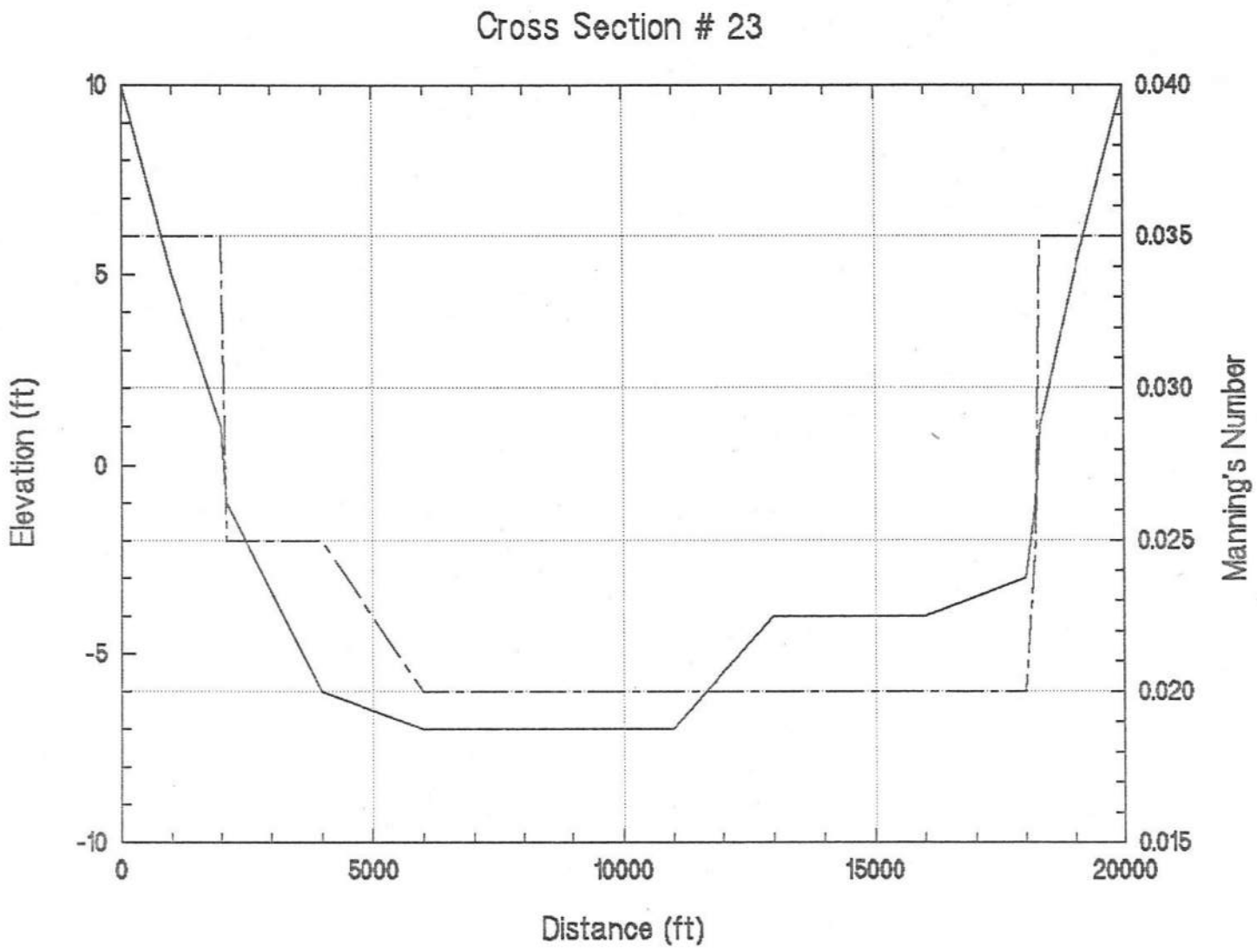
Cross Section # 23
Elevation (ft)
Manning's Number
Distance (ft)
10
5
0
-5
-10
0.040
0.035
0.030
0.025
0.020
0.015
0
5000
10000
15000
20000

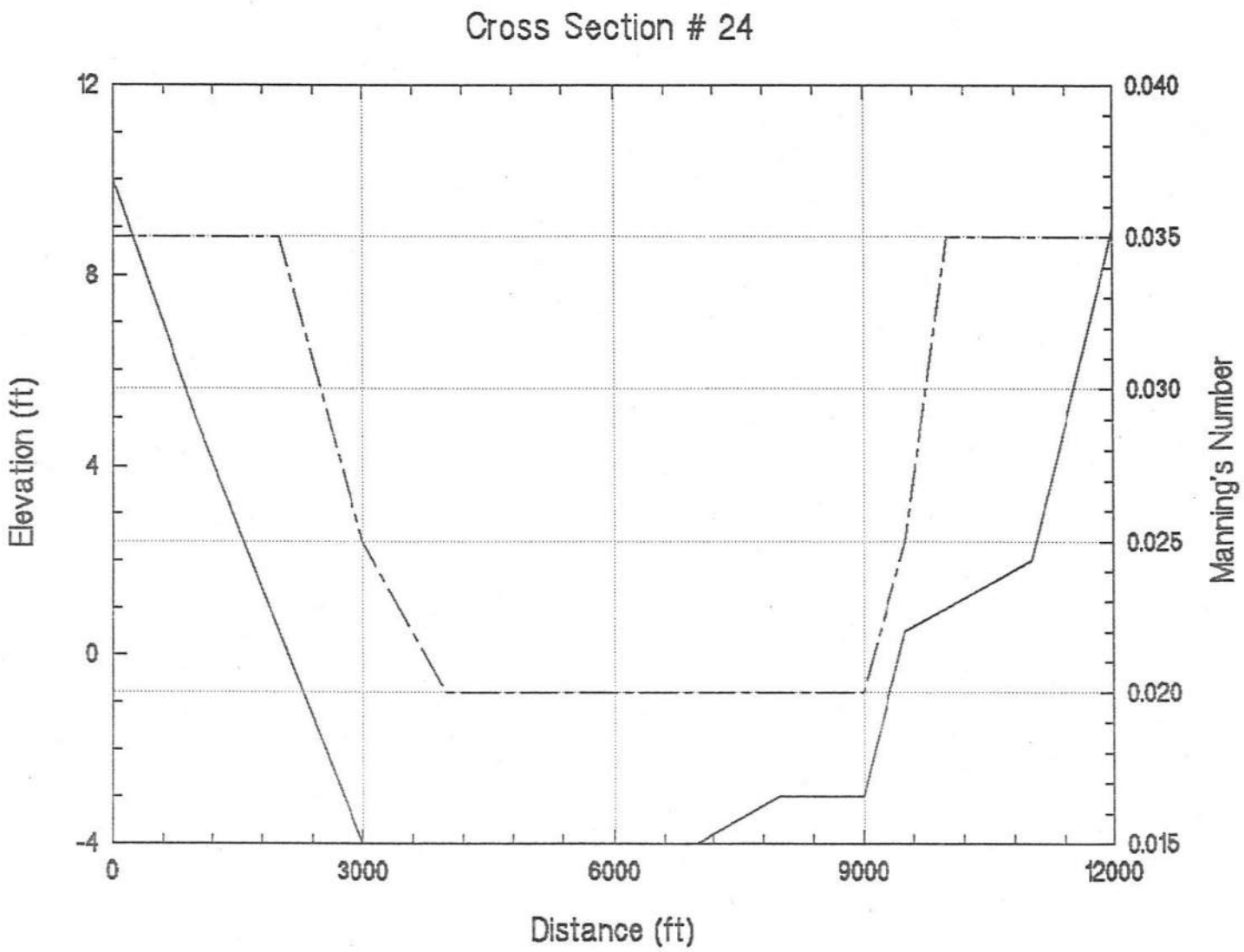
Cross Section # 24
Elevation (ft)
Manning's Number
Distance (ft)
12
8
4
0
-4
0.040
0.035
0.030
0.025
0.020
0.015
0
3000
6000
9000
12000

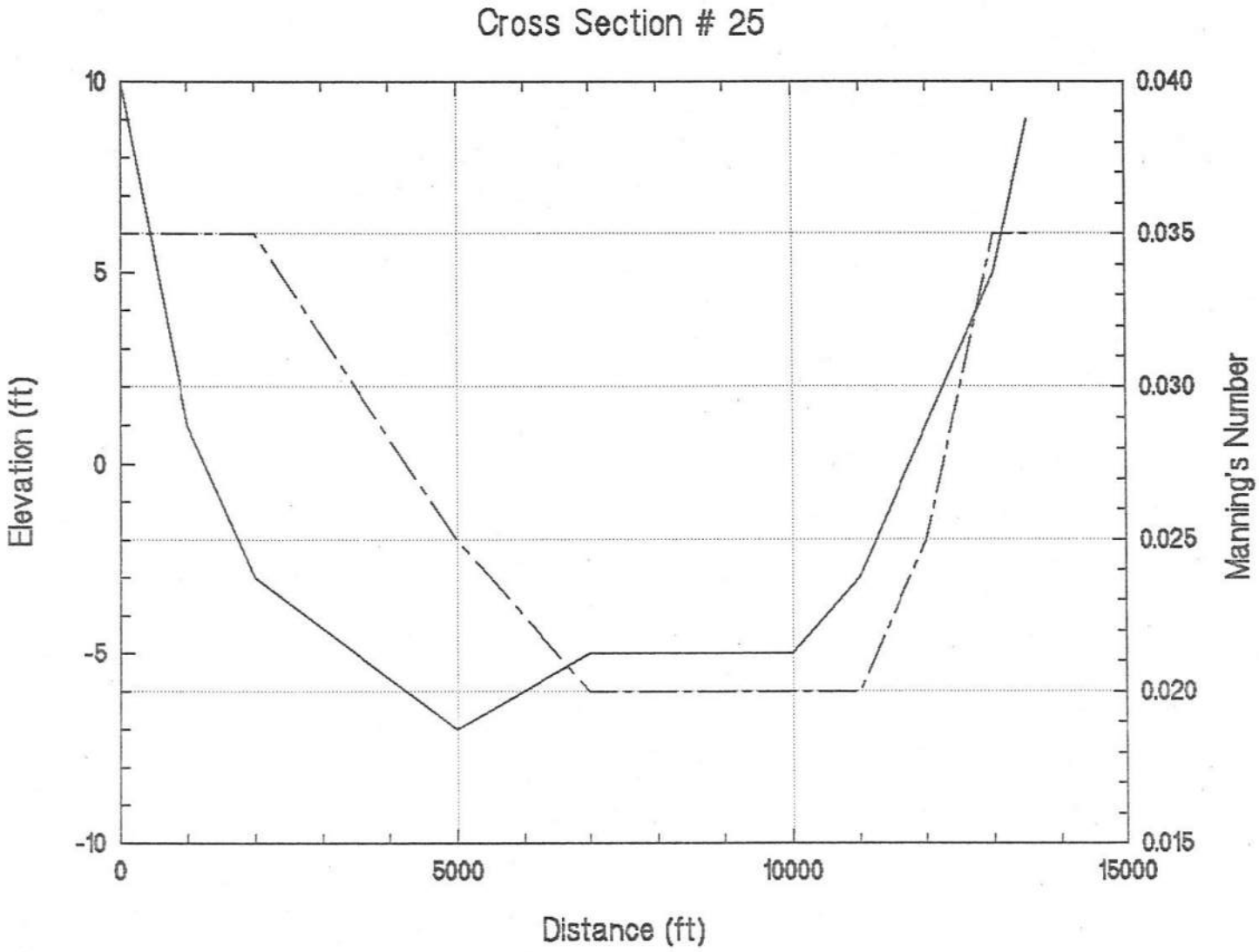
Cross Section # 25
Elevation (ft)
Manning's Number
Distance (ft)
10
5
0
-5
-10
0.040
0.035
0.030
0.025
0.020
0.015
0
5000
10000
15000

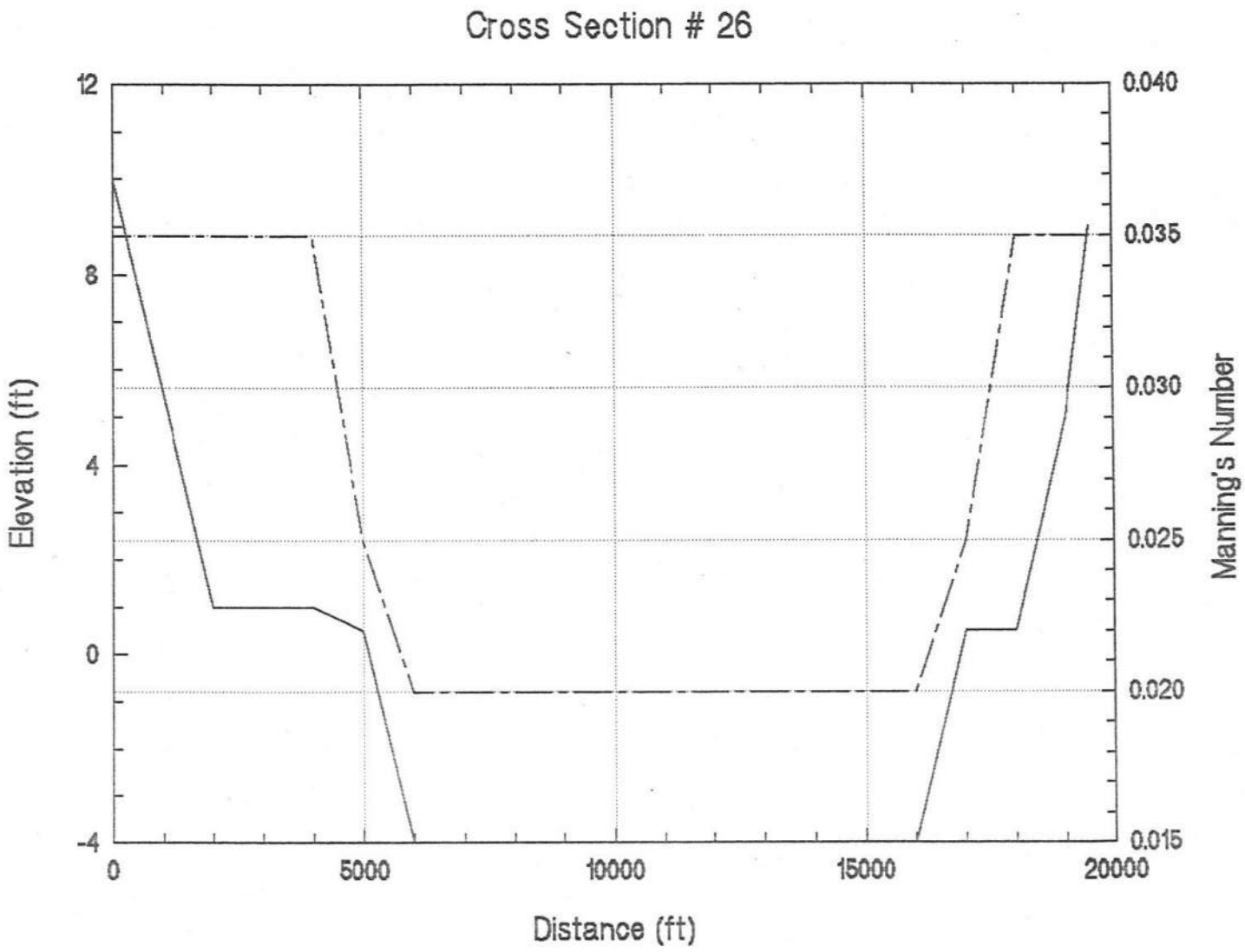
Cross Section # 26
Elevation (ft)
Manning's Number
Distance (ft)
12
8
4
0
-4
0.040
0.035
0.030
0.025
0.020
0.015
0
5000
10000
15000
20000

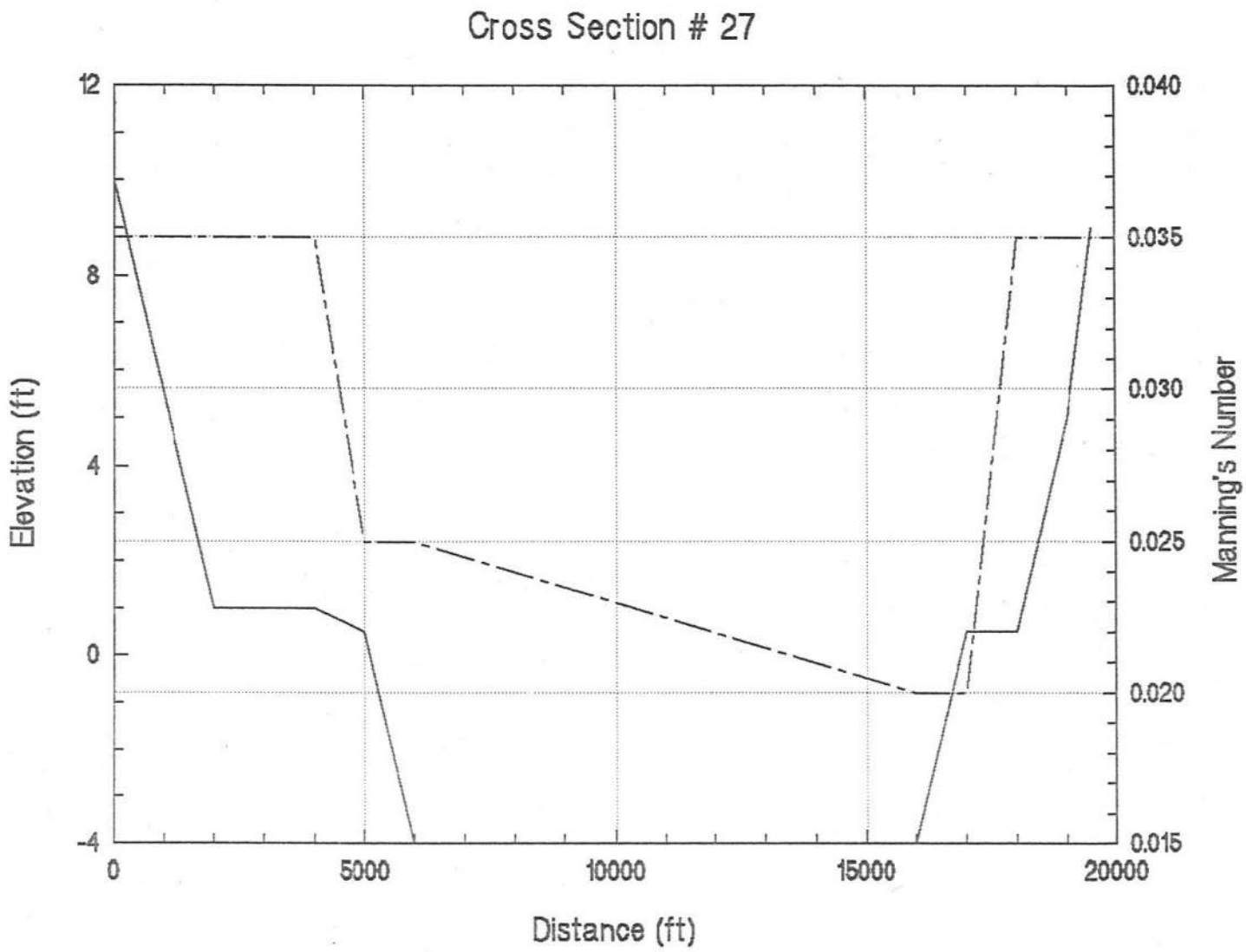
Cross Section # 27
Elevation (ft)
Manning's Number
Distance (ft)
12
8
4
0
-4
0.040
0.035
0.030
0.025
0.020
0.015
0
5000
10000
15000
20000

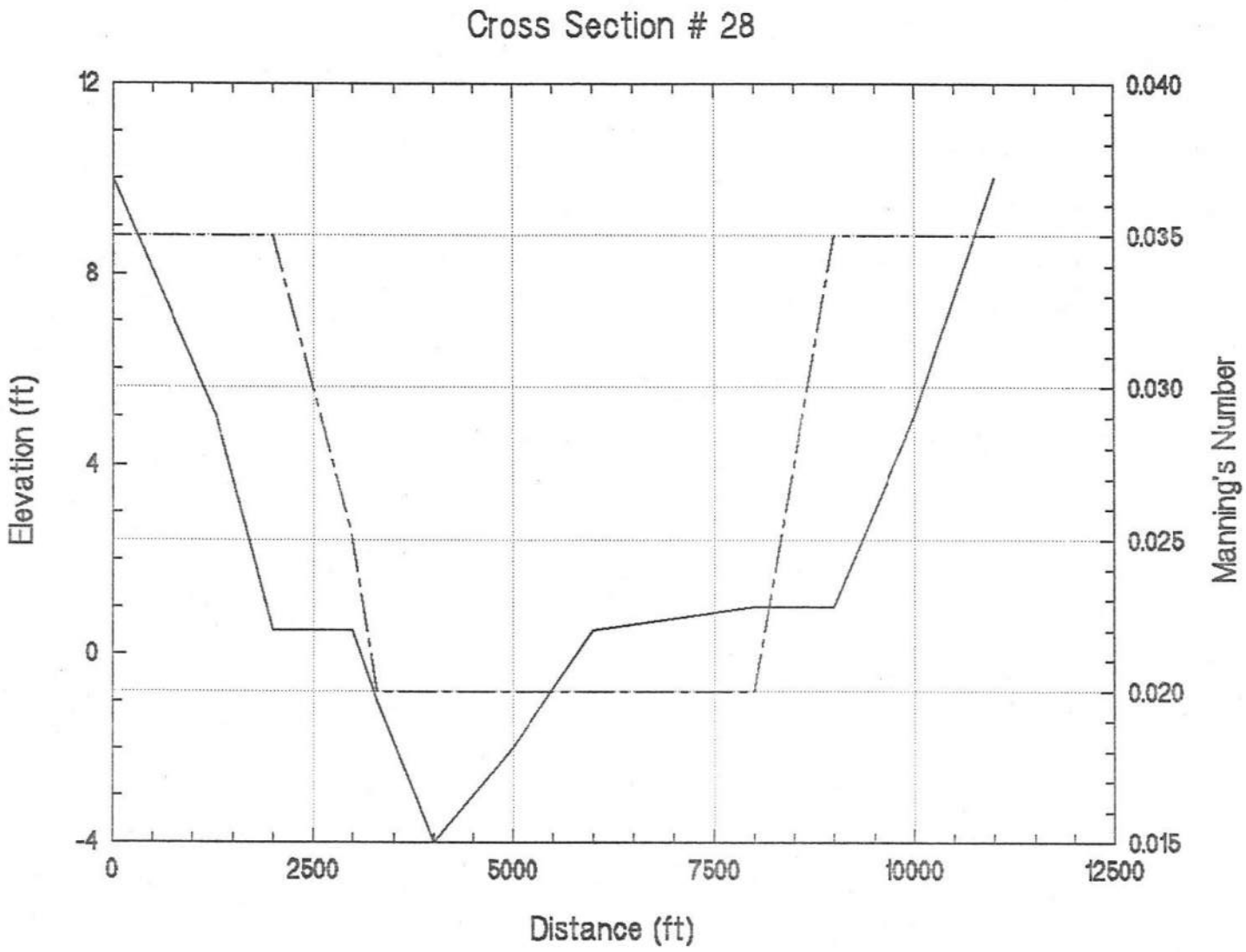
Cross Section # 28
Elevation (ft)
Manning's Number
Distance (ft)
12
8
4
0
-4
0.040
0.035
0.030
0.025
0.020
0.015
0
2500
5000
7500
10000
12500

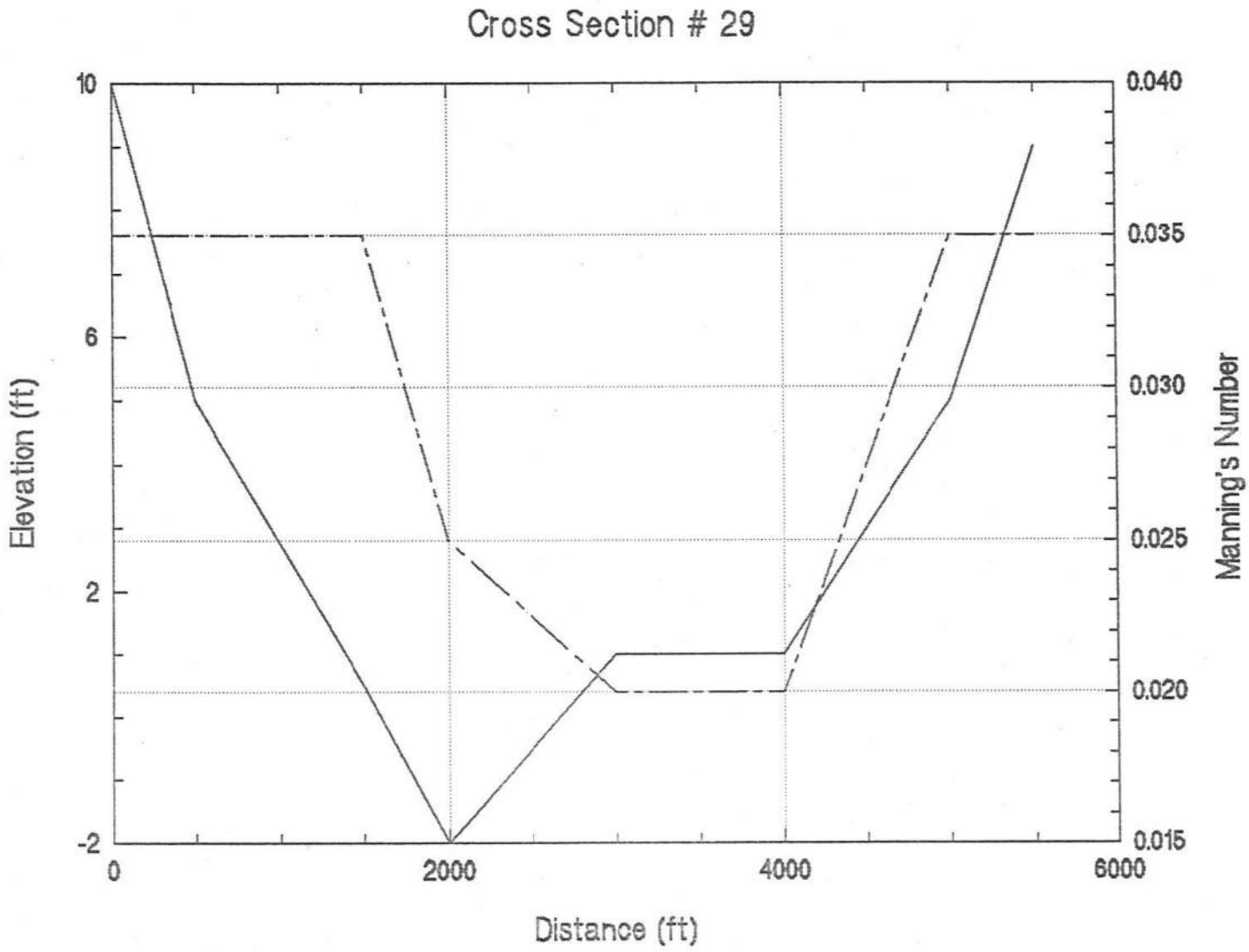
Cross Section # 29
10
6
2
-2
Elevation (ft)
0.040
0.035
0.030
0.025
0.020
0.015
Manning's Number
0
2000
4000
6000
Distance (ft)

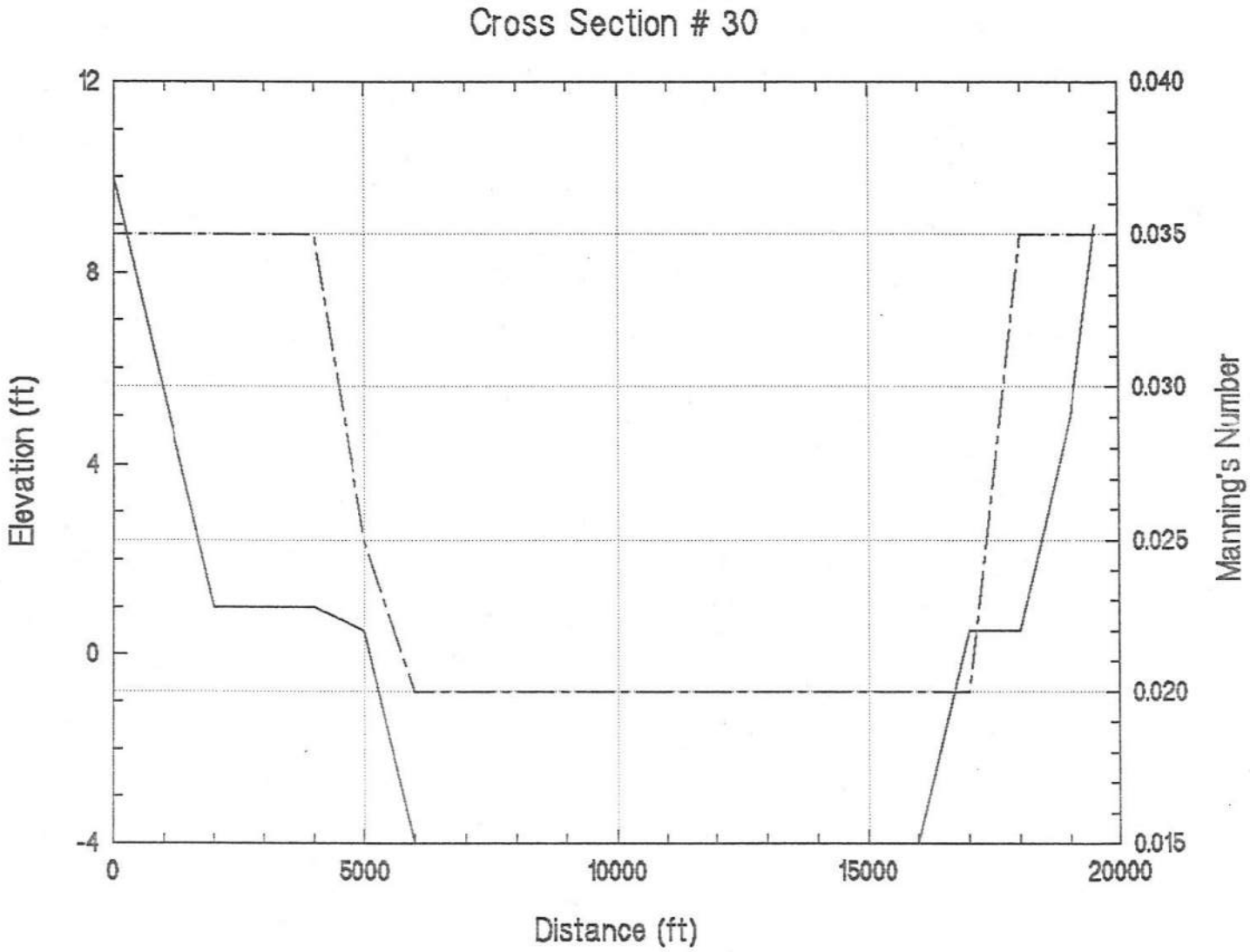
Cross Section # 30
Elevation (ft)
Manning's Number
Distance (ft)
12
8
4
0
-4
0.040
0.035
0.030
0.025
0.020
0.015
0
5000
10000
15000
20000

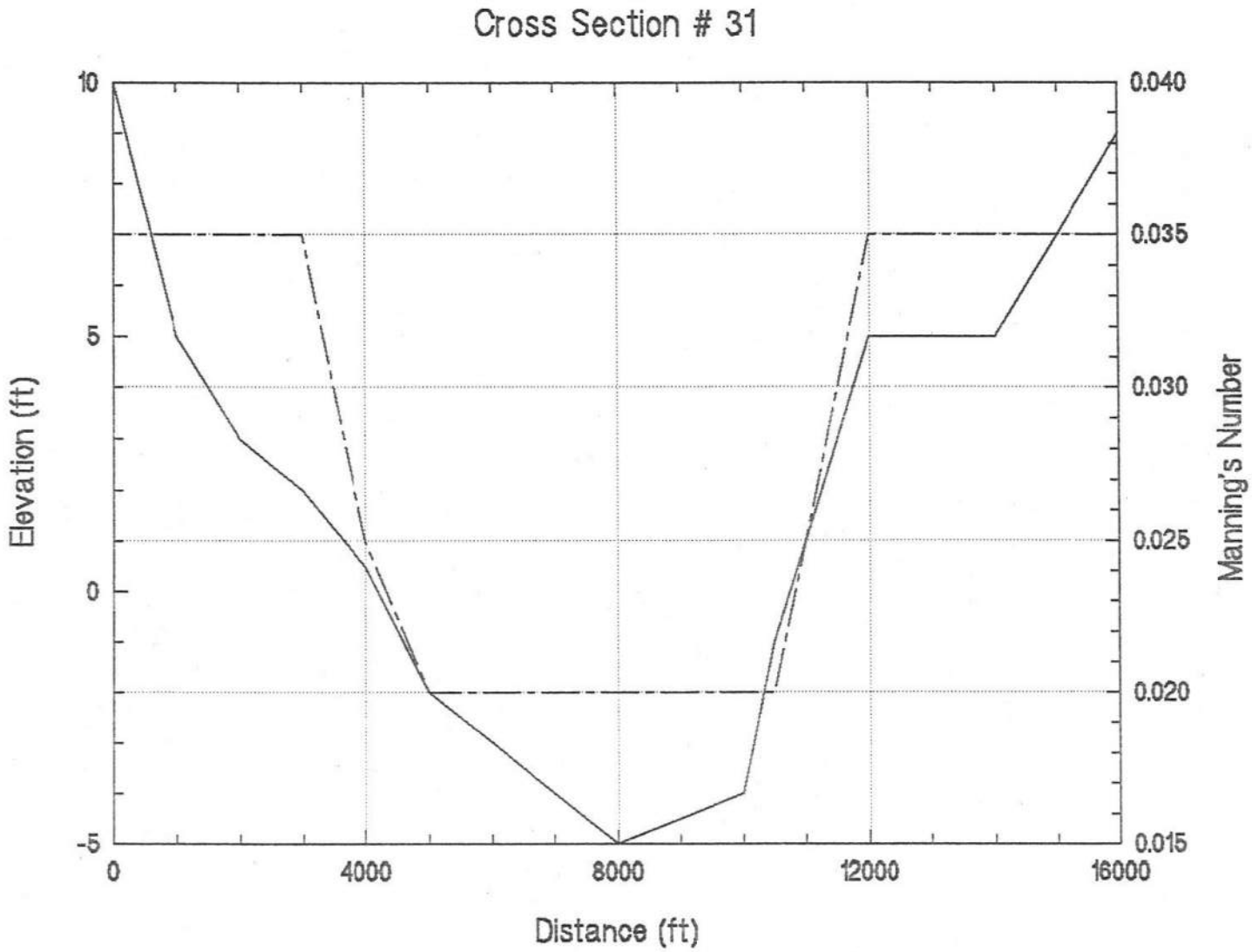
Cross Section # 31
Elevation (ft)
Manning's Number
Distance (ft)
10
5
0
-5
0.040
0.035
0.030
0.025
0.020
0.015
0
4000
8000
12000
16000

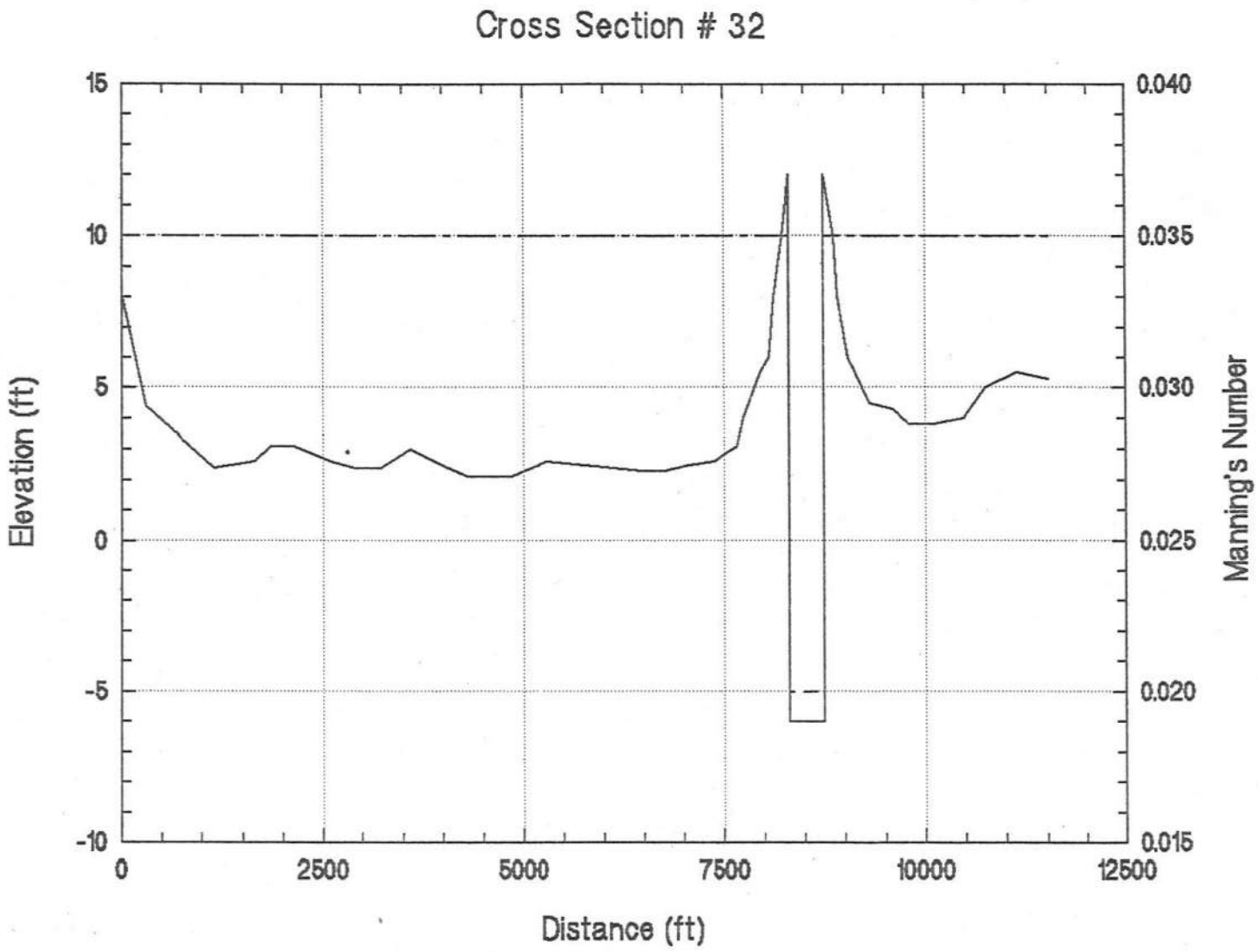
Cross Section # 32
Elevation (ft)
Manning's Number
Distance (ft)
15
10
5
0
-5
-10
0.040
0.035
0.030
0.025
0.020
0.015
0
2500
5000
7500
10000
12500

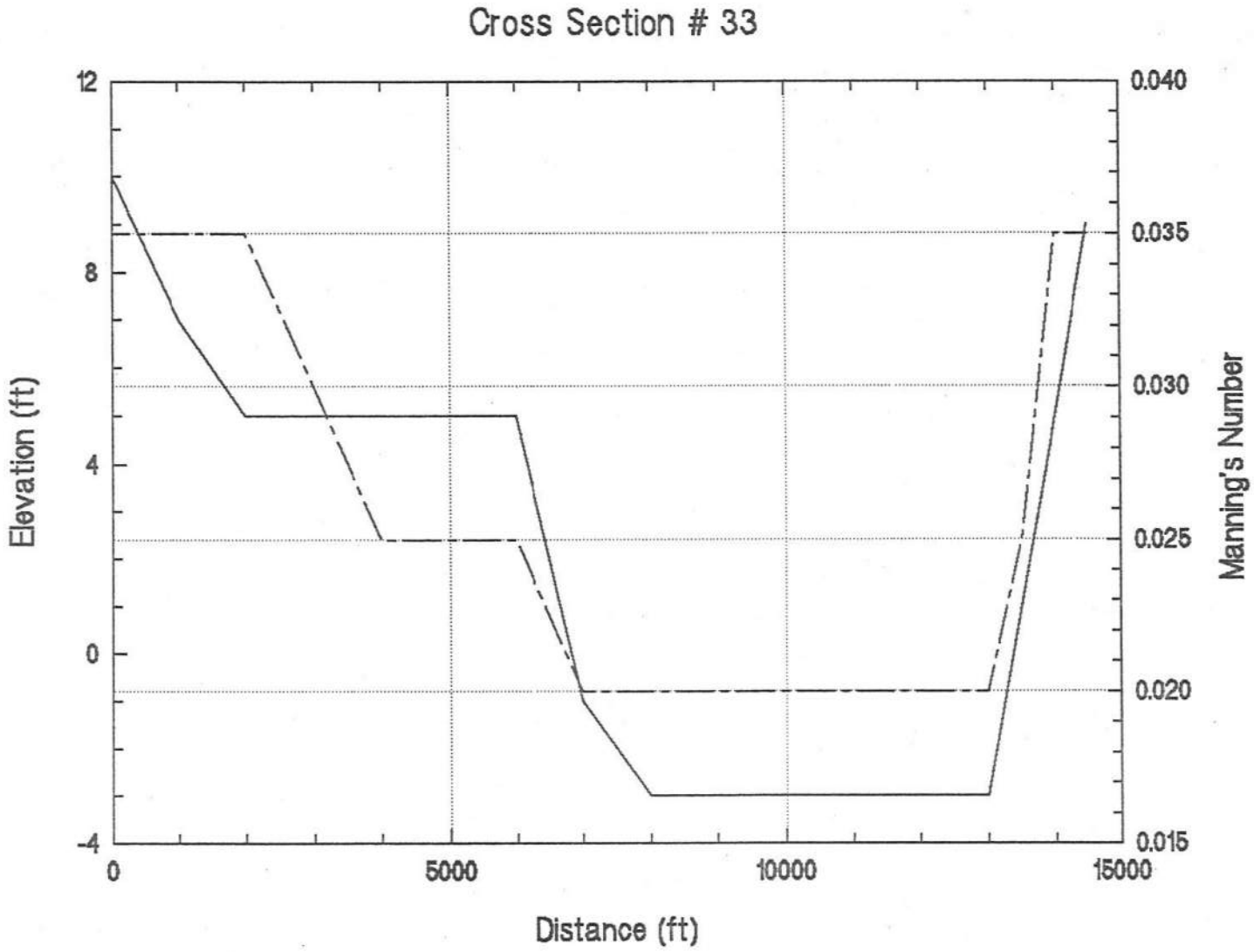
Cross Section # 33
Elevation (ft)
12
8
4
0
-4
0
5000
10000
15000
Distance (ft)
0.040
0.035
0.030
0.025
0.020
0.015
Manning's Number

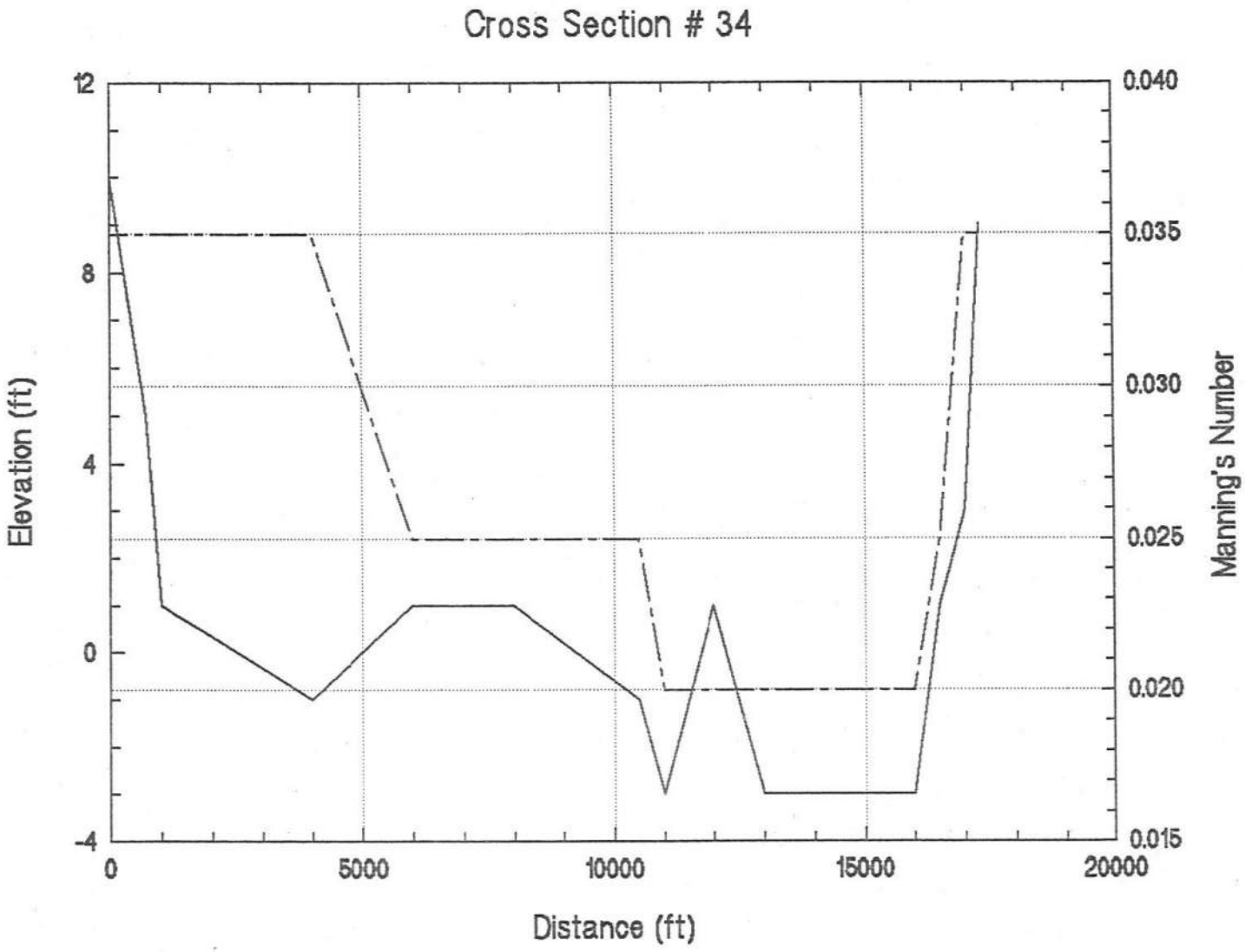
Cross Section # 34
Elevation (ft)
Manning's Number
Distance (ft)
12
8
4
0
-4
0.040
0.035
0.030
0.025
0.020
0.015
0
5000
10000
15000
20000

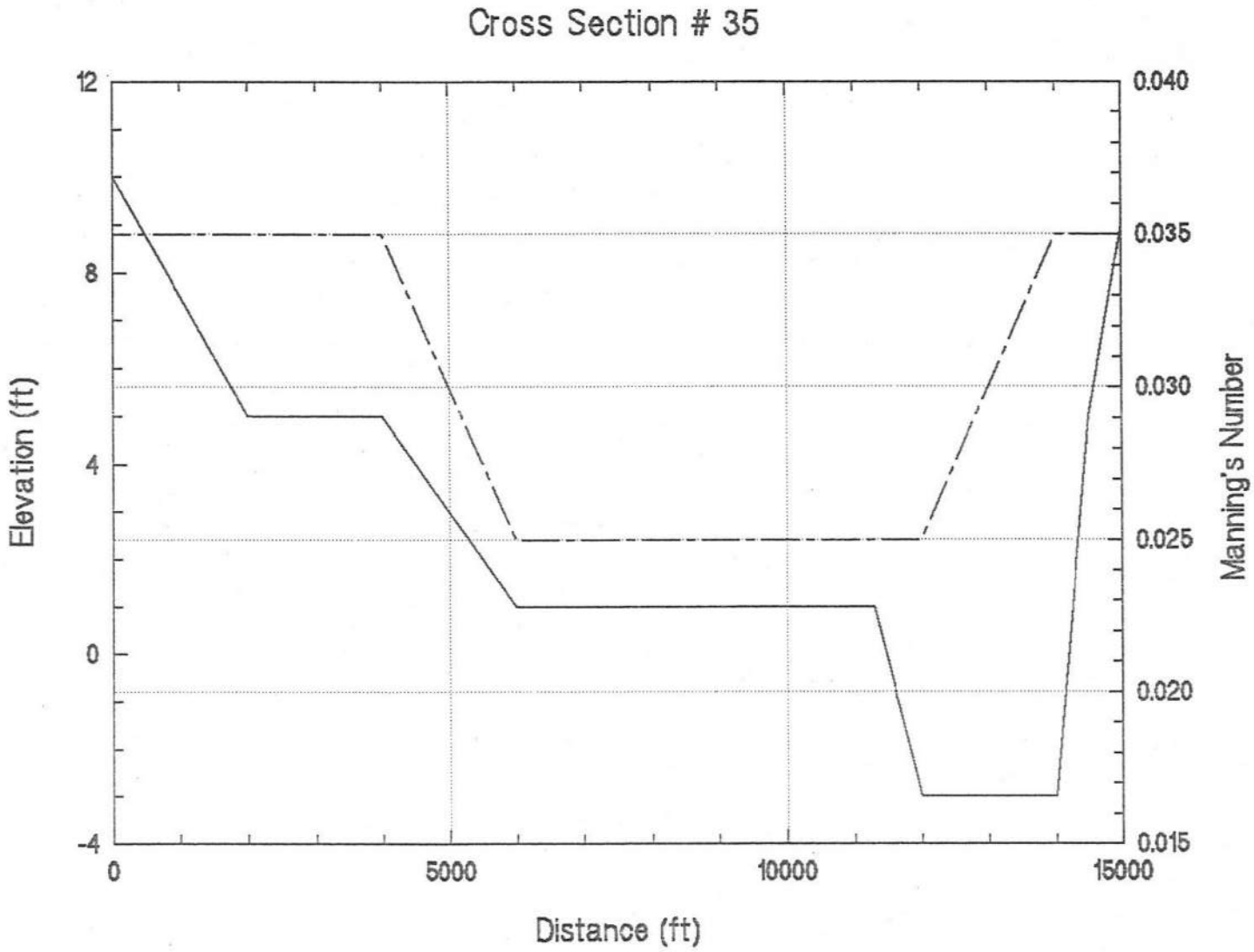
Cross Section # 35
Elevation (ft)
Manning's Number
Distance (ft)
12
8
4
0
-4
0.040
0.035
0.030
0.025
0.020
0.015
0
5000
10000
15000

Appendix B

Specified Temporal Variations of Stillwater Elevation at Node 1, Seaward of Ocean City Inlet.

The stillwater elevation above the mean sea level (the National Geodetic Vertical Datum of 1929) at Node 1, seaward of Ocean City Inlet is plotted as a function of time, t, for the duration $0 \leq t \leq 95$ hr for the specified recurrence interval, T_r, in years and the storm durations of 40 and 60 hr as follows:

T_r (yr)	Duration (hr)	Page	Duration (hr)	Page
10	40	B-2	60	B-3
20	40	B-4	60	B-5
50	40	B-6	60	B-7
100	40	B-8	60	B-9
500	40	B-10	60	B-11

The actual values of the stillwater elevation used for plotting these figures are tabulated in pages B-12 to B-16 for T_r = 10, 20, and 50 yr. and in pages B-17 to B-21 for T_r = 100 and 500 yr. The first column of these tables lists the time, t, (hr) at every half hour, while the second column indicates the still water elevations due to the spring tide only.

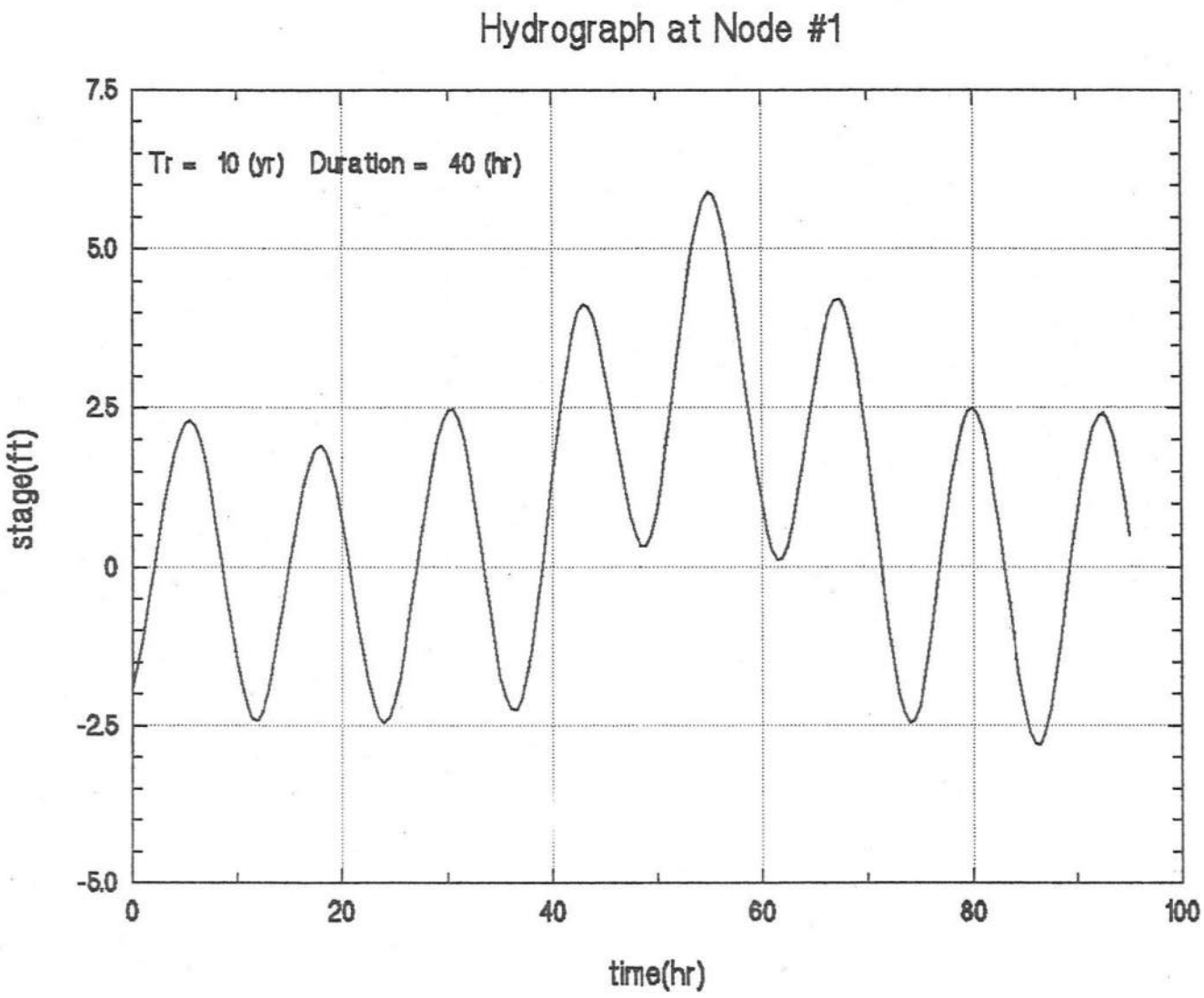
Hydrograph at Node #1
Tr = 10 (yr) Duration = 40 (hr)
stage(ft)
time(hr)
7.5
5.0
2.5
0
-2.5
-5.0
0
20
40
60
80
100

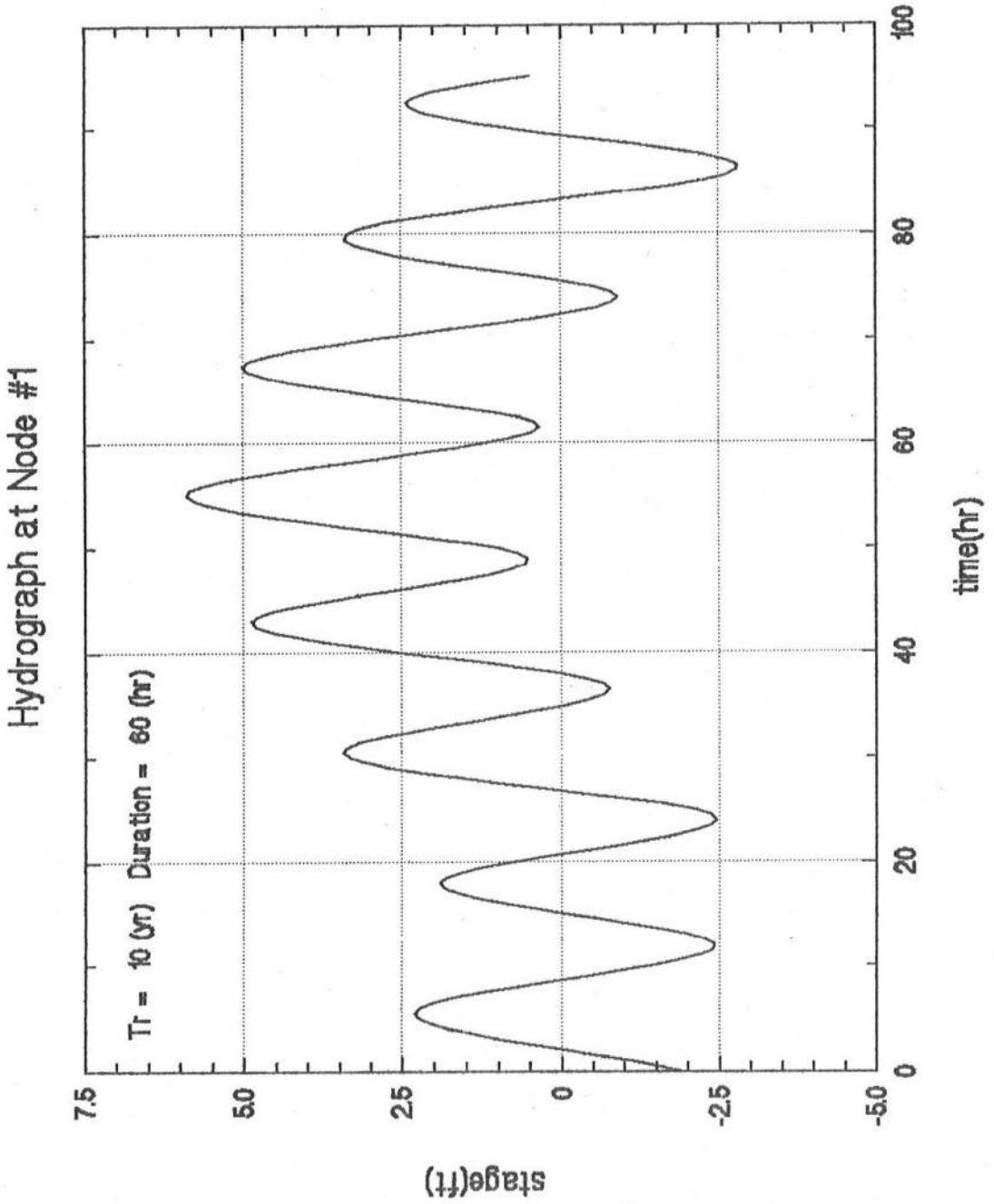
Hydrograph at Node #1
Tr = 10 (yr) Duration = 60 (hr)
stage(ft)
time(hr)
7.5
5.0
2.5
0
-2.5
-5.0
0
20
40
60
80
100

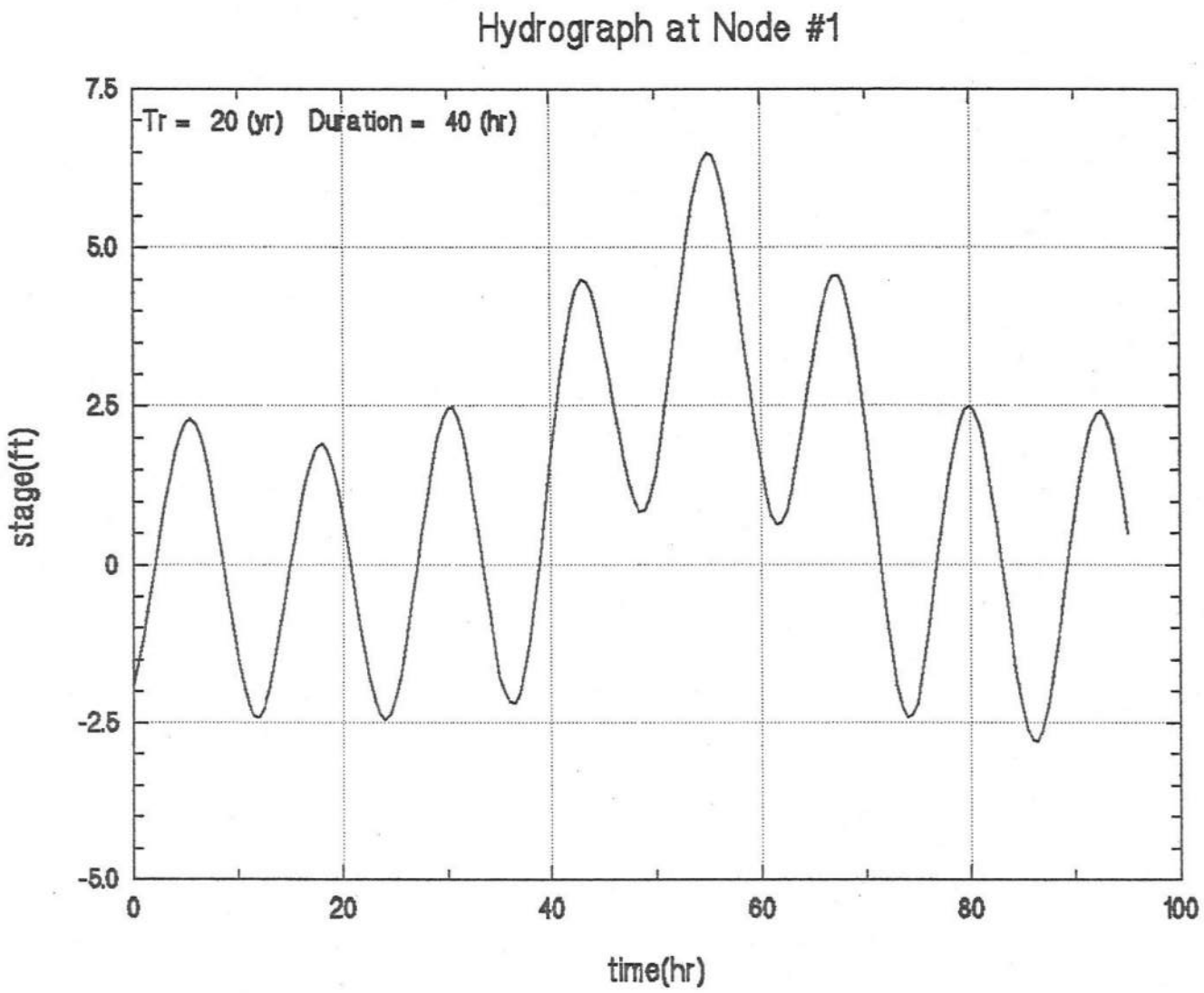
Hydrograph at Node #1
Tr = 20 (yr) Duration = 40 (hr)
7.5
5.0
2.5
0
-2.5
-5.0
stage(ft)
0
20
40
60
80
100
time(hr)

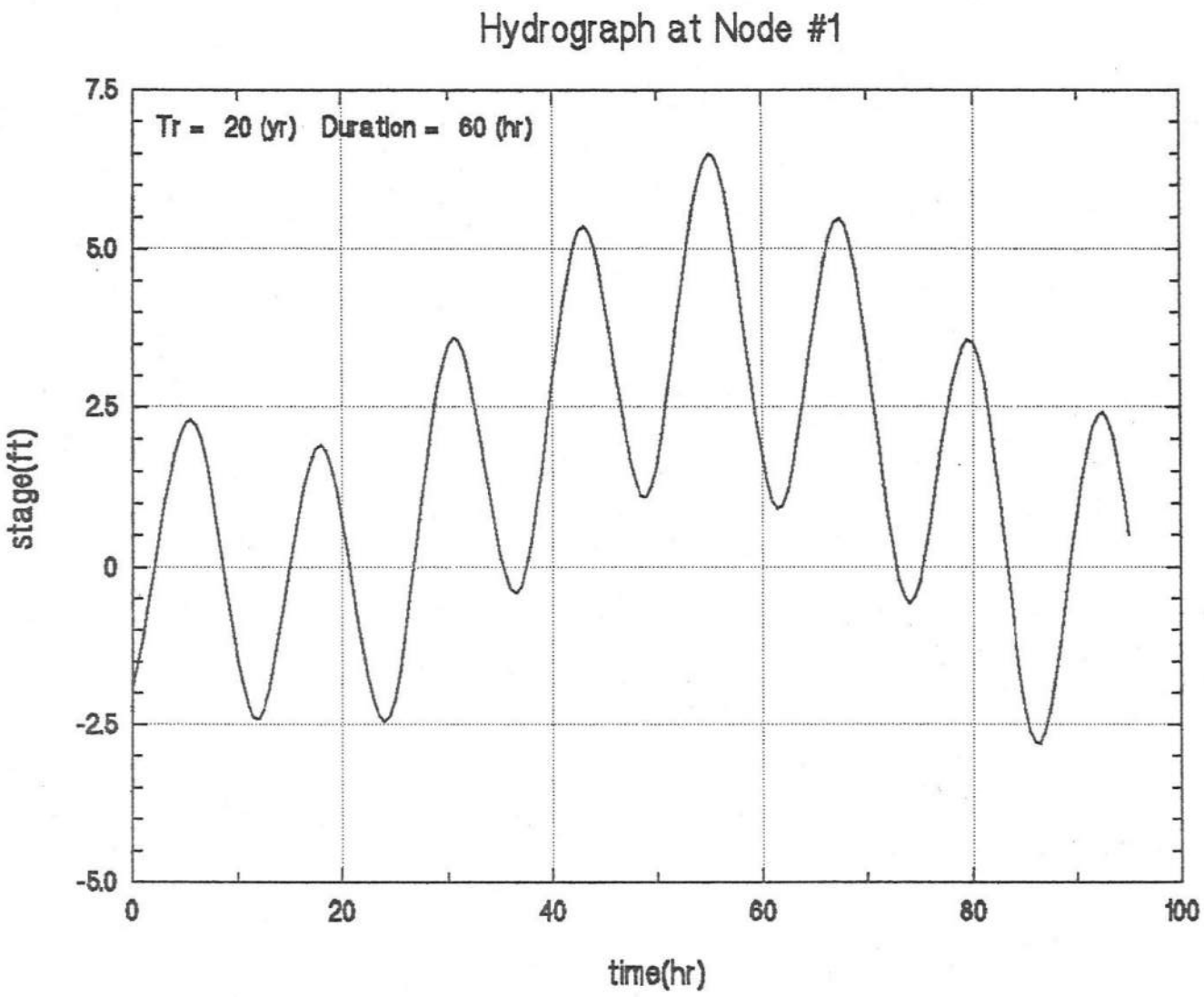
Hydrograph at Node #1
Tr = 20 (yr) Duration = 60 (hr)
stage(ft)
time(hr)
7.5
5.0
2.5
0
-2.5
-5.0
0
20
40
60
80
100

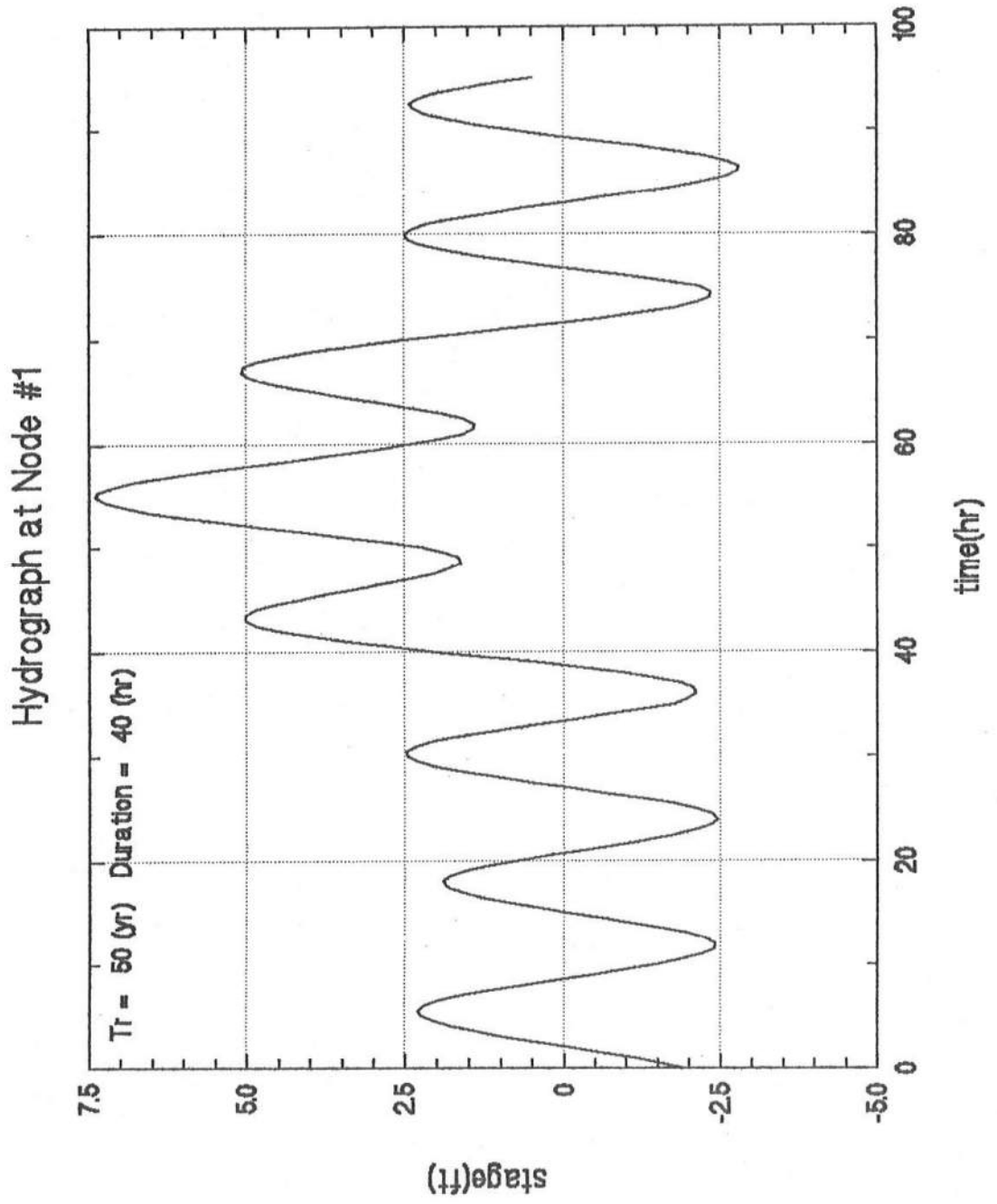
Hydrograph at Node #1
Tr = 50 (yr) Duration = 40 (hr)
stage(ft)
time(hr)
7.5
5.0
2.5
0
-2.5
-5.0
0
20
40
60
80
100

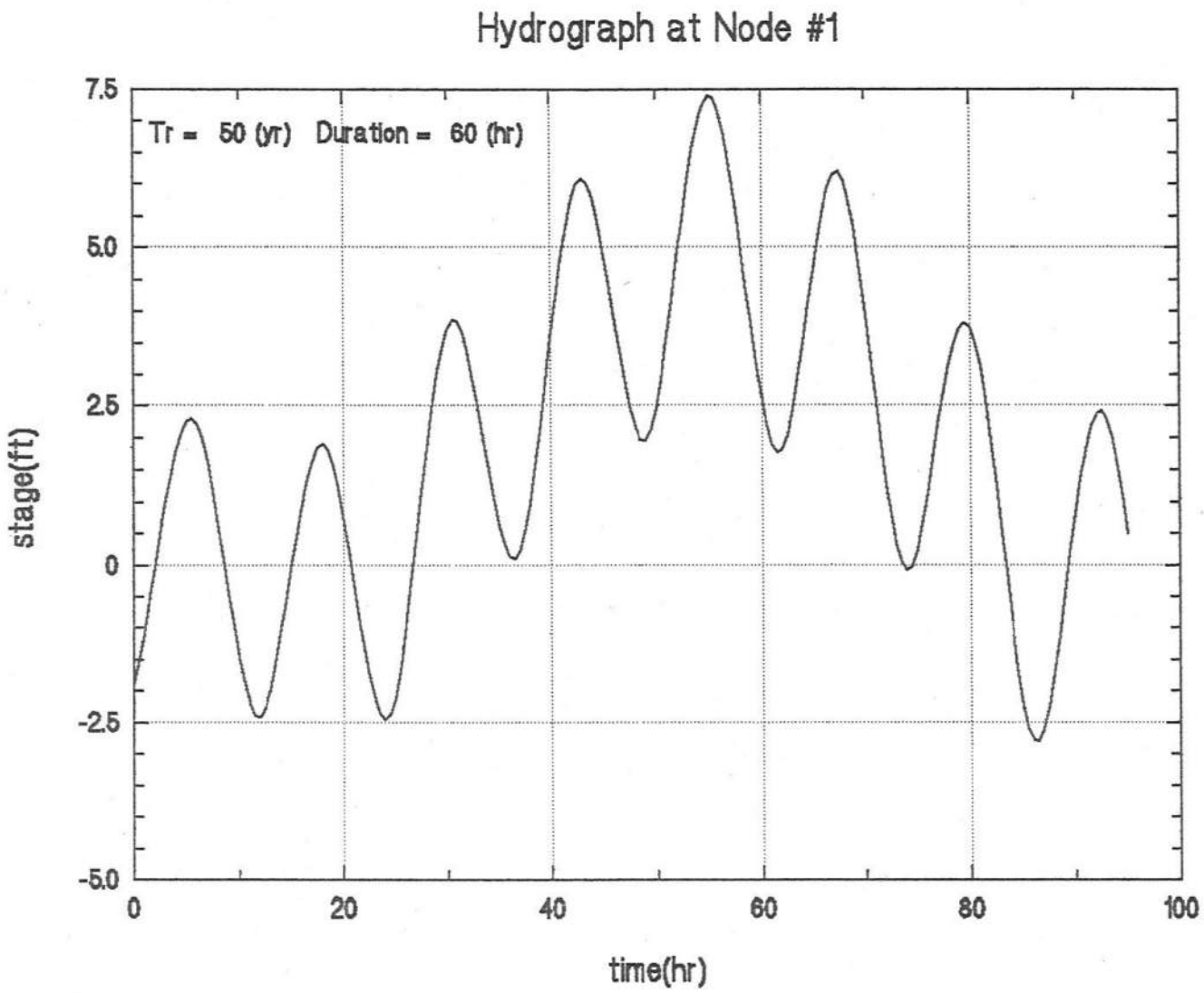
Hydrograph at Node #1
Tr = 50 (yr) Duration = 60 (hr)
stage(ft)
time(hr)
7.5
5.0
2.5
0
-2.5
-5.0
0
20
40
60
80
100

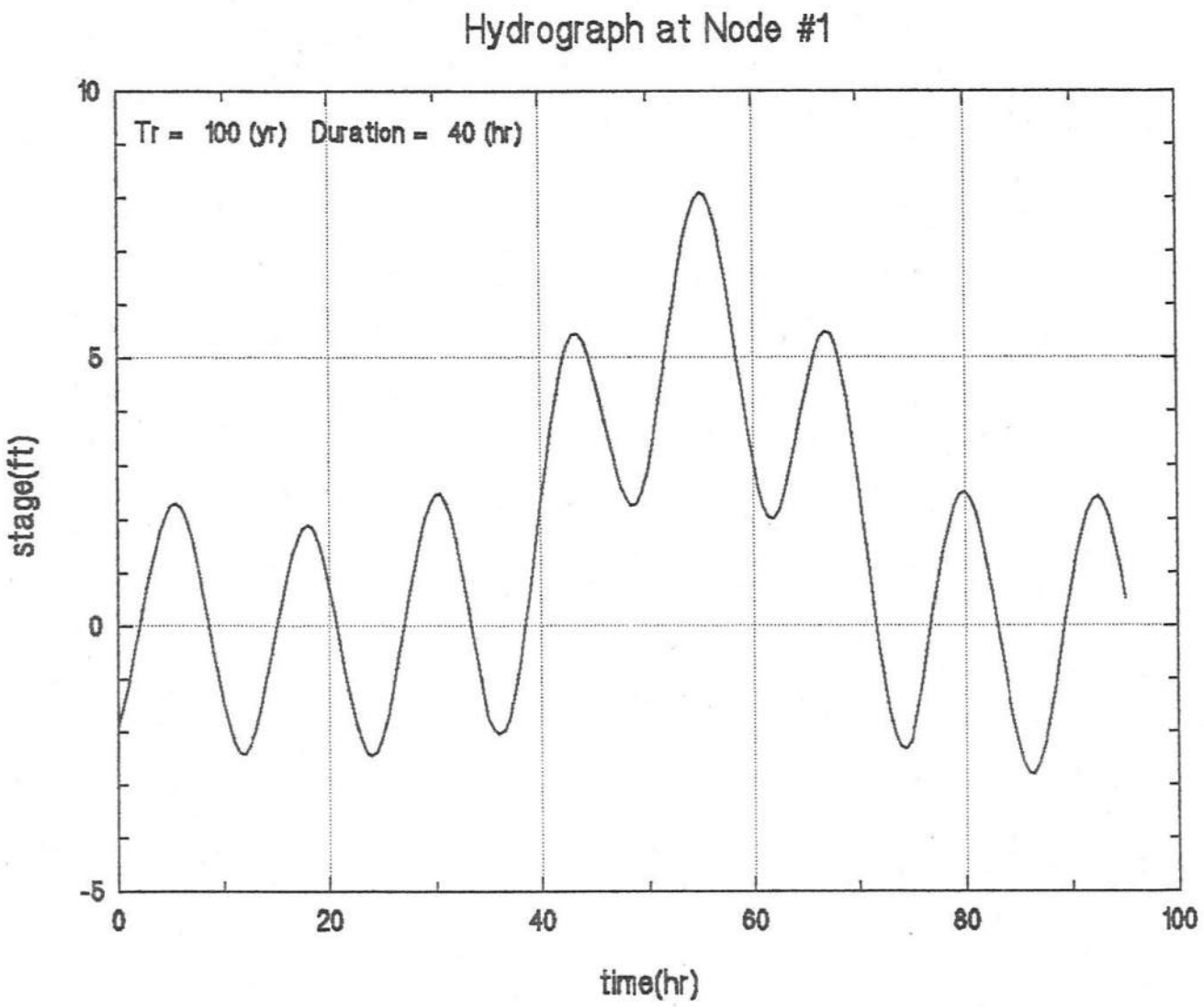
Hydrograph at Node #1
Tr = 100 (yr) Duration = 40 (hr)
stage(ft)
time(hr)
10
5
0
-5
0
20
40
60
80
100

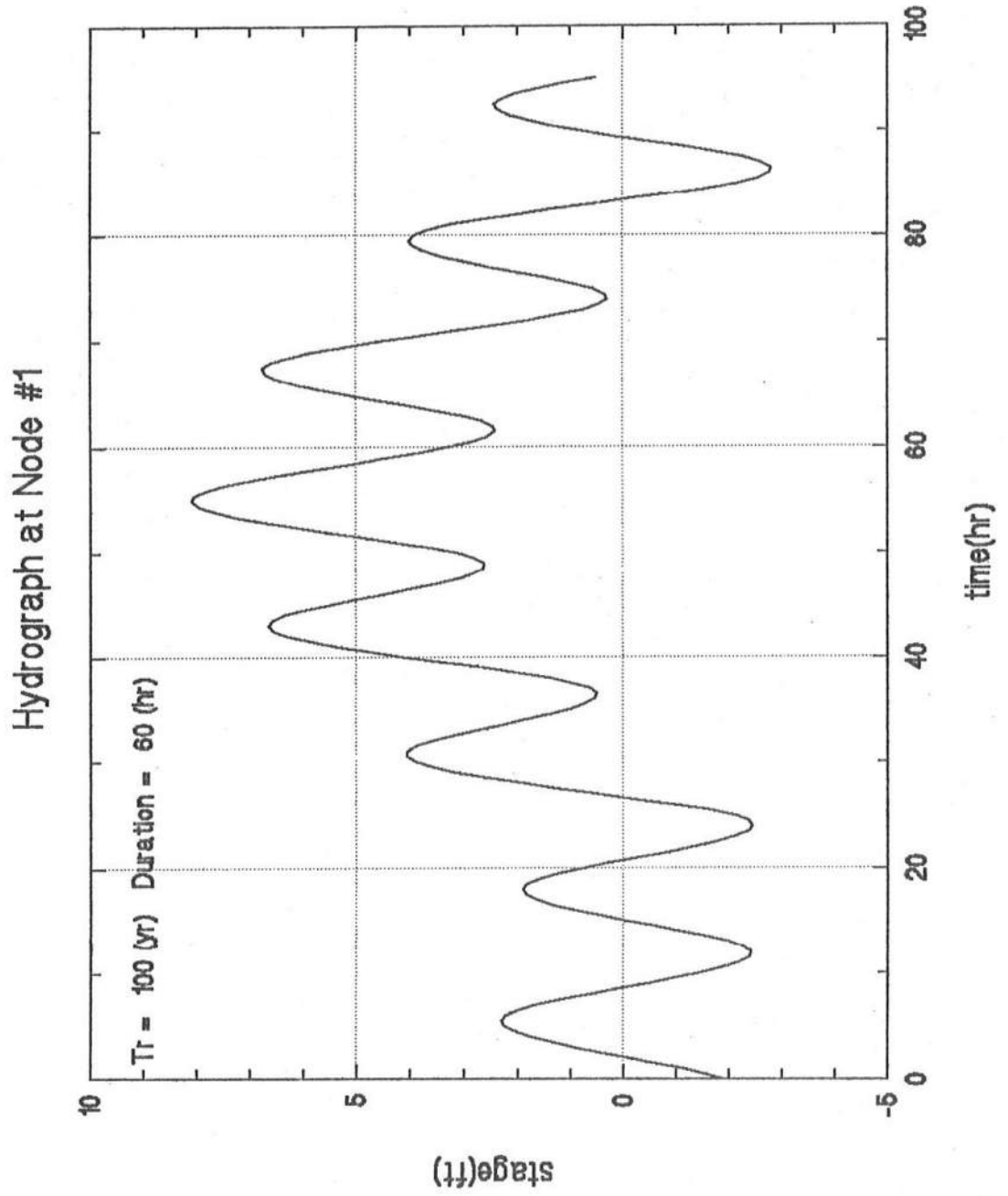
Hydrograph at Node #1
Tr = 100 (yr) Duration = 60 (hr)
stage(ft)
time(hr)
10
5
0
-5
0
20
40
60
80
100

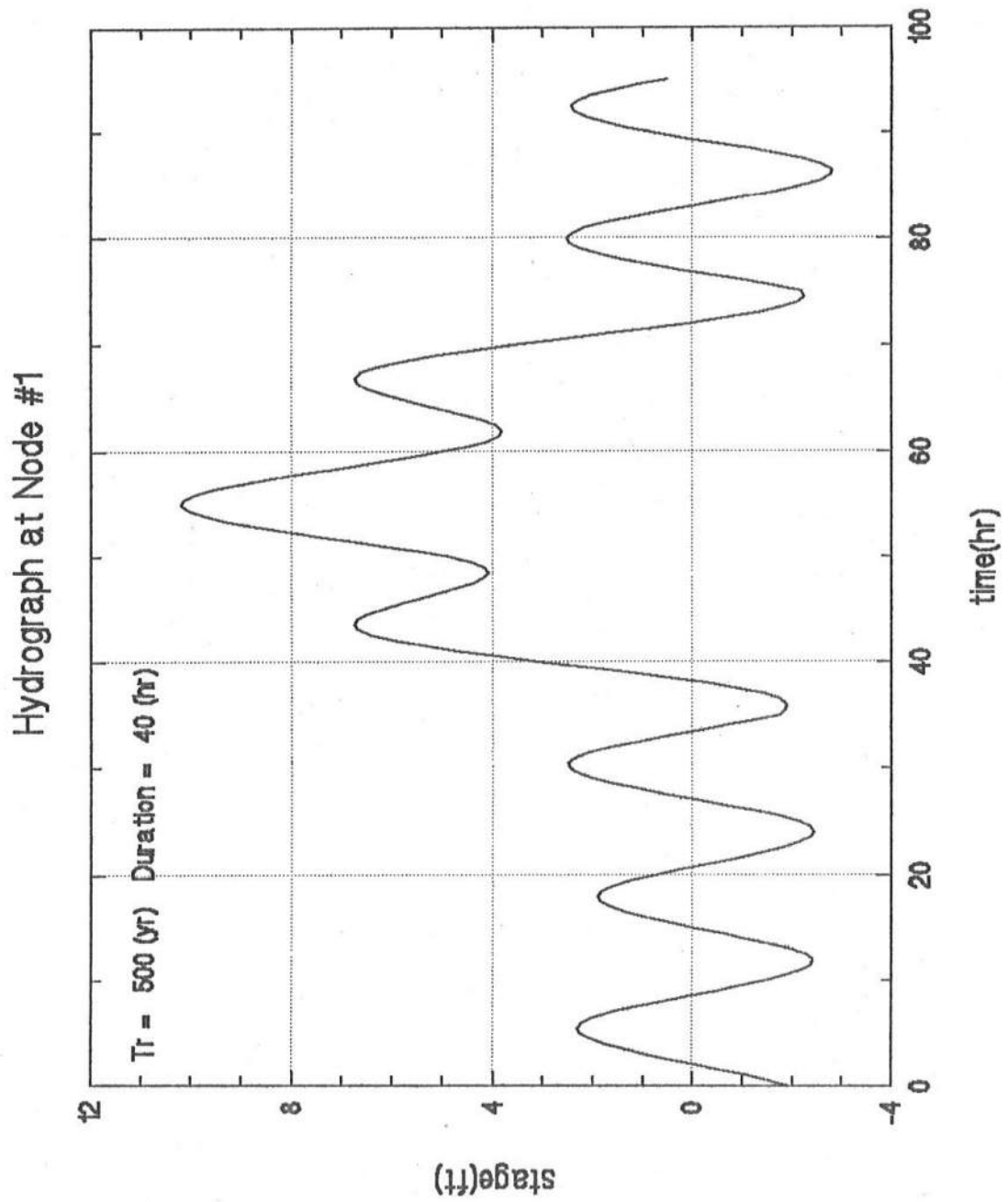
Hydrograph at Node #1
Tr = 500 (yr) Duration = 40 (hr)
stage(ft)
time(hr)
12
8
4
0
-4
0
20
40
60
80
100

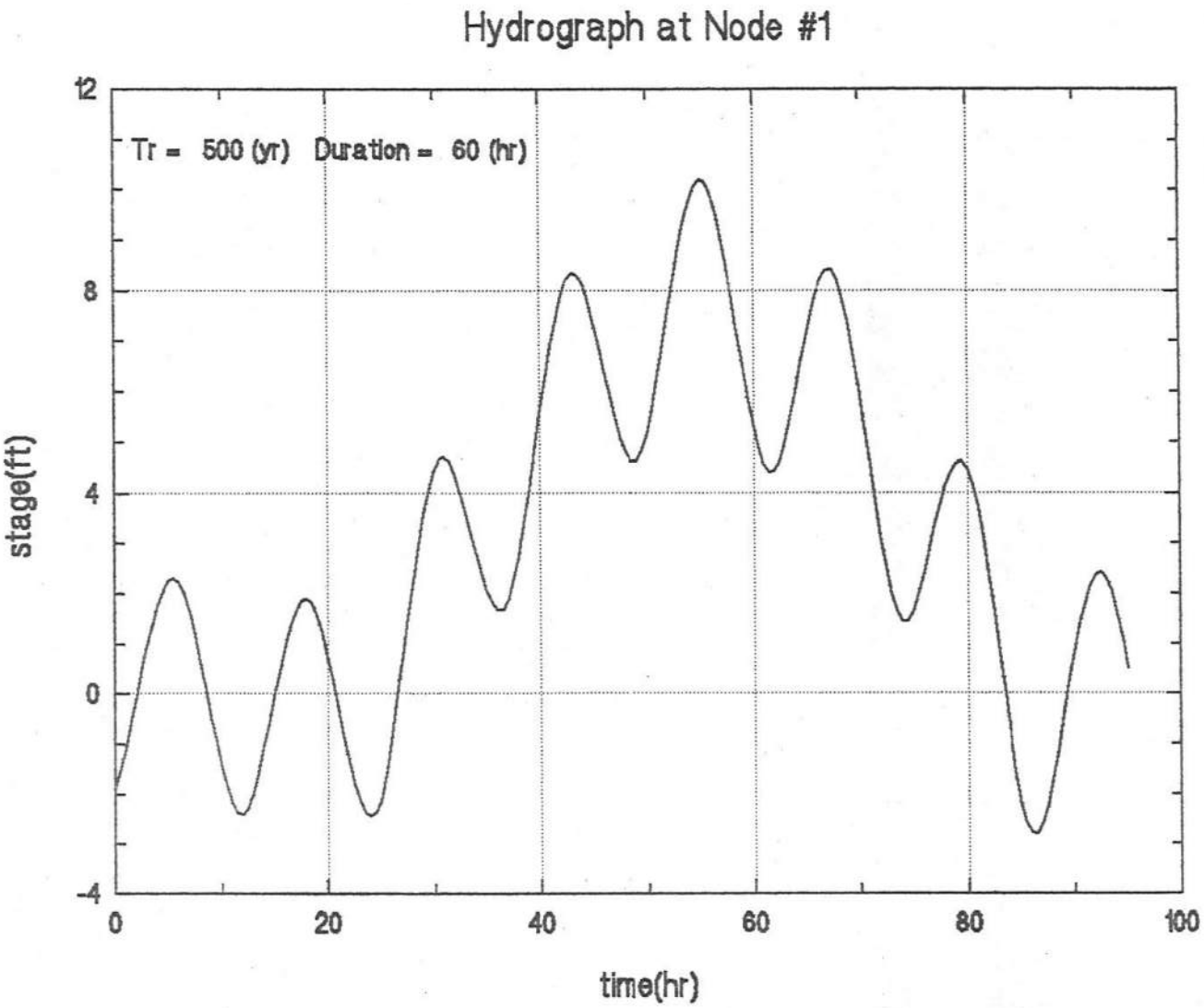
Hydrograph at Node #1
Tr = 500 (yr) Duration = 60 (hr)
stage(ft)
time(hr)
12
8
4
0
-4
0
20
40
60
80
100

Computed surge + spring tides

Return Period:		**T = 10**	**T = 10**	**T = 20**	**T = 20**	**T = 50**	**T = 50**
Duration:		**60**	**40**	**60**	**40**	**60**	**40**
	spring tides						
0.000	-1.920	-1.920	-1.920	-1.920	-1.920	-1.920	-1.920
0.500	-1.560	-1.560	-1.560	-1.560	-1.560	-1.560	-1.560
1.000	-1.100	-1.100	-1.100	-1.100	-1.100	-1.100	-1.100
1.500	-0.580	-0.580	-0.580	-0.580	-0.580	-0.580	-0.580
2.000	-0.050	-0.050	-0.050	-0.050	-0.050	-0.050	-0.050
2.500	0.470	0.470	0.470	0.470	0.470	0.470	0.470
3.000	0.960	0.960	0.960	0.960	0.960	0.960	0.960
3.500	1.390	1.390	1.390	1.390	1.390	1.390	1.390
4.000	1.770	1.770	1.770	1.770	1.770	1.770	1.770
4.500	2.060	2.060	2.060	2.060	2.060	2.060	2.060
5.000	2.250	2.250	2.250	2.250	2.250	2.250	2.250
5.500	2.310	2.310	2.310	2.310	2.310	2.310	2.310
6.000	2.220	2.220	2.220	2.220	2.220	2.220	2.220
6.500	1.990	1.990	1.990	1.990	1.990	1.990	1.990
7.000	1.620	1.620	1.620	1.620	1.620	1.620	1.620
7.500	1.160	1.160	1.160	1.160	1.160	1.160	1.160
8.000	0.640	0.640	0.640	0.640	0.640	0.640	0.640
8.500	0.090	0.090	0.090	0.090	0.090	0.090	0.090
9.000	-0.460	-0.460	-0.460	-0.460	-0.460	-0.460	-0.460
9.500	-0.980	-0.980	-0.980	-0.980	-0.980	-0.980	-0.980
10.000	-1.470	-1.470	-1.470	-1.470	-1.470	-1.470	-1.470
10.500	-1.890	-1.890	-1.890	-1.890	-1.890	-1.890	-1.890
11.000	-2.200	-2.200	-2.200	-2.200	-2.200	-2.200	-2.200
11.500	-2.390	-2.390	-2.390	-2.390	-2.390	-2.390	-2.390
12.000	-2.410	-2.410	-2.410	-2.410	-2.410	-2.410	-2.410
12.500	-2.270	-2.270	-2.270	-2.270	-2.270	-2.270	-2.270
13.000	-1.980	-1.980	-1.980	-1.980	-1.980	-1.980	-1.980
13.500	-1.570	-1.570	-1.570	-1.570	-1.570	-1.570	-1.570
14.000	-1.090	-1.090	-1.090	-1.090	-1.090	-1.090	-1.090
14.500	-0.580	-0.580	-0.580	-0.580	-0.580	-0.580	-0.580
15.000	-0.060	-0.060	-0.060	-0.060	-0.060	-0.060	-0.060
15.500	0.440	0.440	0.440	0.440	0.440	0.440	0.440
16.000	0.900	0.900	0.900	0.900	0.900	0.900	0.900
16.500	1.300	1.300	1.300	1.300	1.300	1.300	1.300
17.000	1.620	1.620	1.620	1.620	1.620	1.620	1.620
17.500	1.830	1.830	1.830	1.830	1.830	1.830	1.830
18.000	1.900	1.900	1.900	1.900	1.900	1.900	1.900
18.500	1.820	1.820	1.820	1.820	1.820	1.820	1.820
19.000	1.590	1.590	1.590	1.590	1.590	1.590	1.590
19.500	1.220	1.220	1.220	1.220	1.220	1.220	1.220

20.000	0.760	0.760	0.760	0.760	0.760	0.760	0.760
20.500	0.240	0.240	0.240	0.240	0.240	0.240	0.240
21.000	-0.300	-0.300	-0.300	-0.300	-0.300	-0.300	-0.300
21.500	-0.830	-0.830	-0.830	-0.830	-0.830	-0.830	-0.830
22.000	-1.330	-1.330	-1.330	-1.330	-1.330	-1.330	-1.330
22.500	-1.770	-1.770	-1.770	-1.770	-1.770	-1.770	-1.770
23.000	-2.130	-2.130	-2.130	-2.130	-2.130	-2.130	-2.130
23.500	-2.370	-2.370	-2.370	-2.370	-2.370	-2.370	-2.370
24.000	-2.450	-2.450	-2.450	-2.450	-2.450	-2.450	-2.450
24.500	-2.370	-2.370	-2.370	-2.370	-2.370	-2.370	-2.370
25.000	-2.120	-2.120	-2.120	-2.120	-2.120	-2.120	-2.120
25.500	-1.720	-1.633	-1.720	-1.617	-1.720	-1.594	-1.720
26.000	-1.210	-1.036	-1.210	-1.004	-1.210	-0.957	-1.210
26.500	-0.640	-0.379	-0.640	-0.332	-0.640	-0.261	-0.640
27.000	-0.050	0.298	-0.050	0.361	-0.050	0.455	-0.050
27.500	0.530	0.965	0.530	1.043	0.530	1.160	0.530
28.000	1.080	1.601	1.080	1.695	1.080	1.836	1.080
28.500	1.560	2.167	1.560	2.276	1.560	2.440	1.560
29.000	1.980	2.672	1.980	2.797	1.980	2.984	1.980
29.500	2.290	3.067	2.290	3.207	2.290	3.418	2.290
30.000	2.460	3.322	2.460	3.477	2.460	3.710	2.460
30.500	2.490	3.436	2.490	3.606	2.490	3.862	2.490
31.000	2.350	3.379	2.350	3.564	2.350	3.843	2.350
31.500	2.050	3.162	2.050	3.362	2.050	3.662	2.050
32.000	1.620	2.813	1.620	3.028	1.620	3.351	1.620
32.500	1.090	2.364	1.090	2.594	1.090	2.938	1.090
33.000	0.510	1.864	0.510	2.108	0.510	2.475	0.510
33.500	-0.080	1.354	-0.080	1.612	-0.080	1.999	-0.080
34.000	-0.670	0.842	-0.670	1.114	-0.670	1.523	-0.670
34.500	-1.230	0.359	-1.230	0.645	-1.230	1.075	-1.230
35.000	-1.750	-0.085	-1.750	0.215	-1.750	0.665	-1.750
35.500	-2.170	-0.430	-2.039	-0.117	-2.016	0.354	-1.980
36.000	-2.480	-0.666	-2.219	-0.340	-2.172	0.151	-2.101
36.500	-2.640	-0.754	-2.249	-0.414	-2.178	0.096	-2.072
37.000	-2.620	-0.663	-2.099	-0.310	-2.005	0.219	-1.864
37.500	-2.420	-0.393	-1.770	-0.028	-1.653	0.520	-1.478
38.000	-2.060	0.036	-1.283	0.413	-1.143	0.980	-0.932
38.500	-1.570	0.593	-0.666	0.982	-0.503	1.567	-0.259
39.000	-1.020	1.208	0.009	1.610	0.194	2.212	0.473
39.500	-0.430	1.862	0.723	2.275	0.930	2.895	1.242
40.000	0.160	2.515	1.434	2.939	1.664	3.575	2.008
40.500	0.720	3.135	2.114	3.571	2.365	4.224	2.742
41.000	1.230	3.705	2.742	4.151	3.014	4.819	3.423
41.500	1.650	4.182	3.277	4.638	3.570	5.323	4.010
42.000	1.980	4.568	3.720	5.034	4.033	5.734	4.504

42.500	2.160	4.802	4.010	5.278	4.343	5.992	4.843
43.000	2.180	4.874	4.137	5.359	4.490	6.088	5.019
43.500	2.030	4.774	4.092	5.269	4.463	6.011	5.020
44.000	1.730	4.523	3.893	5.026	4.282	5.781	4.867
44.500	1.290	4.129	3.550	4.641	3.958	5.408	4.569
45.000	0.760	3.644	3.115	4.163	3.539	4.943	4.175
45.500	0.190	3.116	2.635	3.644	3.076	4.435	3.737
46.000	-0.400	2.567	2.132	3.102	2.588	3.904	3.273
46.500	-0.970	2.036	1.645	2.577	2.116	3.389	2.823
47.000	-1.500	1.542	1.194	2.090	1.679	2.912	2.408
47.500	-1.970	1.107	0.799	1.661	1.298	2.492	2.046
48.000	-2.340	0.769	0.499	1.329	1.011	2.169	1.778
48.500	-2.580	0.559	0.325	1.125	0.849	1.973	1.634
49.000	-2.640	0.527	0.327	1.098	0.862	1.954	1.664
49.500	-2.520	0.673	0.504	1.248	1.049	2.111	1.866
50.000	-2.220	0.997	0.857	1.576	1.411	2.445	2.242
50.500	-1.770	1.468	1.354	2.051	1.917	2.927	2.761
51.000	-1.200	2.057	1.967	2.644	2.538	3.524	3.394
51.500	-0.580	2.694	2.625	3.284	3.202	4.169	4.069
52.000	0.060	3.349	3.298	3.942	3.881	4.831	4.757
52.500	0.680	3.982	3.946	4.576	4.534	5.469	5.417
53.000	1.250	4.562	4.539	5.158	5.132	6.054	6.021
53.500	1.750	5.070	5.057	5.668	5.653	6.565	6.547
54.000	2.150	5.475	5.470	6.075	6.068	6.973	6.965
54.500	2.430	5.759	5.757	6.359	6.357	7.258	7.256
55.000	2.570	5.900	5.900	6.500	6.500	7.400	7.400
55.500	2.530	5.859	5.857	6.459	6.457	7.358	7.356
56.000	2.320	5.645	5.640	6.245	6.238	7.143	7.135
56.500	1.950	5.270	5.257	5.868	5.853	6.765	6.747
57.000	1.470	4.782	4.759	5.378	5.352	6.274	6.241
57.500	0.900	4.202	4.166	4.796	4.754	5.689	5.637
58.000	0.290	3.579	3.528	4.172	4.111	5.061	4.987
58.500	-0.330	2.944	2.875	3.534	3.452	4.419	4.319
59.000	-0.930	2.327	2.237	2.914	2.808	3.794	3.664
59.500	-1.500	1.738	1.624	2.321	2.187	3.197	3.031
60.000	-2.010	1.207	1.067	1.786	1.621	2.655	2.452
60.500	-2.420	0.773	0.604	1.348	1.149	2.211	1.966
61.000	-2.700	0.467	0.267	1.038	0.802	1.894	1.604
61.500	-2.790	0.349	0.115	0.915	0.639	1.763	1.424
62.000	-2.700	0.409	0.139	0.969	0.651	1.809	1.418
62.500	-2.420	0.657	0.349	1.211	0.848	2.042	1.596
63.000	-1.970	1.072	0.724	1.620	1.209	2.442	1.938
63.500	-1.410	1.596	1.205	2.137	1.676	2.949	2.383
64.000	-0.790	2.177	1.742	2.712	2.198	3.514	2.883
64.500	-0.150	2.776	2.295	3.304	2.736	4.095	3.397

65.000	0.470	3.354	2.825	3.873	3.249	4.653	3.885
65.500	1.050	3.889	3.310	4.401	3.718	5.168	4.329
66.000	1.560	4.353	3.723	4.856	4.112	5.611	4.697
66.500	1.970	4.714	4.032	5.209	4.403	5.951	4.960
67.000	2.240	4.934	4.197	5.419	4.550	6.148	5.079
67.500	2.370	5.012	4.220	5.488	4.553	6.202	5.053
68.000	2.320	4.908	4.060	5.374	4.373	6.074	4.844
68.500	2.100	4.632	3.727	5.088	4.020	5.773	4.460
69.000	1.730	4.205	3.242	4.651	3.514	5.319	3.923
69.500	1.240	3.655	2.634	4.091	2.885	4.744	3.262
70.000	0.670	3.025	1.944	3.449	2.174	4.085	2.518
70.500	0.070	2.362	1.223	2.775	1.430	3.395	1.742
71.000	-0.540	1.688	0.489	2.090	0.674	2.692	0.953
71.500	-1.130	1.033	-0.226	1.422	-0.063	2.007	0.181
72.000	-1.670	0.426	-0.893	0.803	-0.753	1.370	-0.542
72.500	-2.140	-0.113	-1.490	0.252	-1.373	0.800	-1.198
73.000	-2.500	-0.543	-1.979	-0.190	-1.885	0.339	-1.744
73.500	-2.700	-0.814	-2.309	-0.474	-2.238	0.036	-2.132
74.000	-2.720	-0.906	-2.459	-0.580	-2.412	-0.089	-2.341
74.500	-2.540	-0.800	-2.409	-0.487	-2.386	-0.016	-2.350
75.000	-2.180	-0.515	-2.180	-0.215	-2.180	0.235	-2.180
75.500	-1.670	-0.081	-1.670	0.205	-1.670	0.635	-1.670
76.000	-1.060	0.452	-1.060	0.724	-1.060	1.133	-1.060
76.500	-0.400	1.034	-0.400	1.292	-0.400	1.679	-0.400
77.000	0.250	1.604	0.250	1.848	0.250	2.215	0.250
77.500	0.860	2.134	0.860	2.364	0.860	2.708	0.860
78.000	1.410	2.603	1.410	2.818	1.410	3.141	1.410
78.500	1.880	2.992	1.880	3.192	1.880	3.492	1.880
79.000	2.230	3.259	2.230	3.444	2.230	3.723	2.230
79.500	2.450	3.396	2.450	3.566	2.450	3.822	2.450
80.000	2.510	3.372	2.510	3.527	2.510	3.760	2.510
80.500	2.400	3.177	2.400	3.317	2.400	3.528	2.400
81.000	2.130	2.822	2.130	2.947	2.130	3.134	2.130
81.500	1.720	2.327	1.720	2.436	1.720	2.600	1.720
82.000	1.200	1.721	1.200	1.815	1.200	1.956	1.200
82.500	0.620	1.055	0.620	1.133	0.620	1.250	0.620
83.000	0.010	0.358	0.010	0.421	0.010	0.515	0.010
83.500	-0.610	-0.349	-0.610	-0.302	-0.610	-0.231	-0.610
84.000	-1.200	-1.026	-1.200	-0.994	-1.200	-0.947	-1.200
84.500	-1.750	-1.663	-1.750	-1.647	-1.750	-1.624	-1.750
85.000	-2.220	-2.220	-2.220	-2.220	-2.220	-2.220	-2.220
85.500	-2.580	-2.580	-2.580	-2.580	-2.580	-2.580	-2.580
86.000	-2.780	-2.780	-2.780	-2.780	-2.780	-2.780	-2.780
86.500	-2.800	-2.800	-2.800	-2.800	-2.800	-2.800	-2.800
87.000	-2.610	-2.610	-2.610	-2.610	-2.610	-2.610	-2.610

87.500	-2.240	-2.240	-2.240	-2.240	-2.240	-2.240	-2.240
88.000	-1.720	-1.720	-1.720	-1.720	-1.720	-1.720	-1.720
88.500	-1.110	-1.110	-1.110	-1.110	-1.110	-1.110	-1.110
89.000	-0.450	-0.450	-0.450	-0.450	-0.450	-0.450	-0.450
89.500	0.200	0.200	0.200	0.200	0.200	0.200	0.200
90.000	0.810	0.810	0.810	0.810	0.810	0.810	0.810
90.500	1.360	1.360	1.360	1.360	1.360	1.360	1.360
91.000	1.810	1.810	1.810	1.810	1.810	1.810	1.810
91.500	2.160	2.160	2.160	2.160	2.160	2.160	2.160
92.000	2.370	2.370	2.370	2.370	2.370	2.370	2.370
92.500	2.430	2.430	2.430	2.430	2.430	2.430	2.430
93.000	2.310	2.310	2.310	2.310	2.310	2.310	2.310
93.500	2.030	2.030	2.030	2.030	2.030	2.030	2.030
94.000	1.610	1.610	1.610	1.610	1.610	1.610	1.610
94.500	1.090	1.090	1.090	1.090	1.090	1.090	1.090
95.000	0.510	0.510	0.510	0.510	0.510	0.510	0.510

Computed surge + spring tides

Return Period:		**T = 100**	**T = 100**	**T = 500**	**T = 500**
Duration:		**60**	**40**	**60**	**40**
	Spring tides				
0.000	-1.920	-1.920	-1.920	-1.920	-1.920
0.500	-1.560	-1.560	-1.560	-1.560	-1.560
1.000	-1.100	-1.100	-1.100	-1.100	-1.100
1.500	-0.580	-0.580	-0.580	-0.580	-0.580
2.000	-0.050	-0.050	-0.050	-0.050	-0.050
2.500	0.470	0.470	0.470	0.470	0.470
3.000	0.960	0.960	0.960	0.960	0.960
3.500	1.390	1.390	1.390	1.390	1.390
4.000	1.770	1.770	1.770	1.770	1.770
4.500	2.060	2.060	2.060	2.060	2.060
5.000	2.250	2.250	2.250	2.250	2.250
5.500	2.310	2.310	2.310	2.310	2.310
6.000	2.220	2.220	2.220	2.220	2.220
6.500	1.990	1.990	1.990	1.990	1.990
7.000	1.620	1.620	1.620	1.620	1.620
7.500	1.160	1.160	1.160	1.160	1.160
8.000	0.640	0.640	0.640	0.640	0.640
8.500	0.090	0.090	0.090	0.090	0.090
9.000	-0.460	-0.460	-0.460	-0.460	-0.460
9.500	-0.980	-0.980	-0.980	-0.980	-0.980
10.000	-1.470	-1.470	-1.470	-1.470	-1.470
10.500	-1.890	-1.890	-1.890	-1.890	-1.890
11.000	-2.200	-2.200	-2.200	-2.200	-2.200
11.500	-2.390	-2.390	-2.390	-2.390	-2.390
12.000	-2.410	-2.410	-2.410	-2.410	-2.410
12.500	-2.270	-2.270	-2.270	-2.270	-2.270
13.000	-1.980	-1.980	-1.980	-1.980	-1.980
13.500	-1.570	-1.570	-1.570	-1.570	-1.570
14.000	-1.090	-1.090	-1.090	-1.090	-1.090
14.500	-0.580	-0.580	-0.580	-0.580	-0.580
15.000	-0.060	-0.060	-0.060	-0.060	-0.060
15.500	0.440	0.440	0.440	0.440	0.440
16.000	0.900	0.900	0.900	0.900	0.900
16.500	1.300	1.300	1.300	1.300	1.300
17.000	1.620	1.620	1.620	1.620	1.620
17.500	1.830	1.830	1.830	1.830	1.830
18.000	1.900	1.900	1.900	1.900	1.900
18.500	1.820	1.820	1.820	1.820	1.820
19.000	1.590	1.590	1.590	1.590	1.590
19.500	1.220	1.220	1.220	1.220	1.220

20.000	0.760	0.760	0.760	0.760	0.760
20.500	0.240	0.240	0.240	0.240	0.240
21.000	-0.300	-0.300	-0.300	-0.300	-0.300
21.500	-0.830	-0.830	-0.830	-0.830	-0.830
22.000	-1.330	-1.330	-1.330	-1.330	-1.330
22.500	-1.770	-1.770	-1.770	-1.770	-1.770
23.000	-2.130	-2.130	-2.130	-2.130	-2.130
23.500	-2.370	-2.370	-2.370	-2.370	-2.370
24.000	-2.450	-2.450	-2.450	-2.450	-2.450
24.500	-2.370	-2.370	-2.370	-2.370	-2.370
25.000	-2.120	-2.120	-2.120	-2.120	-2.120
25.500	-1.720	-1.575	-1.720	-1.520	-1.720
26.000	-1.210	-0.921	-1.210	-0.811	-1.210
26.500	-0.640	-0.206	-0.640	-0.041	-0.640
27.000	-0.050	0.528	-0.050	0.748	-0.050
27.500	0.530	1.252	0.530	1.526	0.530
28.000	1.080	1.945	1.080	2.274	1.080
28.500	1.560	2.568	1.560	2.950	1.560
29.000	1.980	3.130	1.980	3.566	1.980
29.500	2.290	3.581	2.290	4.071	2.290
30.000	2.460	3.891	2.460	4.435	2.460
30.500	2.490	4.061	2.490	4.657	2.490
31.000	2.350	4.059	2.350	4.708	2.350
31.500	2.050	3.896	2.050	4.597	2.050
32.000	1.620	3.602	1.620	4.354	1.620
32.500	1.090	3.206	1.090	4.010	1.090
33.000	0.510	2.759	0.510	3.613	0.510
33.500	-0.080	2.301	-0.080	3.205	-0.080
34.000	-0.670	1.841	-0.670	2.794	-0.670
34.500	-1.230	1.409	-1.230	2.411	-1.230
35.000	-1.750	1.015	-1.750	2.065	-1.750
35.500	-2.170	0.719	-1.953	1.817	-1.870
36.000	-2.480	0.532	-2.046	1.676	-1.881
36.500	-2.640	0.492	-1.990	1.682	-1.743
37.000	-2.620	0.630	-1.755	1.865	-1.426
37.500	-2.420	0.946	-1.341	2.225	-0.931
38.000	-2.060	1.420	-0.769	2.742	-0.279
38.500	-1.570	2.021	-0.069	3.385	0.501
39.000	-1.020	2.680	0.689	4.085	1.338
39.500	-0.430	3.377	1.484	4.822	2.211
40.000	0.160	4.070	2.276	5.555	3.080
40.500	0.720	4.731	3.035	6.255	3.914
41.000	1.230	5.340	3.741	6.900	4.694
41.500	1.650	5.855	4.352	7.452	5.378
42.000	1.980	6.278	4.869	7.910	5.967

42.500	2.160	6.547	5.232	8.213	6.399
43.000	2.180	6.654	5.430	8.353	6.665
43.500	2.030	6.587	5.454	8.318	6.754
44.000	1.730	6.368	5.321	8.129	6.685
44.500	1.290	6.005	5.044	7.796	6.469
45.000	0.760	5.549	4.670	7.368	6.155
45.500	0.190	5.050	4.251	6.895	5.793
46.000	-0.400	4.527	3.805	6.398	5.402
46.500	-0.970	4.021	3.373	5.917	5.022
47.000	-1.500	3.552	2.974	5.470	4.673
47.500	-1.970	3.139	2.628	5.079	4.374
48.000	-2.340	2.823	2.375	4.783	4.166
48.500	-2.580	2.633	2.245	4.612	4.077
49.000	-2.640	2.619	2.287	4.617	4.158
49.500	-2.520	2.782	2.502	4.796	4.409
50.000	-2.220	3.122	2.889	5.150	4.829
50.500	-1.770	3.607	3.418	5.649	5.388
51.000	-1.200	4.209	4.059	6.263	6.057
51.500	-0.580	4.857	4.742	6.922	6.764
52.000	0.060	5.522	5.437	7.596	7.479
52.500	0.680	6.163	6.104	8.245	8.163
53.000	1.250	6.750	6.712	8.838	8.786
53.500	1.750	7.263	7.242	9.356	9.327
54.000	2.150	7.672	7.663	9.770	9.756
54.500	2.430	7.958	7.956	10.057	10.054
55.000	2.570	8.100	8.100	10.200	10.200
55.500	2.530	8.058	8.056	10.157	10.154
56.000	2.320	7.842	7.833	9.940	9.926
56.500	1.950	7.463	7.442	9.556	9.527
57.000	1.470	6.970	6.932	9.058	9.006
57.500	0.900	6.383	6.324	8.465	8.383
58.000	0.290	5.752	5.667	7.826	7.709
58.500	-0.330	5.107	4.992	7.172	7.014
59.000	-0.930	4.479	4.329	6.533	6.327
59.500	-1.500	3.877	3.688	5.919	5.658
60.000	-2.010	3.332	3.099	5.360	5.039
60.500	-2.420	2.882	2.602	4.896	4.509
61.000	-2.700	2.559	2.227	4.557	4.098
61.500	-2.790	2.423	2.035	4.402	3.867
62.000	-2.700	2.463	2.015	4.423	3.806
62.500	-2.420	2.689	2.178	4.629	3.924
63.000	-1.970	3.082	2.504	5.000	4.203
63.500	-1.410	3.581	2.933	5.477	4.582
64.000	-0.790	4.137	3.415	6.008	5.012
64.500	-0.150	4.710	3.911	6.555	5.453

65.000	0.470	5.259	4.380	7.078	5.865
65.500	1.050	5.765	4.804	7.556	6.229
66.000	1.560	6.198	5.151	7.959	6.515
66.500	1.970	6.527	5.394	8.258	6.694
67.000	2.240	6.714	5.490	8.413	6.725
67.500	2.370	6.757	5.442	8.423	6.609
68.000	2.320	6.618	5.209	8.250	6.307
68.500	2.100	6.305	4.802	7.902	5.828
69.000	1.730	5.840	4.241	7.400	5.194
69.500	1.240	5.251	3.555	6.775	4.434
70.000	0.670	4.580	2.786	6.065	3.590
70.500	0.070	3.877	1.984	5.322	2.711
71.000	-0.540	3.160	1.169	4.565	1.818
71.500	-1.130	2.461	0.371	3.825	0.941
72.000	-1.670	1.810	-0.379	3.132	0.111
72.500	-2.140	1.226	-1.061	2.505	-0.651
73.000	-2.500	0.750	-1.635	1.985	-1.306
73.500	-2.700	0.432	-2.050	1.622	-1.803
74.000	-2.720	0.292	-2.286	1.436	-2.121
74.500	-2.540	0.349	-2.323	1.447	-2.240
75.000	-2.180	0.585	-2.180	1.635	-2.180
75.500	-1.670	0.969	-1.670	1.971	-1.670
76.000	-1.060	1.451	-1.060	2.404	-1.060
76.500	-0.400	1.981	-0.400	2.885	-0.400
77.000	0.250	2.499	0.250	3.353	0.250
77.500	0.860	2.976	0.860	3.780	0.860
78.000	1.410	3.392	1.410	4.144	1.410
78.500	1.880	3.726	1.880	4.427	1.880
79.000	2.230	3.939	2.230	4.588	2.230
79.500	2.450	4.021	2.450	4.617	2.450
80.000	2.510	3.941	2.510	4.485	2.510
80.500	2.400	3.691	2.400	4.181	2.400
81.000	2.130	3.280	2.130	3.716	2.130
81.500	1.720	2.728	1.720	3.110	1.720
82.000	1.200	2.065	1.200	2.394	1.200
82.500	0.620	1.342	0.620	1.616	0.620
83.000	0.010	0.588	0.010	0.808	0.010
83.500	-0.610	-0.176	-0.610	-0.011	-0.610
84.000	-1.200	-0.911	-1.200	-0.801	-1.200
84.500	-1.750	-1.605	-1.750	-1.550	-1.750
85.000	-2.220	-2.220	-2.220	-2.220	-2.220
85.500	-2.580	-2.580	-2.580	-2.580	-2.580
86.000	-2.780	-2.780	-2.780	-2.780	-2.780
86.500	-2.800	-2.800	-2.800	-2.800	-2.800
87.000	-2.610	-2.610	-2.610	-2.610	-2.610

87.500	-2.240	-2.240	-2.240	-2.240	-2.240
88.000	-1.720	-1.720	-1.720	-1.720	-1.720
88.500	-1.110	-1.110	-1.110	-1.110	-1.110
89.000	-0.450	-0.450	-0.450	-0.450	-0.450
89.500	0.200	0.200	0.200	0.200	0.200
90.000	0.810	0.810	0.810	0.810	0.810
90.500	1.360	1.360	1.360	1.360	1.360
91.000	1.810	1.810	1.810	1.810	1.810
91.500	2.160	2.160	2.160	2.160	2.160
92.000	2.370	2.370	2.370	2.370	2.370
92.500	2.430	2.430	2.430	2.430	2.430
93.000	2.310	2.310	2.310	2.310	2.310
93.500	2.030	2.030	2.030	2.030	2.030
94.000	1.610	1.610	1.610	1.610	1.610
94.500	1.090	1.090	1.090	1.090	1.090
95.000	0.510	0.510	0.510	0.510	0.510

Appendix C

Computed Temporal Variations of Stillwater Elevation at Existing Roadway

The computed temporal variations of the stillwater elevation at the existing Roadway and the specified temporal variations of the stillwater elevation at Node 1 are plotted for spring tide only in page C-2 and for the specified recurrence interval, T_r (yr.), and the storm durations of 40 and 60 hr in pages C-3 to C-12 as follows:

T_r (yr)	Duration (hr)	Page	Duration (hr)	Page
10	40	C-3	60	C-4
20	40	C-5	60	C-6
50	40	C-7	60	C-8
100	40	C-9	60	C-10
500	40	C-11	60	C-12

It is noted that the computed temporal variations of the stillwater elevation for the raised Roadway with minimum elevations of 3.5, 4.0, 4.5 and 5.0 ft have been determined to be identical to those for the existing Roadway for a given storm.

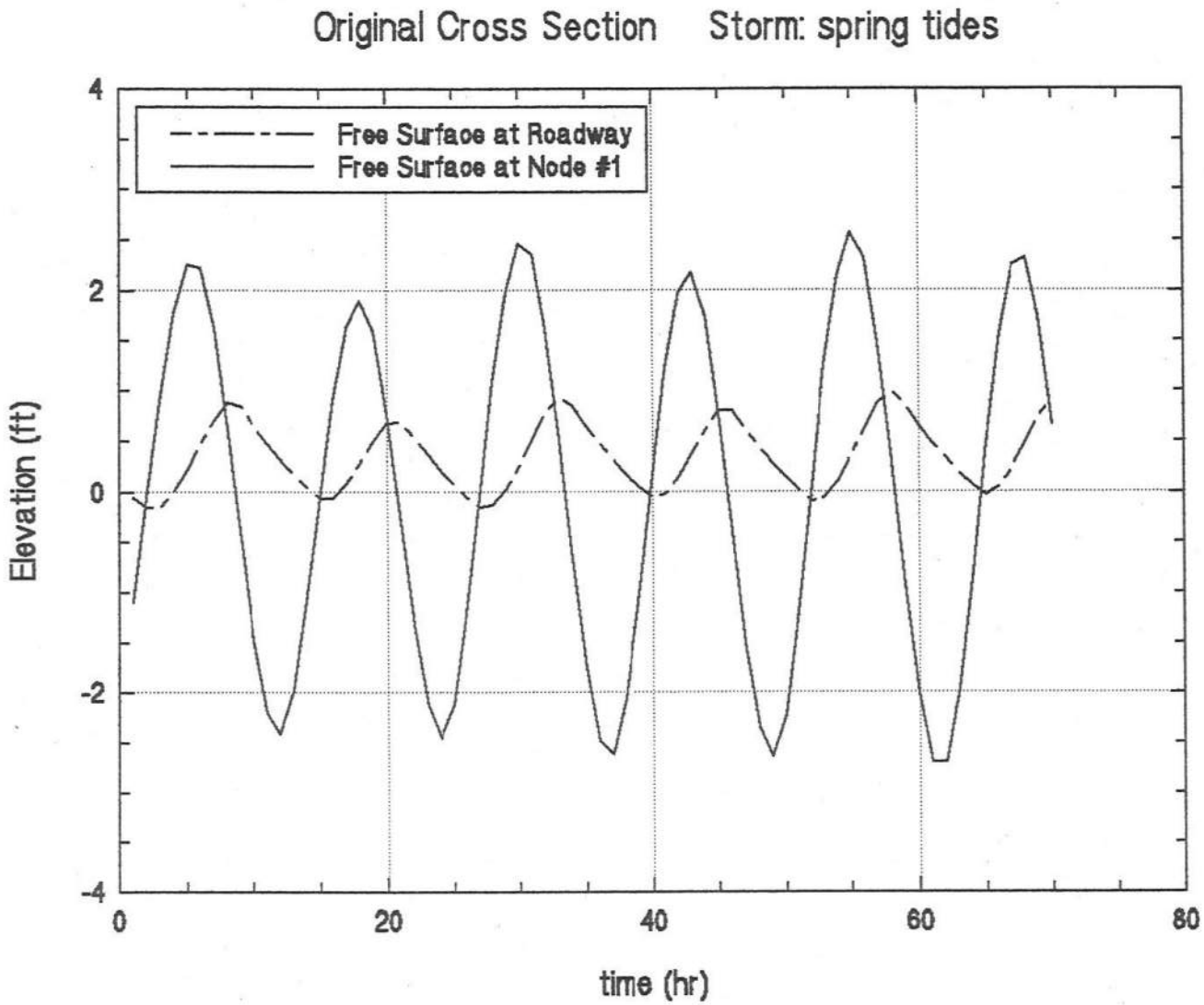
Original Cross Section Storm: spring tides
Free Surface at Roadway
Free Surface at Node #1
Elevation (ft)
time (hr)
4
2
0
-2
-4
0
20
40
60
80

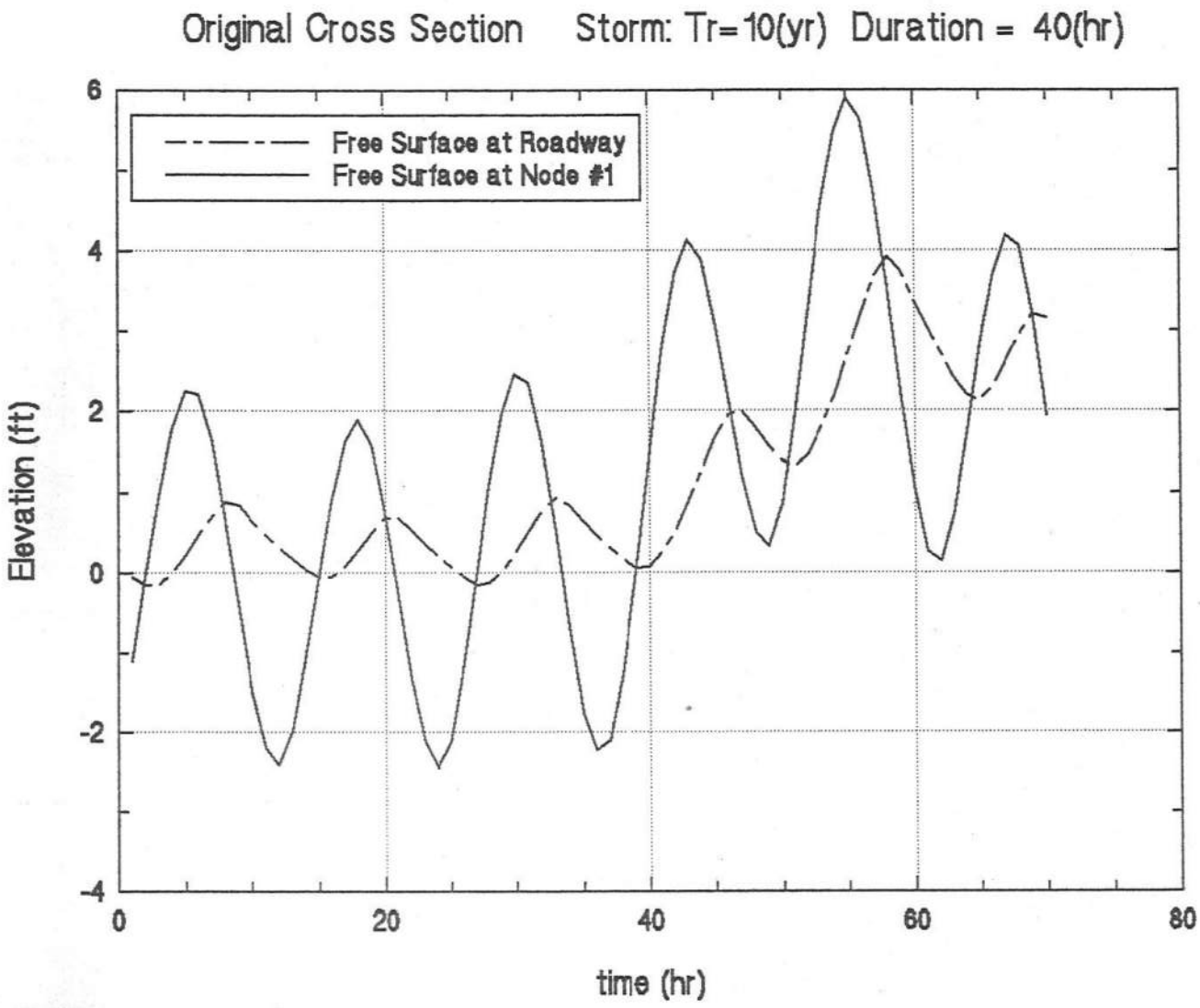
Original Cross Section Storm: Tr=10(yr) Duration = 40(hr)
Free Surface at Roadway
Free Surface at Node #1
Elevation (ft)
time (hr)
6
4
2
0
-2
-4
0
20
40
60
80

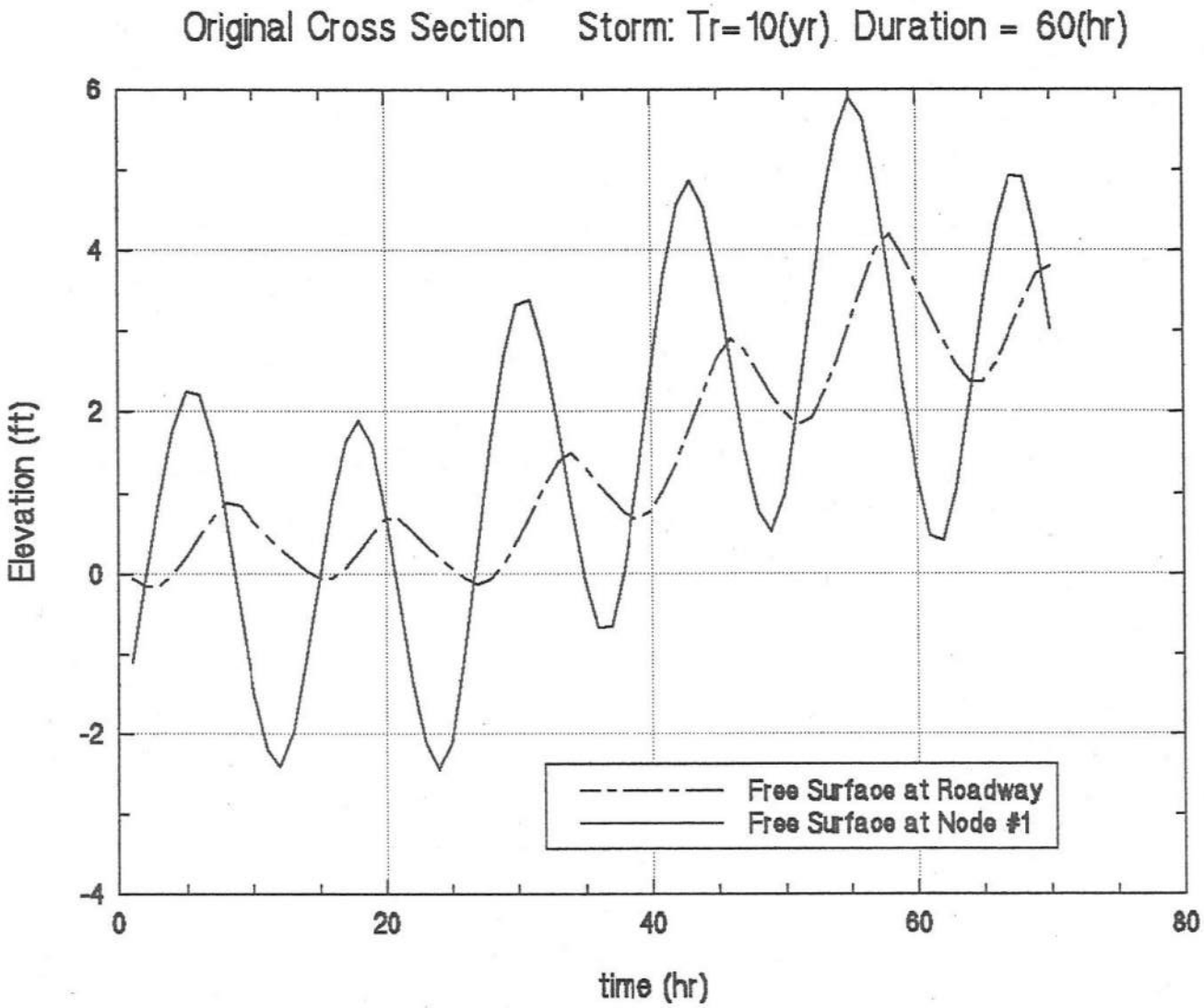
Original Cross Section Storm: Tr=10(yr) Duration = 60(hr)
Elevation (ft)
6
4
2
0
-2
-4
0
20
40
60
80
time (hr)
Free Surface at Roadway
Free Surface at Node #1

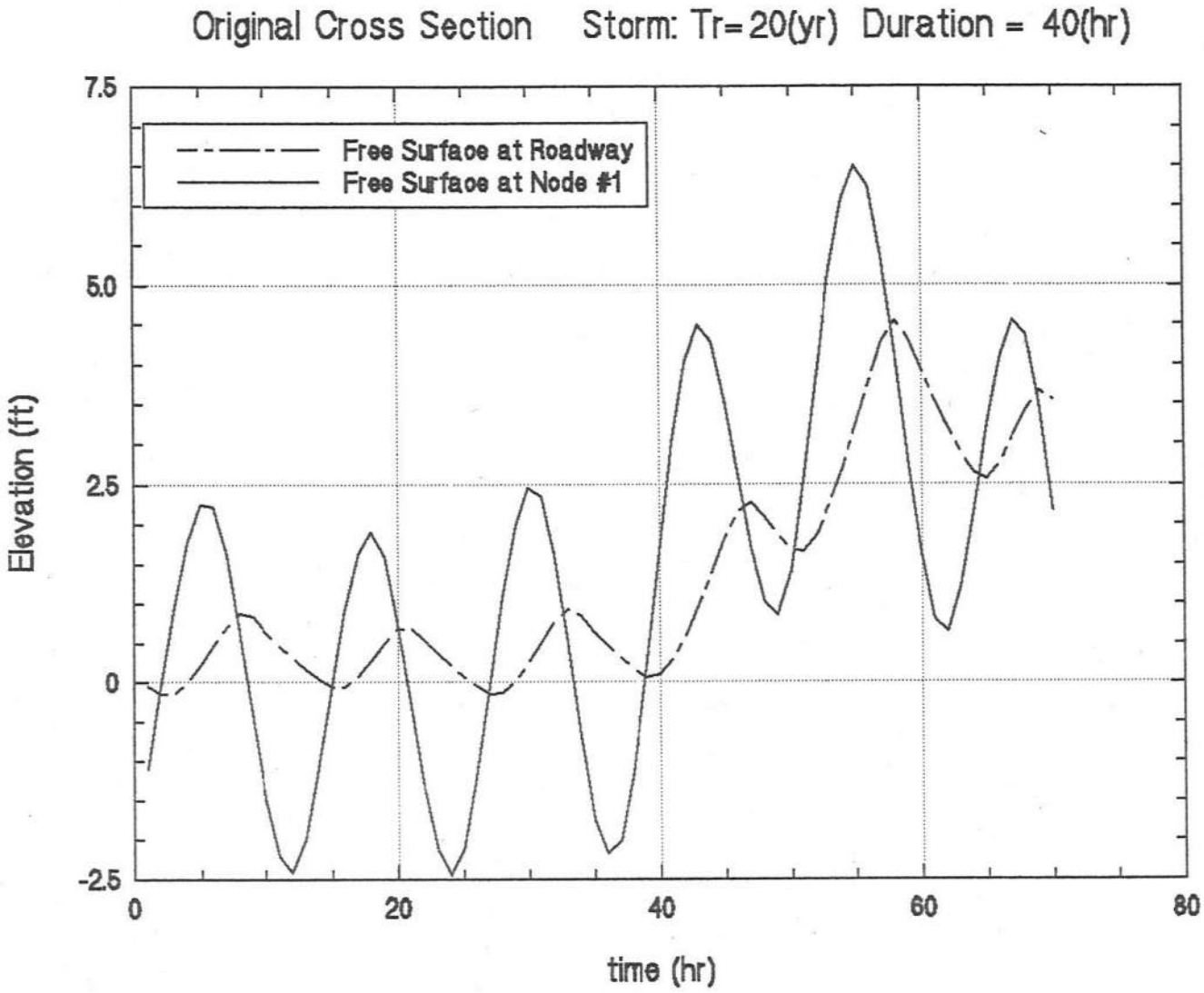
Original Cross Section Storm: Tr=20(yr) Duration = 40(hr)
Free Surface at Roadway
Free Surface at Node #1
Elevation (ft)
7.5
5.0
2.5
0
-2.5
0
20
40
60
80
time (hr)

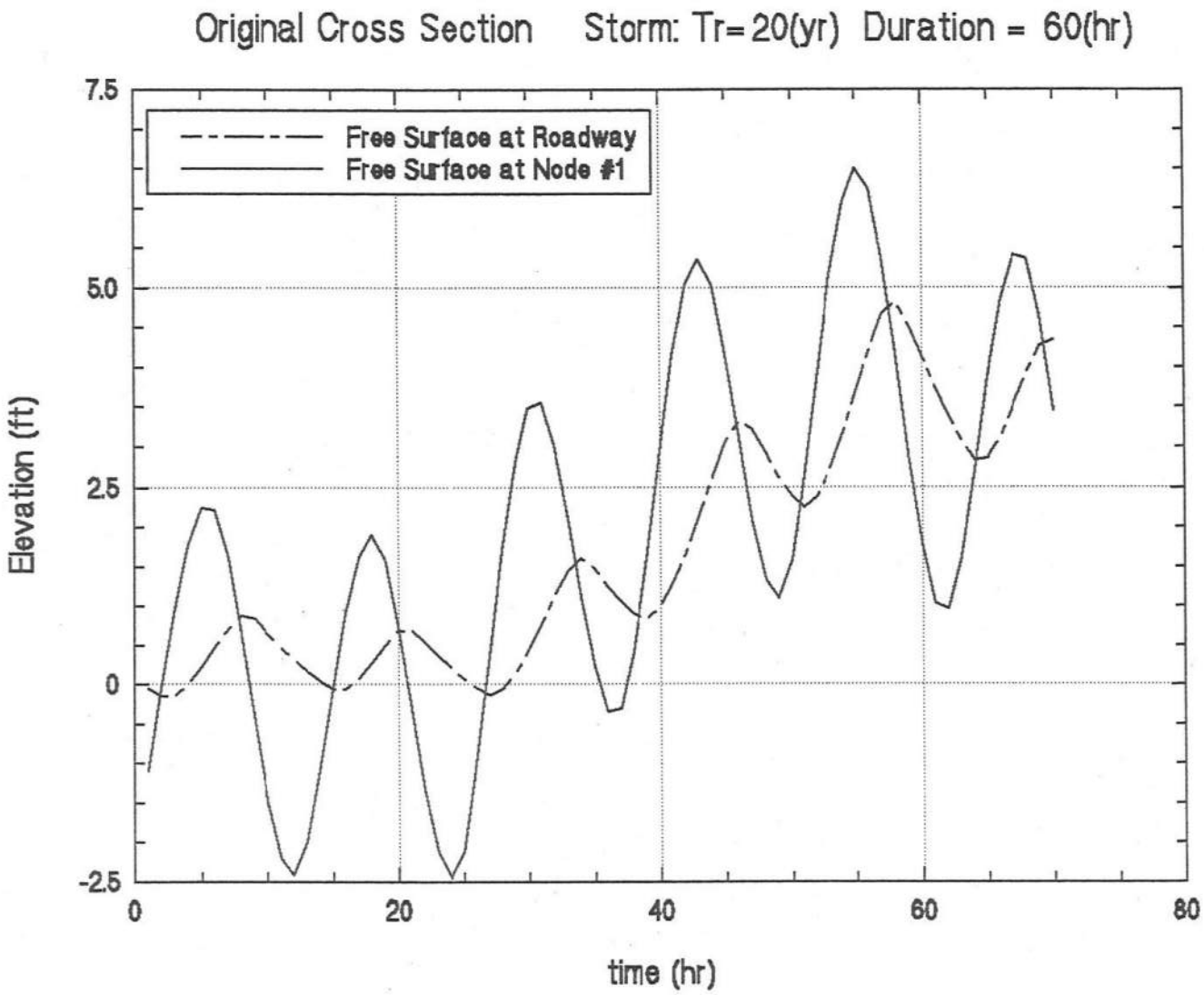
Original Cross Section Storm: Tr=20(yr) Duration = 60(hr)
Free Surface at Roadway
Free Surface at Node #1
Elevation (ft)
7.5
5.0
2.5
0
-2.5
0
20
40
60
80
time (hr)

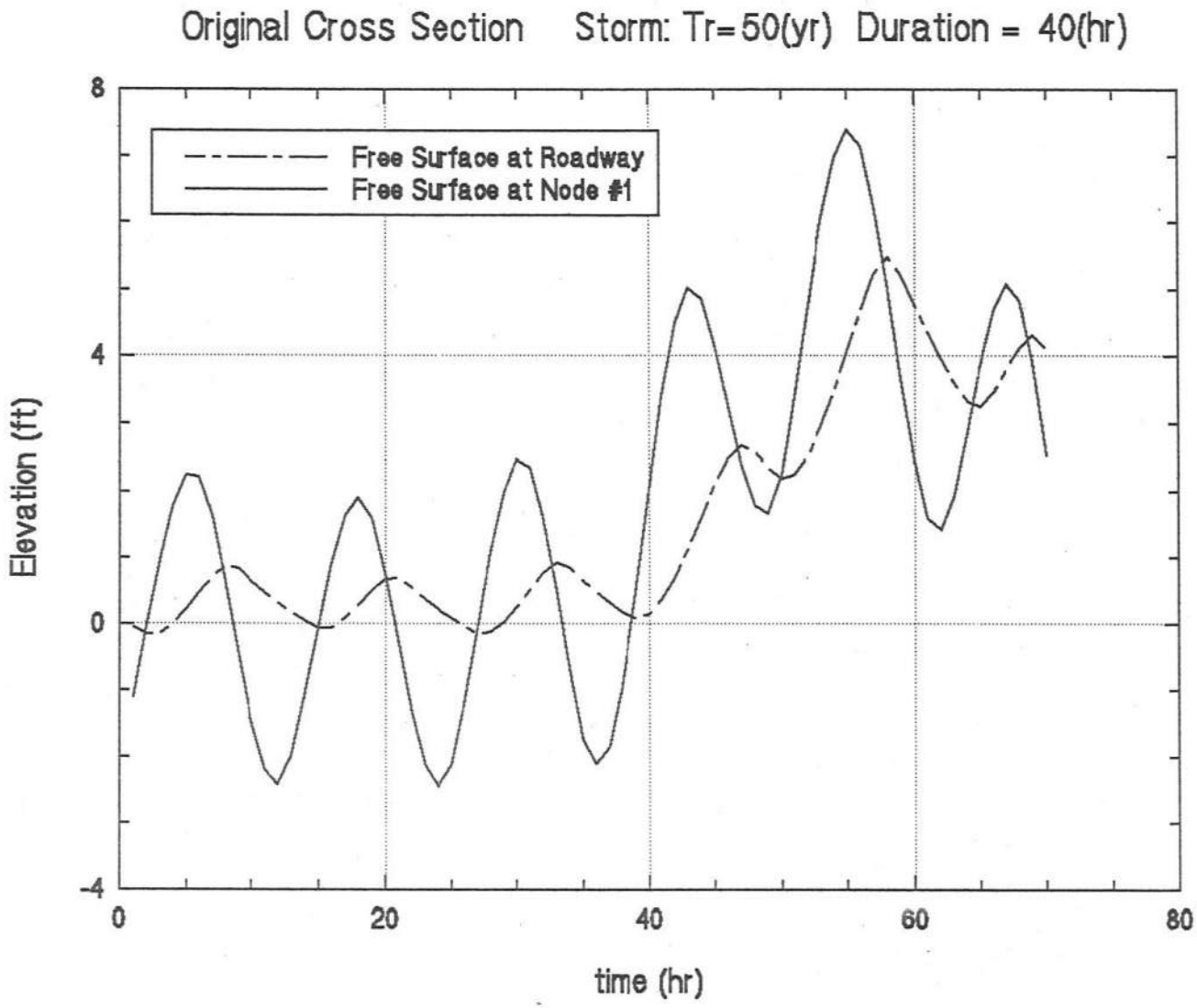
Original Cross Section Storm: Tr=50(yr) Duration = 40(hr)
Free Surface at Roadway
Free Surface at Node #1
Elevation (ft)
8
4
0
-4
0
20
40
60
80
time (hr)

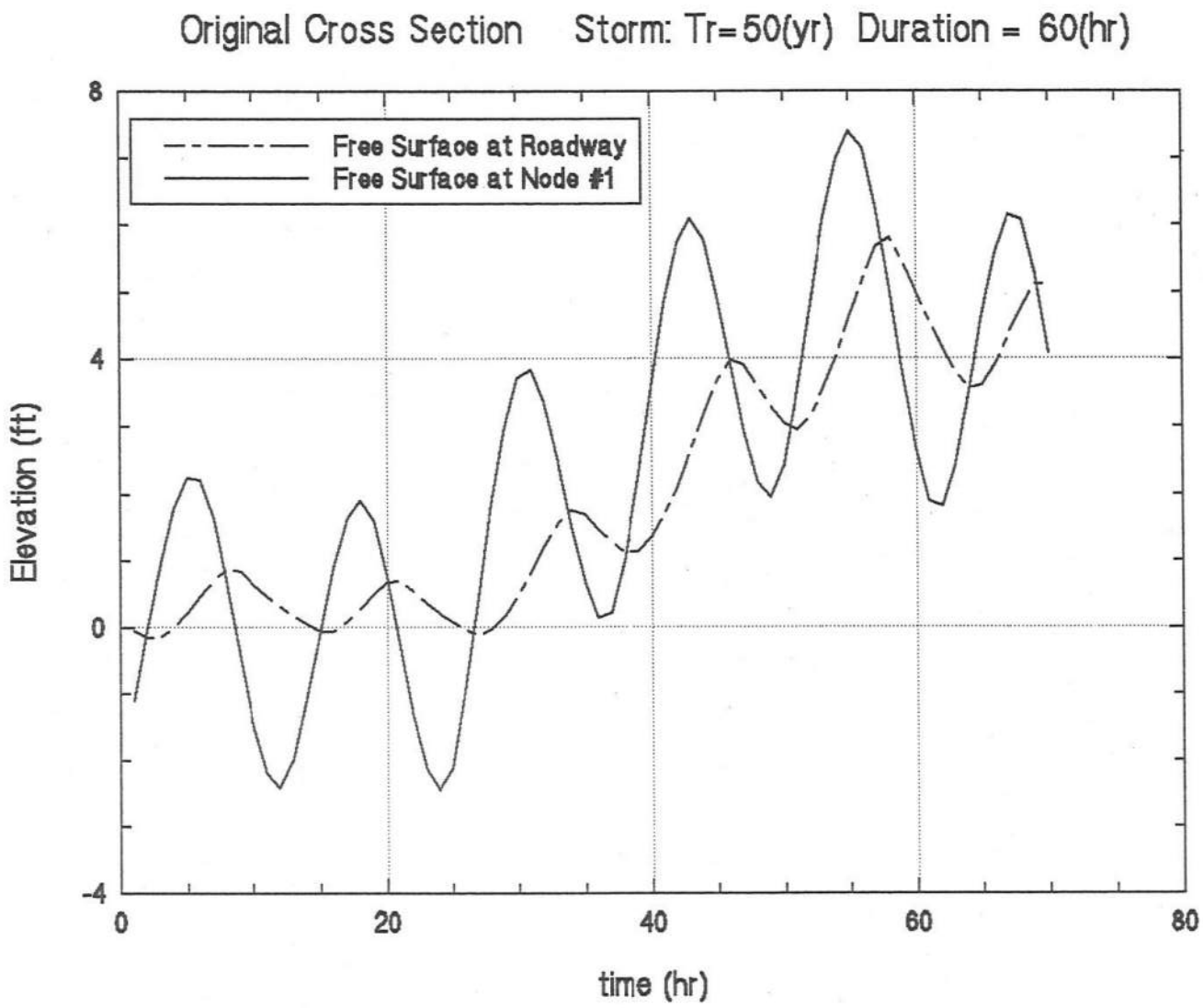
Original Cross Section Storm: Tr=50(yr) Duration = 60(hr)
Free Surface at Roadway
Free Surface at Node #1
Elevation (ft)
8
4
0
-4
0
20
40
60
80
time (hr)

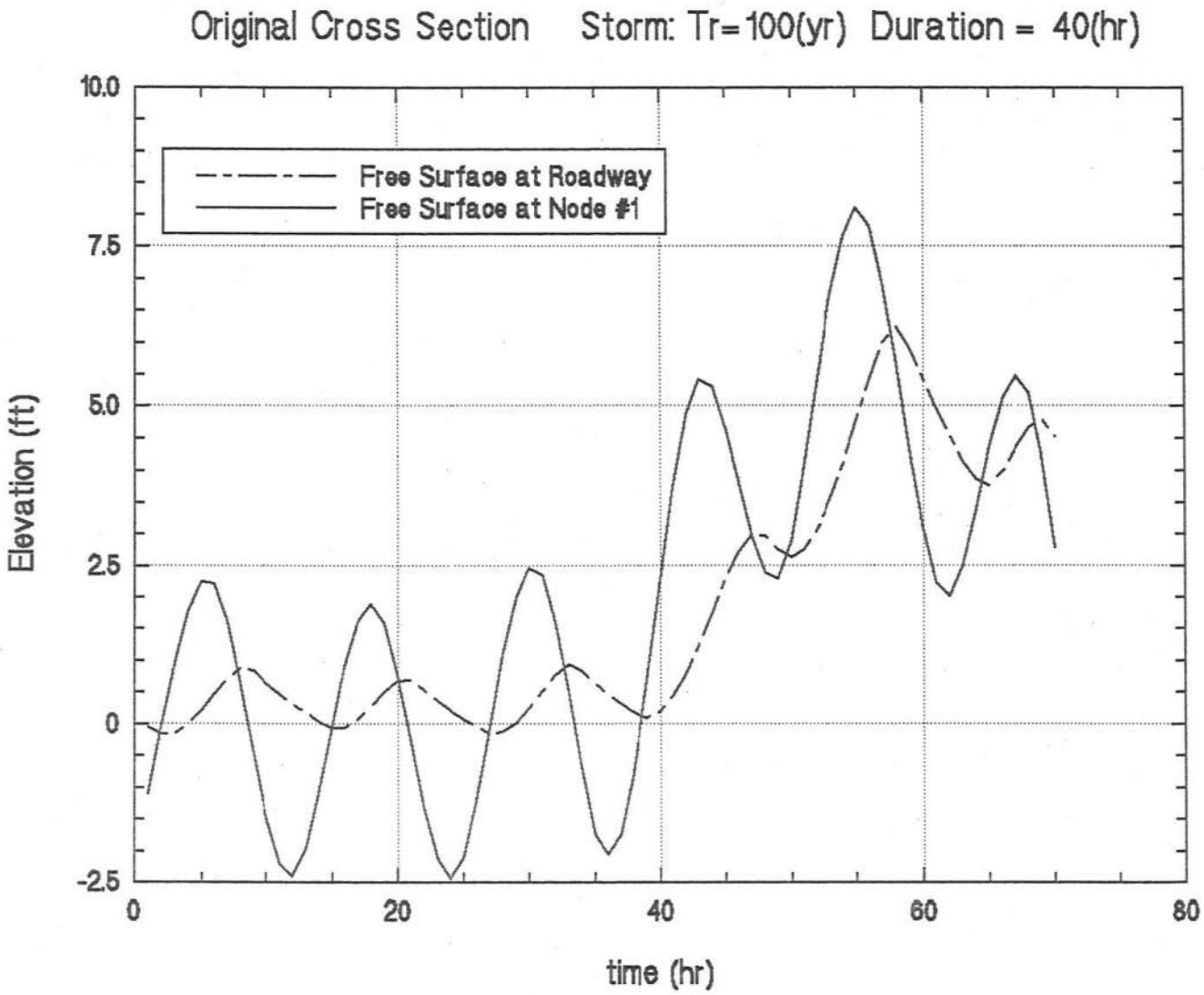
Original Cross Section Storm: Tr=100(yr) Duration = 40(hr)
Free Surface at Roadway
Free Surface at Node #1
Elevation (ft)
10.0
7.5
5.0
2.5
0
-2.5
0
20
40
60
80
time (hr)

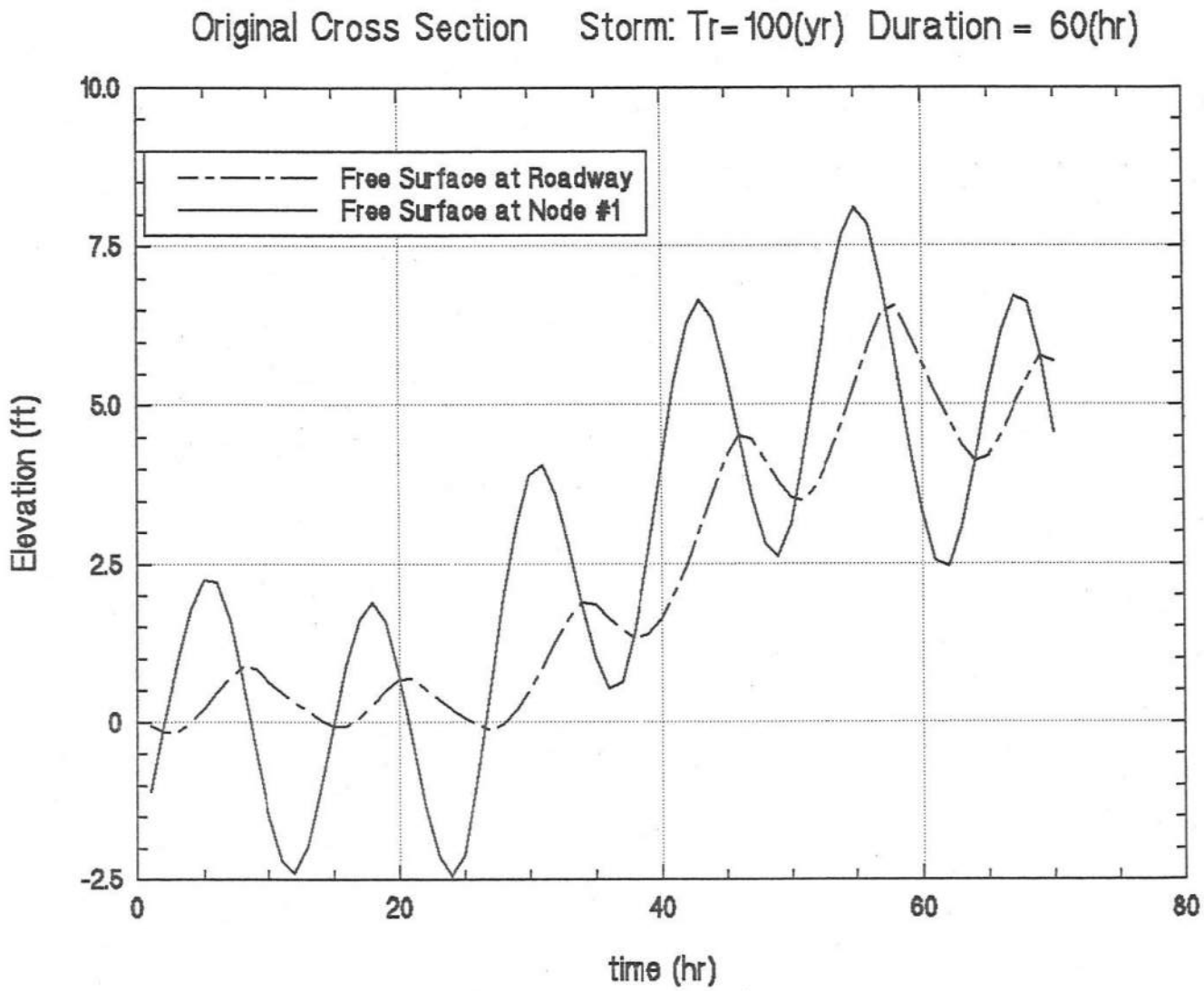
Original Cross Section Storm: Tr=100(yr) Duration = 60(hr)
Free Surface at Roadway
Free Surface at Node #1
Elevation (ft)
time (hr)
10.0
7.5
5.0
2.5
0
-2.5
0
20
40
60
80

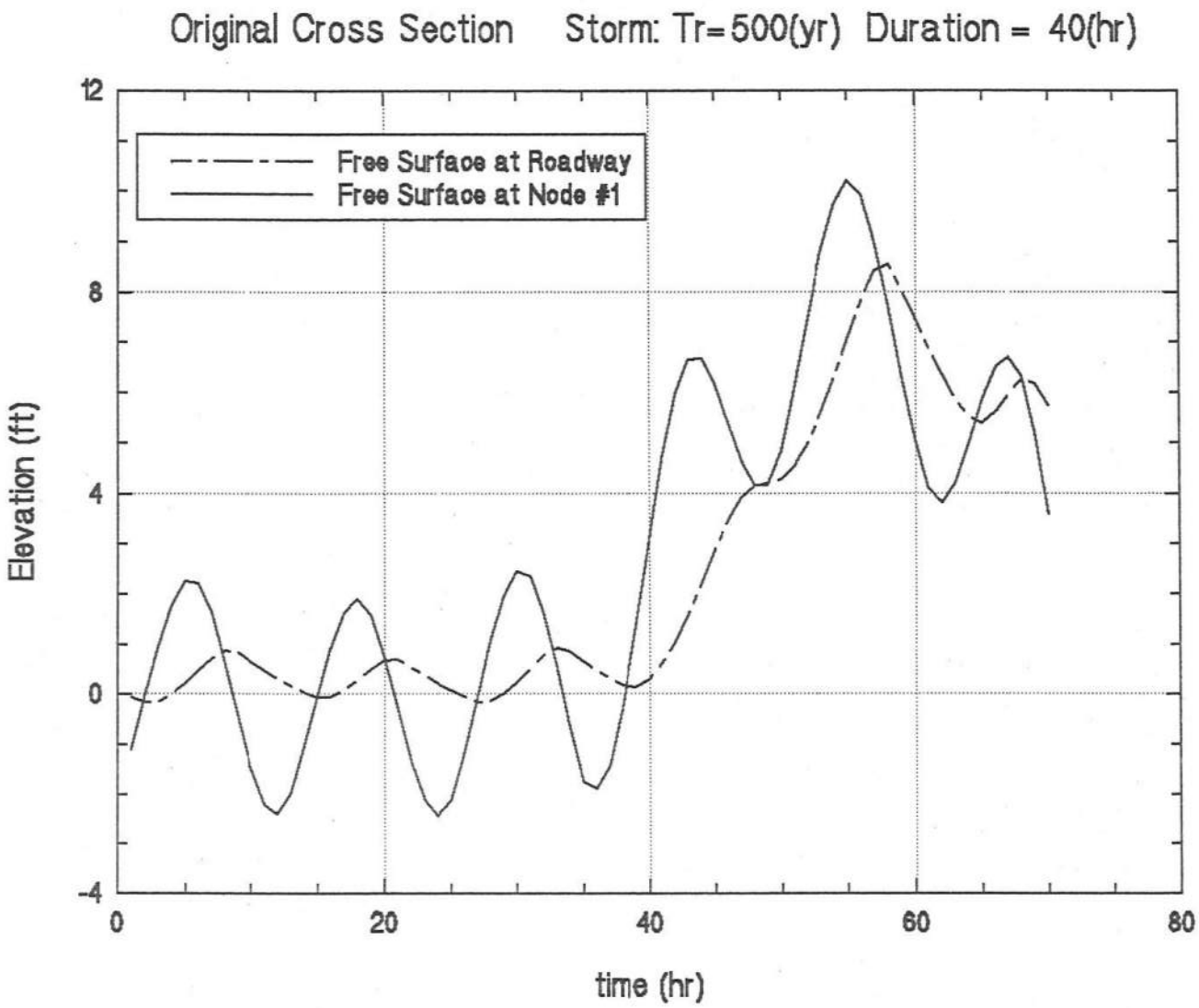
Original Cross Section Storm: Tr=500(yr) Duration = 40(hr)
Free Surface at Roadway
Free Surface at Node #1
Elevation (ft)
12
8
4
0
-4
0
20
40
60
80
time (hr)

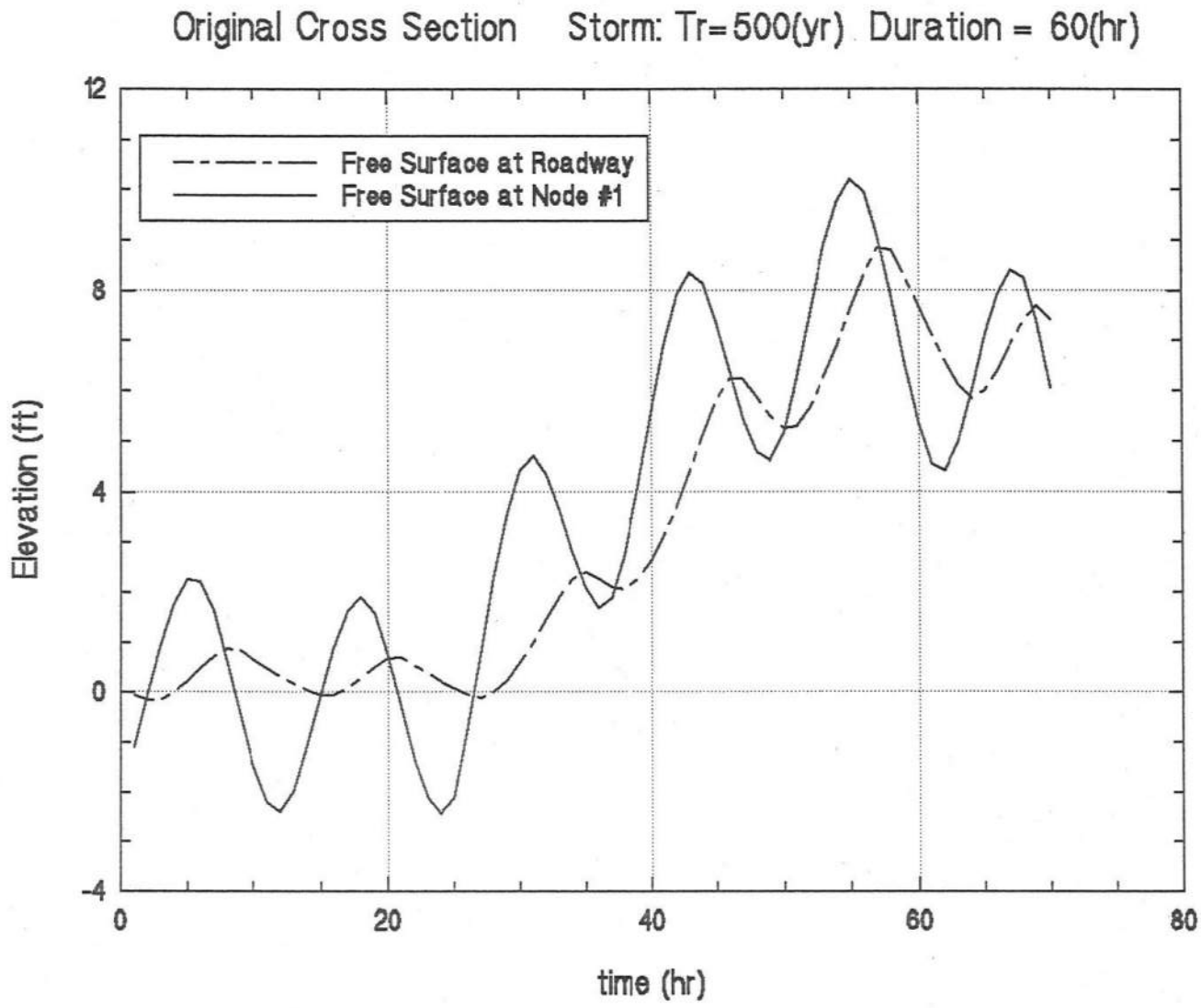
Original Cross Section Storm: Tr=500(yr) Duration = 60(hr)
Free Surface at Roadway
Free Surface at Node #1
Elevation (ft)
12
8
4
0
-4
0
20
40
60
80
time (hr)

Appendix D

Report of Preliminary Hydraulic Study

The second author of this report conducted a preliminary hydraulic study associated with the Roadway improvement project for Delaware Route 54 as a consultant to the firm Rummel • Klepper & Kahl. The report of this preliminary study is attached herein where the page number used in the original report is not changed for convience.

The conclusion of this preliminary study based on simple analyses was that the increase of the roadway elevation would be the most straightforward way to improve vehicle passage during storms in comparison to other alternatives such as bridges, culverts and an elevated permeable roadway. The raised impermeable roadway will not increase the peak stillwater elevation but may increase the stillwater elevation slightly before and after the peak of storm surge. The present study , based on a numerical model, indicates that the raised impermeable roadway with the minimum elevations in the range of 3.5 to 5.0 ft will cause practically no increase in the stillwater elevation during storms.

Hydraulic Study Associated with Roadway Improvement Project for Delaware Route 54

by

Nobuhisa Kobayashi

January, 1993

Center for Applied Coastal Research
Department of Civil Engineering
University of Delaware
Newark, Delaware 19716

ABSTRACT

Available data on storm stuge on Little Assawoman Bay and the part of the Assawoman Bay in Sussex County is reviewed and synthesized to estimate design stillwater elevations for the roadway improvement project for Delaware Route 54. Available data appears to be based on numerical models calibrated using very limited field data. Simple hydraulic analysis procedures are proposed for estimating the flow through the Ditch and the overflow over the raodway for the specified stillwater elevations on the two bays. Example calculations indicate that the overflow over the existing roadway is not negligible as compared to the flow thorugh the Ditch. As a result, roadway improvement alterativess based on discharge considerations, such as bridges and culverts, would require discharge capacities similar to that of the Ditch. A more direct way to improve vehicle passage during storms is to increase the roadway elevation. An elevated permeable roadway may need to be elevated about 7 ft above the mean sea level to satisfy the new construction requirements. A raised impermeable roadway will not increase the peak stillwater elevation as long as the peak stillwater elevations on both bays are the same and occur at the same time during storms. Before and after the peak of storm surge, the raised roadway will increase the stillwater elevation. However, its increase will be well below 1 ft unless large water velocities are reduced significantly by the raised roadway.

Contents

1 INTRODUCTION

1.1 Background

The firm, Rummel · Klepper & Kahl, was planning to perform a preliminary investigation to provide roadway improvement alternatives for Delaware Route 54. The need to investigate possible hydraulic modifications caused by the proposed roadway improvement alternatives was identified by the firm. The representatives from the firm met with Nobu Kobayashi, Associate Director, Center for Applied Coastal Research, on October 27 and December 15, 1992. This report is written on the basis of the discussions during these meetings and materials provided by the firm.

1.2 Objectives and Scope

The objectives of this preliminary hydraulic study are as follows:

1. Synthesize and interpret available data collected by the firm on the existing hydraulic and hydrographic characteristics of the part of Assawoman Bay in Sussex County and Little Assawoman Bay.

2. Develop preliminary analysis procedures to examine the existing hydraulic characteristics in the vicinity of the proposed roadway improvement site.

3. Develop preliminary analysis procedures to assess the degree of hydraulic modifications associated with roadway improvement alternatives.

4. Propose mitigation measures to reduce the hydraulic modifications if they are found to be significant.

This report is written for the firm Rummel · Klepper & Kahl, so that the firm will be able to investigate possible hydraulic modifications caused by the proposed roadway improvement

alternatives under the supervision of the consultant, Nobu Kobayashi. The tasks of the consultant include:

1. Synthesize and interpret the collected data.
2. Develop the hydraulic analysis procedures and examine the computed results obtained by the firm.
3. Propose various aspects and options which need to be investigated in this study.
4. Review the hydraulic part of the final report as well as recommend future studies, if any.
5. Attend public hearings to explain the results of this study, if requested.

2 SYNTHESIS OF COLLECTED DATA

Available data collected so far are summarized and synthesized in the following.

2.1 FEMA Flood Map

The Flood Insurance Rate Map (Community-Panel Number 100029 0295E, Sussex County, Delaware, Unincorporated Areas) was revised on April 2, 1992 by the Federal Emergency Management Agency (FEMA). Dewberry & Davis provided additional information for this map. The proposed roadway improvement site is in the vicinity of Transect 14 from the Atlantic Ocean shoreline to Assawoman Bay along the Delaware-Maryland borderline. Table 1 summarizes the flood insurance zone data along Transect 14.

The row number in Table 1 increases landward from row 1 at the Atlantic Ocean shoreline. The proposed roadway improvement site approximately corresponds to the locations of rows 3 and 4. The stillwater elevation is the maximum elevation of the free surface with no waves

Table 1: FEMA Flood Insurance Zone Data

Row	Stillwater Elevation in Feet, NGVD				Zone	Base Flood Elevation (Feet, NGVD*)
	10-Year	50-Year	100-Year	500-Year		
1	6.1	7.7	8.5	10.0	V7	11–13
2	6.1	7.7	8.5	10.0	A7	9–11
3	5.5	6.1	7.0	8.8	A7	7–9
4	2.9	4.5	5.5	7.6	A7	6–7

*Due to map scale limitations, base flood elevations shown on the map represent average elevations for the zones depicted.

during the storm of the specified recurrence interval of 10, 50, 100 and 500 years. The elevation is relative to the National Geodetic Vertical Datum (mean sea level) of 1929. The base flood elevation was explained in more detail in the report entitled, "Flood Insurance Study: Supplement-Wave Height Analysis," published in 1982 by the Federal Emergency Management Agency. The base flood elevation accounts for the effects of waves during the 100-year storm and is given by

$$\text{Base Flood Elevation} = \text{100-year Stillwater Elevation} + 0.7\ H \tag{1}$$

where H is the local wave height during the 100-year storm and the wave crest elevation is assumed to be $0.7\ H$ above the stillwater elevation. The local wave height H is limited by the maximum breaking height H_b

$$H \leq H_b = 0.78h \tag{2}$$

where h is the local stillwater depth and H_b is assumed to be given by $H_b = 0.78\ h$. The V zone in row 1 in Table 1 corresponds to the zone where $H \geq 3$ ft, while the A zone in rows 2, 3 and 4 corresponds to the zone whre $H < 3$ ft. This implies that at the proposed roadway improvement site, the wave height during the 100-year storm will be less than 3 ft and the

difference between the base flood elevation and the 100-year stillwater elevation will be less than 2.1 ft using (1).

It should be noted that the base flood elevation has been proposed to account for wave action effects on structures. All new construction is generally required to be elevated such that the first floor, including basement, is above the base flood elevation in V and A zones. On the other hand, the hydraulic characteristics at the proposed roadway improvement site are mostly determined by the stillwater elevations with no waves. As a result, the base flood elevations listed in the Flood Insurance Rate Map should be regarded as the upper limit of the 100-year water elevations along Delaware Route 54. However, the Flood Insurance Rate Map revised on April 2, 1992 appears to be based on flooding and wave action from the Atlantic Ocean only and may not have accounted for flooding and wave action from Assawoman Bay.

2.2 Flood Data from U. S. Army Corps of Engineers

The U. S. Army Corps of Engineers, Philadelphia District, provided preliminary flood information for Assawoman and Little Assawoman Bays on October 20, 1992. This data was prepared as part of the Sussex County, Delaware Type 19 Flood Insurance Study for FEMA, and as such is subject to final review, approval, and adoption by FEMA. This implies that the Flood Insurance Rate Map revised on April 2, 1992 may be revised again in the near future.

A numerical model was used to simulate storm surges through the inlet at Ocean City, Maryland. Flow into the Assawoman–Little Assawoman Bay system was assumed to be solely a function of flow through Ocean City Inlet, neglecting overtopping of the barrier island, contributions from Assawoman Canal, and freshwater runoff. It was noted, "although the Ditch is a relatively narrow connection between Little Assawoman and Assawoman Bays,

Table 2: Computed Stillwater Elevations for Both Bays

Location	Stillwater Elevation in Feet, NGVD			
	10-Year	50-Year	100-Year	500-Year
Both Bays	3.8	5.4	6.0	10.2

almost the entire area along Delaware State Route 54 from Bayville to its crossing of the Ditch is low (under 4.0 feet NGVD) and routinely floods at spring tide." However, overflow over Delaware State Route 54 appears to have not been included in the numerical model. In any case, the numerical output displaying the spatial and temporal variations of the free surface and water velocities will be very useful to examine the existing large-scale hydraulic characteristics.

Table 2 summarizes the computed stillwater elevations for the recurrence intervals of 10, 50, 100 and 500 years for the part of Assawoman Bay in Sussex County as well as for Little Assawoman Bay in Fenwich Island. The same stillwater elevation on both bays for given recurrence interval implies that the peak elevations on both bays are predicted to be the same but might not occur at the same time during the storm. The stillwater elevation listed in Table 2 falls between the stillwater elevations in rows 3 and 4 in Table 1 except for the 500-year recurrence interval. For the 500-year storm, the stillwater elevations on both bays in Table 2 were assumed to be the same as that on the ocean shoreline because of breaching of the barrier dune in several places.

The study of the U. S. Army Corps of Engineers, Philadelphia District, indicated little historical data for the bays other than for the 1991 Halloween Storm on Little Assawoman Bay. The peak elevation recorded at the NOAA tide gage at Ocean City, Maryland was 5.5 feet (NGVD), while the Delaware Department of Natural Resources and Environmental

Table 3: Earlier Estimates of Stillwater Elevations for Part of Assawoman Bay in Maryland

Stillwater Elevation in Feet, NGVD					
10-Year		50-Year		100-Year	
COE	FIS	COE	FIS	COE	FIS
2.8	2.9	4.4	4.6	5.6	5.6

Control (DNREC) reported a peak elevation of 4.0 feet (NGVD) on Little Assawoman Bay in Fenwick Island. Table 2 suggests that the recurrence interval associated with this storm on Little Assawoman Bay is slightly greater than 10 years, which appears to be reasonable.

Tables 1 and 2 may be compared with the results given in the earlier report entitled, "Reducing the Flood Damage Potential in Ocean City, Maryland," dated April 1984 and prepared by IEP, Inc. and L. R. Johnston Associates. This report summarized the stillwater elevations for the part of Assawoman Bay in Maryland compiled by the Corps of Engineers (COE) and for the Flood Insurance Studies (FIS) as shown in Table 3. The estimated stillwater elevations by COE and FIS were very similar but it is suspected that these estimates were not independent. Comparing the values in row 4 in Table 1 and Table 3, it is obvious that the stillwater elevations in row 4 in Table 1 were based on the earlier estimates given in Table 3. The stillwater elevation of 2.9 feet for the 10-year storm is too small relative to the reported peak elevation of 4.0 feet on Little Assawoman Bay during the 1991 Halloween Storm.

In conclusion, the recent study by the U. S. Army Corps of Engineers, Philadelphia District appears to be up to date and the results listed in Table 2 are more reliable than the earlier results included in the Flood Insurance Rate Map.

2.3 Other Design Considerations

The maximum stillwater elevation during a design storm may be estimated using Table 2. The effects of waves during the design storm may be accounted for using (1) and (2). The wave crest elevation may be assumed to be 0.7 H above the stillwater elevation. The local wave height H may be assumed to be smaller than 3 feet and should not exceed the breaking height $H_b = 0.78\,h$ where h is the local stillwater depth. This criterion yields

$$H < 3 \text{ ft} \qquad \text{for} \qquad h > 3.8 \text{ ft} \tag{3a}$$

$$H \leq 0.78\,h \qquad \text{for} \qquad h \leq 3.8 \text{ ft} \tag{3b}$$

The stillwater elevations listed in Table 2 include the effects of astronomical tides. However, it is desirable to collect tidal data with no storm effects since spring tide occurs at or near the time of new or full moon, and rises highest from the mean sea level. The study by the U. S. Army Corps of Engineers, Philadelphia District has indicated that Delaware State Route 54 from Bayville to the Ditch routinely floods at spring tide.

The greenhouse effect and resulting increase in the earth's temperature may accelerate the mean sea-level rise. The rise of sea level relative to land level was about one foot over the past century along the East Coast of the United States (Dean et al. 1987). One needs to answer the question of whether one should design or upgrade a structure with the anticipation of future sea-level rise or retrofit the structure when the rise occurs (Titus et al. 1987). The effects of the relative sea-level rise on bays and estuaries were reviewed by the ASCE Task Committee on Sea-Level Rise and Its Effects on Bays and Estuaries (1992). It should be stated that the stillwater elevations given in Table 2 do not include the relative sea-level rise in the future. In any case, the future sea-level rise during the service life of

Table 4: Calculated Risk for Different Recurrence Intervals

T_r (years)	Stillwater Elevation (feet)	Risk		
		N = 10 years	N = 20 years	N = 30 years
10	3.8	0.65	0.88	0.96
50	5.4	0.18	0.33	0.45
100	6.0	0.10	0.18	0.26

the improved roadway will be small relative to the stillwater elevation difference associated with the different recurrence intervals shown in Table 2. This implies that the selection of an appropriate recurrence interval will be crucial.

The risk, that is, the probability that the design stillwater elevation will be exceeded during the service life of N years may be estiamted by (Linsley et al. 1992)

$$\text{Risk} = 1 - \left(1 - \frac{1}{T_r}\right)^N \tag{4}$$

where T_r is the recurrence interval. Table 4 shows the calculated values of the risk using (4) for T_r = 10, 50 and 100 years and N = 10, 20 and 30 years. The increase of the recurrence interval T_r from 10 years to 50 years will reduce the risk significantly for the service life N = 10–30 years but will result in the increase of the stillwater elevation of 1.6 feet. The increase of T_r form 50 years to 100 years will reduce the risk modestly with the corresponding modest increse of the stillwater elevation of 0.6 feet. This simple analysis suggests the necessity of considering various factors in determining the design stillwater elevation.

3 FLOW THROUGH THE DITCH

The flow through the Ditch is analyzed to examine the water exchange between Assawoman Bay and Little Assawoman Bay. The estimated discharge through the Ditch will be compared

with the discharge over the existing roadway to assess whether the effect of the overflow over the roadway is negligible or not in the large-scale numerical modeling performed by the U. S. Army Corps of Engineers, Philadelphia District.

3.1 Hydraulic Analysis Procedure

The flow through the Ditch is similar to the flow through an inlet as depicted in Fig. 1. The representative length and width of the Ditch are denoted by L and B, respectively. The representative depth in the Ditch below the mean sea level (MSL, NGVD) is denoted by d in Fig. 1 where η is the stillwater elevation above the mean sea level. The waterdepth h below the stillwater level is given by $h = (d + \eta)$. The stillwater levels far from the Ditch are essentially horizontal. The horizontal stillwter elevations south and north of the Ditch are denoted by η_s and η_n, respectively. If $\eta_s > \eta_n$, the difference between the hydrostatic pressures south and north of the Ditch forces the flow in the Ditch from the south to the north as shown in Fig. 1 where V is the average water velocity in the Ditch and taken to be positive for $\eta_s > \eta_n$. If $\eta_s = \eta_n$, $V = 0$ and no flow occurs in the Ditch. If $\eta_s < \eta_n$, the difference between the hydrostatic pressures north and south of the Ditch causes the flow in the Ditch from the north to the south. For $\eta_s < \eta_n$, V is negative and the flow direction is opposite to that shown in Fig. 1.

The hydraulic analysis of the flow through the Ditch is based on the following energy equation for water per unit weight as described in the Shore Protection Manual (1984) for hydraulic currents in inlets

$$\eta_s - \eta_n = \left(k_{en} + k_{ex} + \frac{fL}{4R}\right) \frac{|V|V}{2g} \tag{5}$$

where k_{en} = entrance loss coefficient; k_{ex} = exit loss coefficient; f = Darcy-Weisbach friction factor; g = gravitational acceleration; and R = hydraulic radius defined as $R = (A/P)$ with

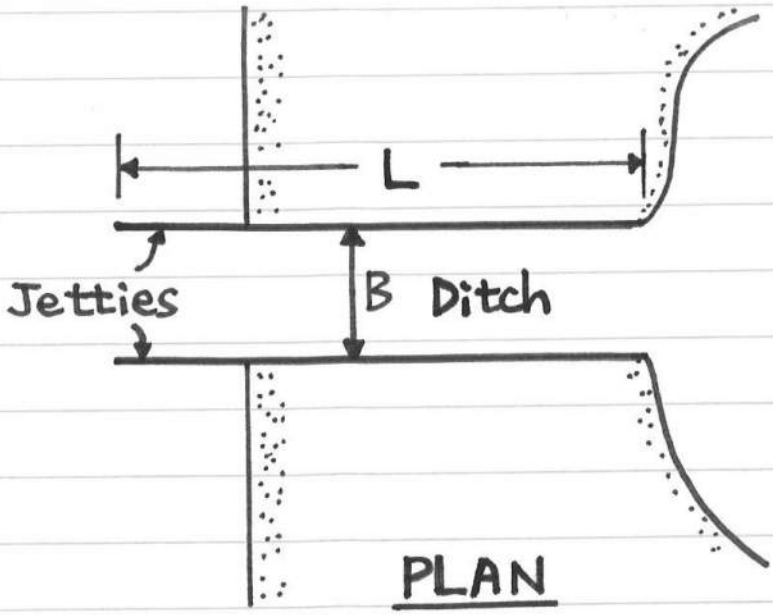

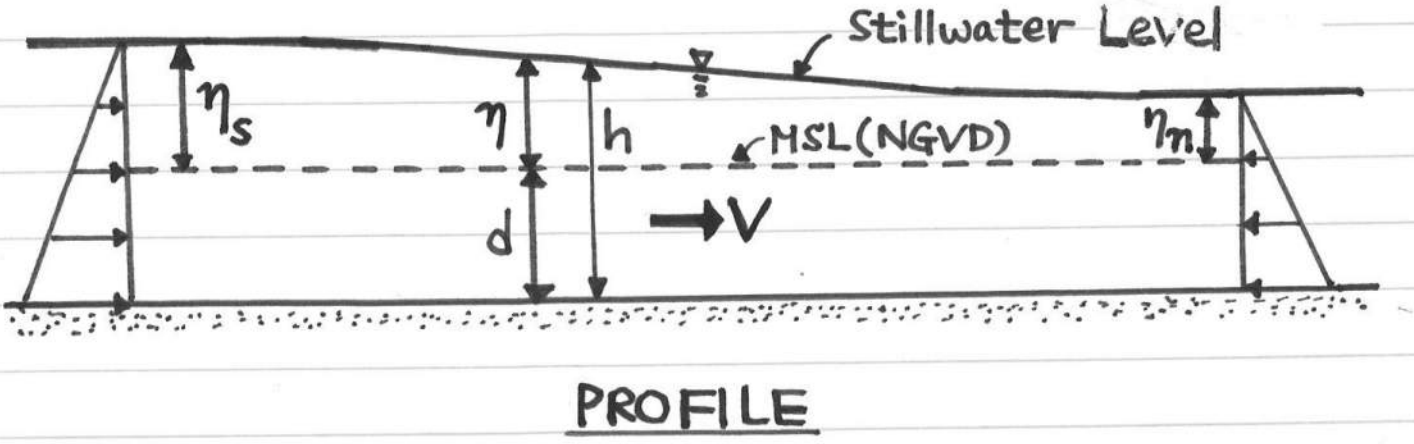

Figure 1: Definition Sketch for Flow through Ditch

A = cross-section area; and P = wetted perimeter where the bottom friction acts. The cross section in the Ditch may be assumed to be approximately rectangular and expressed by $A \simeq Bh$, $P \simeq (B + 2h)$, and $h \simeq [d + (\eta_s + \eta_n)/2]$. The hydraulic radius R in (5) may then be approximated by

$$R \simeq \frac{B[d + 0.5(\eta_s + \eta_n)]}{B + 2d + \eta_s + \eta_n} \tag{6}$$

The typical values of k_{en}, k_{ex} and f in (5) are as follows: k_{en} = 0–0.2, $k_{ex} \simeq 1.0$, and f = 0.01–0.07. For most calculations, the Shore Protection Manual (1984) suggests that k_{en} = 0.2, $k_{ex} = 1.0$ and $f = 0.03$ if no data is available to calibrate these empirical coefficients.

The absolute value $|V|$ of the water velocity V in the Ditch can be obtained from (5)

$$|V| = \left(k_{en} + k_{ex} + \frac{fL}{4R}\right)^{-0.5} (2g\,|\eta_s - \eta_n|)^{0.5} \tag{7}$$

where $V > 0$ for $\eta_s > \eta_n$, $V = 0$ for $\eta_s = \eta_n$, and $V < 0$ for $\eta_s < \eta_n$. The discharge Q through the Ditch is given by $Q = VA$ which may be approximated as

$$Q \simeq VB[d + 0.5(\eta_s + \eta_n)] \tag{8}$$

During a storm, η_s and η_n vary with respect to time t. Accordingly, the values of V and Q in the Ditch vary with time t. A numerical model for Assawoman and Little Assawoman Bays connected with the Ditch would hence be required to predict the temporal variations of V and Q in the Ditch. In this preliminary study, the typical values of V and Q are estimated for the ranges of the stillwater elevations η_s and η_n estimated from Table 2.

3.2 Example Calculations

The map used for the Beach Access Study (Scale 1" = 200', Sheet No. C-5) dated October, 1989 is used to estimate the following values:

Representative Ditch Length $L \simeq$ 1,400 ft

Representative Ditch Width $B \simeq 200$ ft

The representative water depth d in the Ditch below the mean sea level (NGVD) is not available. The following value of d is assumed as a reasonable guess:

Representative Water Depth in the Ditch $d \simeq 10$ ft

which must be replaced by a more accurate value if bathymetry data is available. In addition, the following standard values of the empirical coefficients are assumed:

Entrance Loss Coefficient	$k_{en} \simeq 0.2$
Exit Loss Coefficient	$k_{ex} \simeq 1.0$
Darcy-Weisbach Friction Factor	$f \simeq 0.03$

The peak values of the stillwater elevations η_s and η_n for the storms of the recurrence intervals of 10, 50 and 100 years may be assumed to be the same as those listed in Table 2. For the 500-year storm, the flow through the Ditch would be secondary since the entire area under consideration would be flooded severely. The simple analysis procedure based on (6), (7) and (8) yields the same absolute values of V and Q even if the values of η_s and η_n are exchanged. As a result, the following example calculations will be limited to the case where $\eta_s > \eta_n$ for which $V > 0$ and $Q > 0$. The peak values of the stillwater elevations η_s and η_n on both bays listed in Table 2 are the same but may last over different intervals. Consequently, $(\eta_s - \eta_n) = 0.1$, 0.5, 1.0 and 2.0 ft are used in the following example calculations.

Table 5 shows the calculated values of R, V and Q for $\eta_s = 3.8$, 5.4 and 6.0 ft, corresponding to the recurrence interval $T_r = 10$, 50 and 100 years in Table 2. The hydraulic radius R calculated using (6) is slightly larger than the assumed water depth $d = 10$ ft. The average water velocity V in the Ditch calculated using (7) is mostly determined by the

Table 5: Calculated Water Velocity and Discharge in the Ditch

η_s (ft)	η_n (ft)	$\eta_s - \eta_n$ (ft)	R (ft)	V (ft/s)	Q (ft^3/s)
3.8	3.7	0.1	12.1	1.8	4,900
	3.3	0.5	11.9	3.9	10,700
	2.8	1.0	11.7	5.5	14,700
	1.8	2.0	11.3	7.8	19,900
5.4	5.3	0.1	13.3	1.8	5,500
	4.9	0.5	13.2	4.0	12,200
	4.4	1.0	13.0	5.7	16,900
	3.4	2.0	12.6	8.0	22,900
6.0	5.9	0.1	13.8	1.8	5,800
	5.5	0.5	13.6	4.0	12,700
	5.0	1.0	13.4	5.7	17,700
	4.0	2.0	13.0	8.0	24,000

assumed stillwater elevation difference $(\eta_s - \eta_n) = 0.1$, 0.5, 1.0 and 2.0 ft. The discharge Q in the Ditch calculated using (8) increases with the increase of $(\eta_s - \eta_n)$ and η_s. Table 5 suggests that the discharge Q in the Ditch may vary with time during a storm but is of the order of 10,000 ft^3/s as long as $|\eta_s - \eta_n| = 0.1$–2.0 ft and $d \simeq 10$ ft.

4 OVERFLOW OVER THE ROADWAY

The discharge of water over the existing roadway between Assawoman and Little Assawoman Bays is estimated using a simple hydraulic analysis procedure and compared with the discharge in the Ditch listed in Table 5.

4.1 Hydraulic Analysis Procedure

The flow over the idealized dip of the roadway is depicted in Fig. 2. The idealized dip is characterized by its length L_c and its crest elevation Z_c above the mean sea level (MSL,

NGVD). For simplicity, Z_c is assumed to be constant over the length L_c. The water depth below the stillwater level and the depth-averaged velocity at the crest of the dip are denoted by h_c and V_c, respectively. The stillwater levels far from the dip are essentially horizontal. The horizontal stillwater elevations south and north of the dip are denoted by η_s and η_n, respectively, in the same way as the analysis for the flow through the Ditch in Section 3.1. The following analysis is limited to the case of $\eta_s \geq \eta_n$ since the results obtained for $\eta_s > \eta_n$ will be valid even for $\eta_s < \eta_n$ if η_s and η_n are exchanged.

For the case of $\eta_s > \eta_n$ as shown in Fig. 2, the water south of the dip converges toward the dip in a manner similar to a steady sink flow. The depth-averaged velocity V south of the dip increases to V_c at the crest of the dip as the water approaches the dip because of the conservation of water mass which requires that the discharge over the dip is the same as the discharge through the side of an aproximately half cylinder as depicted in Fig. 2. The stillwater elevation η above MSL corresponding to the velocity V decreases from η_s far from the dip to η_c at the crest of the dip as the velocity V increases from essentially zero far from the dip to V_c at the crest of the dip. This is because the potential energy per unit water weight represented by η is converted into the kinetic energy per unit water weight expressed as $V^2/(2g)$ where g is the gravitational acceleration. On the other hand, the diverging flow north of the dip is similar to a jet flow issuing from the dip. The kinetic energy per unit water weight, $V_c^2/(2g)$, of the water issuing from the dip will be dissipated in the jet flow.

For the converging sink flow south of the dip, energy dissipation may simply be neglected and the energy equation per unit water weight may be expressed as

$$\eta + \frac{V^2}{2g} \simeq \text{ constant for converging flow} \tag{9}$$

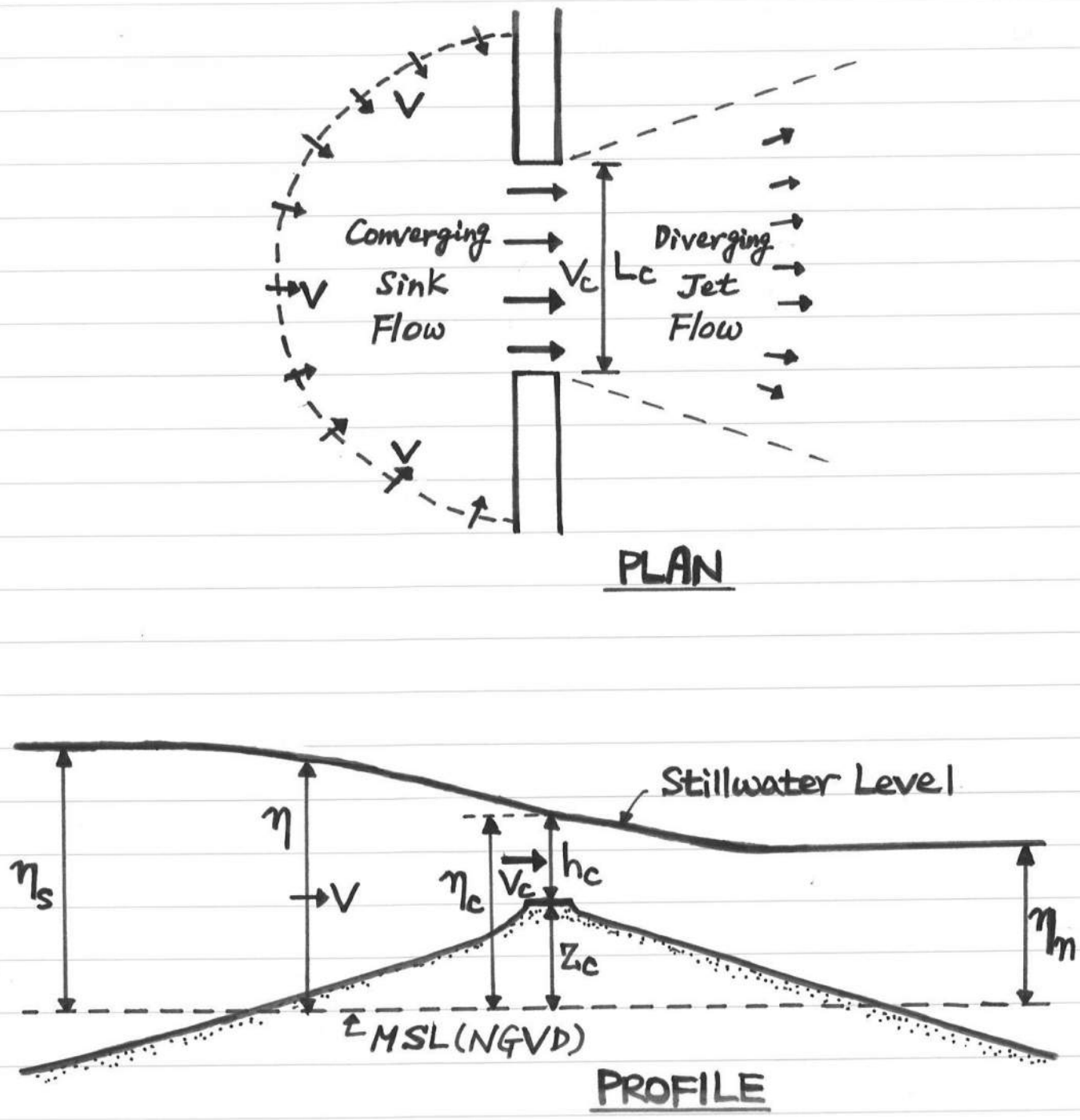

Figure 2: Definition Sketch for Overflow over Roadway

which implies that η becomes the maximum when $V = 0$. Equating the left hand side of (9) far south of the dip and at the crest of the dip, we obtain

$$\eta_s \simeq \eta_c + \frac{V_c^2}{2g} \tag{10}$$

where η_s corresponds to the stillwater elevation estimated for the case of no overflow over the roadway. Eq. (10) yields

$$V_c \simeq [2g(\eta_s - \eta_c)]^{0.5} \quad \text{for } \eta_s \geq \eta_c \tag{11}$$

The depth h_c at the crest of the dip is given by

$$h_c = \eta_c - Z_c \quad \text{for } \eta_c \geq Z_c \tag{12}$$

The discharge Q_c over the dip is then expressed as

$$Q_c = V_c \, h_c \, L_c \tag{13}$$

For given η_s, Z_c and L_c, the values of V_c, h_c and Q_c can be estimated using (11), (12) and (13) provided η_c is known.

If $\eta_c > \eta_n$ as shown in Fig. 2, the flow over the crest of the dip is similar to the steady flow over a spillway or a weir. The flow at the crest of the dip may then be assumed to be critical. For the critical flow, $V_c = \sqrt{gh_c}$, which yields $\eta_c = (2\eta_s + Z_c)/3$ using (11) and (12). If the calculated value of $(2\eta_s + Z_c)/3$ is not greater than η_n, the critical flow will not occur at the crest of the dip. For this case, it may simply be assumed that $\eta_c \simeq \eta_n$ to avoid the analysis of the diverging jet flow. Combining both cases, η_c may be estimated as

$$\eta_c \simeq \max\left[\frac{2\eta_s + Z_c}{3} \, , \, \eta_n\right] \tag{14}$$

where max indicates the larger value of the two quantities in the square brackets. For $\eta_s = \eta_n > Z_c$, (14) yields $\eta_c = \eta_n = \eta_s$ and $V_c = 0$ from (11). The depth h_c given by (12)

Table 6: Three Idealized Dips of Existing Roadway

Dip Number	Z_c (ft)	L_c (ft)
1	2.5	400
2	2.1	1,000
3	2.5	1,000

will then become the maximum

$$\max\ h_c = \eta_s - Z_c \quad \text{for } \eta_s = \eta_n > Z_c \tag{15}$$

Further, the stillwater elevation η in the vicinity of the dip will be the maximum and equal to $\eta_s = \eta_n$ if the peak stillwater elevations on both bays are equal and occur at the same time. In other words, if the peak duration of a storm is sufficiently long, the peak stillwater elevations on both bays will be essentially horizontal as implied in Table 2. This situation is similar to the essenetially horizontal stillwater elevation in the vicinity of the roadway at high tide when the water velocity V is essentially zero.

4.2 Example Calculations

The map used for the Beach Access Study (Scale 1" = 200', Sheet No. C-5) dated October, 1989 is used to identify three dips of the existing roadway as listed in Table 6 where the elevation in the map is assumed to be relative to the mean sea level (NGVD). More detailed examination of the topography of the existing roadway may yield more accurate geometry of the dips but the essential results of the following example calculations are expected to remain valid.

Example calculations are made for $\eta_s = 3.8$, 5.4 and 6.0 ft, and $(\eta_s - \eta_n) = 0.1$, 0.5, 1.0 and 2.0 ft to compare the calculated results with those shown in Table 5. Table 7 shows the

calculated values of η_c, h_c, and V_c using (14), (12) and (11), respectively for $Z_c = 2.1$ and 2.5 ft. The calculated values of h_c and Z_c may be compared with the maximum value of h_c based on (15). The difference of the stillwater elevations η_s and η_c is equal to the velocity head, $V_c^2/(2g)$, on the basis of (10). The values of $(\eta_s - \eta_c)$ in Table 7 are no more than about 1 ft since the velocity V_c is typically less than about 8 ft/s and $g = 32.2$ ft/s^2. The calculated values of V_c at the crests of the dips for given η_s and η_n are similar to those of the velocity V in the Ditch listed in Table 5.

Table 8 shows the discharge Q_c calculated using (13) for each of the three dips as well as the sum of the discharge Q_c for the three dips for $\eta_s = 3.8$, 5.4 and 6.0 ft, and $(\eta_s - \eta_n) =$ 0.1, 0.5, 1.0 and 2.0 ft. Comparison of Tables 5 and 8 indicates that the sum of the discharge Q_c over the dips is of the same order of magnitude as the discharge Q in the Ditch for given η_s and η_n. The simple analysis procedures employed herein may not be very accurate but the overflow over the existing roadway is not negligible as compared to the flow through the Ditch. The peak stillwater elevations on both bays given in Table 2 were based on the assumption of negligible overflow effects. Nevertheless, the peak stillwater elevations given in Table 2 may still be reliable since the water velocity is essentially zero during the peak of the storm surge provided the peak stillwater elevations on both bays are the same as presented in Table 2 and occur at the same time. The overflow over the existing roadway will modify the temporal variation of the stillwater elevation on Little Assawoman Bay during a storm, although it may not modify the peak stillwater elevation.

5 ROADWAY IMPROVEMENT ALTERNATIVES AND HYDRAULIC EFFECTS

The maximum value of h_c for $\eta_s = 3.8$, 5.4 and 6.0 ft shown in Table 7 may be regarded as the peak stillwater depth on the crest of the existing roadway for the recurrence interval

Table 7: Calculated Values of η_c, h_c and V_c at Crests of Dips

η_s (ft)	Z_c (ft)	max h_c (ft)	η_n (ft)	η_c (ft)	h_c (ft)	V_c (ft/s)
3.8	2.1	1.7	3.7	3.7	1.6	2.5
			3.3	3.3	1.2	5.7
			2.8	3.23	1.13	6.1
			1.8	3.23	1.13	6.1
	2.5	1.3	3.7	3.7	1.2	2.5
			3.3	3.37	0.87	5.3
			2.8	3.37	0.87	5.3
			1.8	3.37	0.87	5.3
5.4	2.1	3.3	5.3	5.3	3.2	2.5
			4.9	4.9	2.8	5.7
			4.4	4.4	2.3	8.0
			3.4	4.3	2.2	8.4
	2.5	2.9	5.3	5.3	2.8	2.5
			4.9	4.9	2.4	5.7
			4.4	4.43	1.93	7.9
			3.4	4.43	1.93	7.9
6.0	2.1	3.9	5.9	5.9	3.8	2.5
			5.5	5.5	3.4	5.7
			5.0	5.0	2.9	8.0
			4.0	4.7	2.6	9.1
	2.5	3.5	5.9	5.9	3.4	2.5
			5.5	5.5	3.0	5.7
			5.0	5.0	2.5	8.0
			4.0	4.83	2.33	8.7

Table 8: Calculated Discharge Q_c over Three Dips

η_s (ft)	η_n (ft)	Q_c (ft^3/s)			Sum of Q_c (ft^3/s)
		Dip 1	Dip 2	Dip 3	
3.8	3.7	1,200	4,000	3,000	8,200
	3.3	1,800	6,800	4,600	13,200
	2.8	1,800	6,900	4,600	13,300
	1.8	1,800	6,900	4,600	13,300
5.4	5.3	2,800	8,000	7,000	17,800
	4.9	5,500	16,000	13,700	35,200
	4.4	6,100	18,400	15,200	39,700
	3.4	6,100	18,500	15,200	39,800
6.0	5.9	3,400	9,500	8,500	21,400
	5.5	6,800	19,400	17,100	43,300
	5.0	8,000	23,200	20,000	51,200
	4.0	8,100	23,700	20,300	52,100

T_r = 10, 50 and 100 years, respectively, on the basis of the peak stillwater elevations on both bays listed in Table 2. The maximum value of h_c on the crest of the roadway with its elevation Z_c = 2.1 ft is estimated to be 1.7, 3.3 and 3.9 ft for T_r = 10, 50 and 100 years, respectively. The water velocity V_c on the crest of the roadway will be essenteially zero when the water depth h_c becomes the maximum. The water depth h_c will be reduced by about 1 ft when the water velocity V_c becomes as large as about 8 ft/s. In addition, wave effects and other factors will need to be considered as explained in Section 2.3.

One of the objectives of the roadway improvement is to improve the vehicle passage during storms. To quantify the vehicle passage improvement, it will be necessary to establish the criterion of the vehicle passage based on the water depth h_c, the water velocity V_c, and other factors including wind waves. If this criterion is exceeded, no vehicle passage will be allowed. The frequency and duration of no vehicle passage could then be estimated by predicting the temporal variations of h_c, V_c and wind waves for various storms with different recurrence

intervals. Roadway improvement alternatives could be compared by predicting how much each alternative would reduce the frequency and duration of no vehicle passage. However, the present hydraulic analysis does not examine the temporal variations of the stillwater depth h_c and the water velocity V_c on the crest of the roadway during storms since no data is available on the temporal variations of the stillwater elevations on both bays. As a result, roadway improvement alternatives are evaluated in terms of their possible capabilities in reducing the peak stillwater depth on the crest of the improved roadway. Furthermore, hydraulic considerations associated with the alternatives are given concisely to minimize adverse effects if any.

5.1 Bridges

Bridges may be built at the locations of the dips of the existing roadway to raise the elevation of the roadway but allow water to flow under the bridges. Since the length L_c of each of the dips as listed in Table 6 is relatively large, it may be required to concentrate the flow in a narrower channel. Since the estimated discharge Q_c for each of the dips listed in Table 8 is of the same order of magnitude as the discharge through the Ditch, the cross-sectional area of the channel under the bridge may become as large as that of the Ditch. Dredging of the channel may then become necessary. The dredged channel will allow water to flow even under non-storm conditions unlike the existing roadway. Hydraulic and environmental effects of the dredged channel on Assawoman and Little Assawoman Bays will need to be assessed. Furthermore, the dredged channel will not lower the peak stillwater elevations on both bays which will be essentially horizontal. Consequently, flooding on the remaining segments of the existing roadway will need to be mitigated separately. In short, bridges combined with dredged channels may improve the water exchange between Assawoman and Little Assawoman Bays but will not be very effective in reducing the peak stillwater depth

on the entire roadway under investigation.

5.2 Culverts

A culvert is a buried barrel or pipe used to allow water to flow from one side to the other side of a roadway. Culverts are present under the existing roadway. The culvert hydraulics are described in hydraulic textbooks (e.g., Linsley et al. 1992). Under the conditions of submerged entrance and outlet, the energy equation per unit water weight used to estimate the water velocity in the culvert is similar to (5) for the flow through the Ditch. Consequently, the water velocity in the culvert can be as large as the water velocity in the Ditch. However, the discharge through the culvert is much smaller than the discharge through the Ditch because the cross-sectional area of the culvert is much smaller than that of the Ditch. Relatedly, the discharge through the existing culverts is much smaller than the discharge over the crest of the existing roadway during storms. The existing culverts may be beneficial to the water exchange between Assawoman and Little Assawoman Bays under normal conditions of no overflow over the roadway.

5.3 Elevated Permeable Roadway

A simple and direct way to reduce the peak stillwater depth on the crest of the roadway is to raise the elevation of the roadway since the peak stillwater elevation is essentially horizontal. If the discharge over the existing roadway during storms is to be maintained, the elevated roadway will need to be permeable. The elevated roadway may be designed such that water will be allowed to flow under the elevatged roadway. However, the elevated roadway itself will need to be designed to withstand current and wave forces during storms. As discussed in relation to (1), the elevated roadway may be required to be constructed such that the roadway is above the base flood elevation defined by (1). Assuming that the Flood Insurance

Rate Map revised on April 2, 1992 will soon be re-revised using the results tabulated in Table 2, the base flood elevation will be about 7 ft above the mean sea level (NGVD). Since the existing roadway is only 2–3 ft above the mean sea level, an elevation increase of 4–5 ft will be necessary. This will cause great inconvenience to residents along the existing roadway.

5.4 Raised Impermeable Roadway

A simple way to raise the elevation of the roadway is to place fill on the existing roadway. The raised impermeable roadway will reduce or eliminate the discharge over the raised roadway during storms. Environmental effects of the raised roadway on Little Assawoman Bay will need to be examined. These effects will be limited to the duration of overflow over the roadway at the time when the discharge through the Ditch is large. Consequently, long-term effects may not be appreciable. In addition, the raised roadway will need to be paved against currents and waves during storms. The pavement of the existing roadway will give a sufficient guideline since the raised roadway will be subjected to the current and wave forces less than those acting on the existing roadway.

One of the major concerns regarding the raised impermeable roadway is whether the raised roadway would raise the stillwater elevation in a manner similar to the backwater effect behind a dam in a river as shown in Fig. 3. Water in a river flows essentially parallel to the sloping bottom due to the component of the gravity force parallel to the bottom. The free surface for steady uniform flow in the river is parallel to the sloping bottom. The presence of a dam in the river reduces the water velocity and the free surface behind the dam becomes essentially horizontal. If the crest elevation of the dam is increased, the stillwater elevation behind the dam will increase so that the stillwater level behind the raised dam will become essentially horizontal. As a result, the increase of the stillwater elevation will be approximately equal to the increase of the crest elevation of the dam.

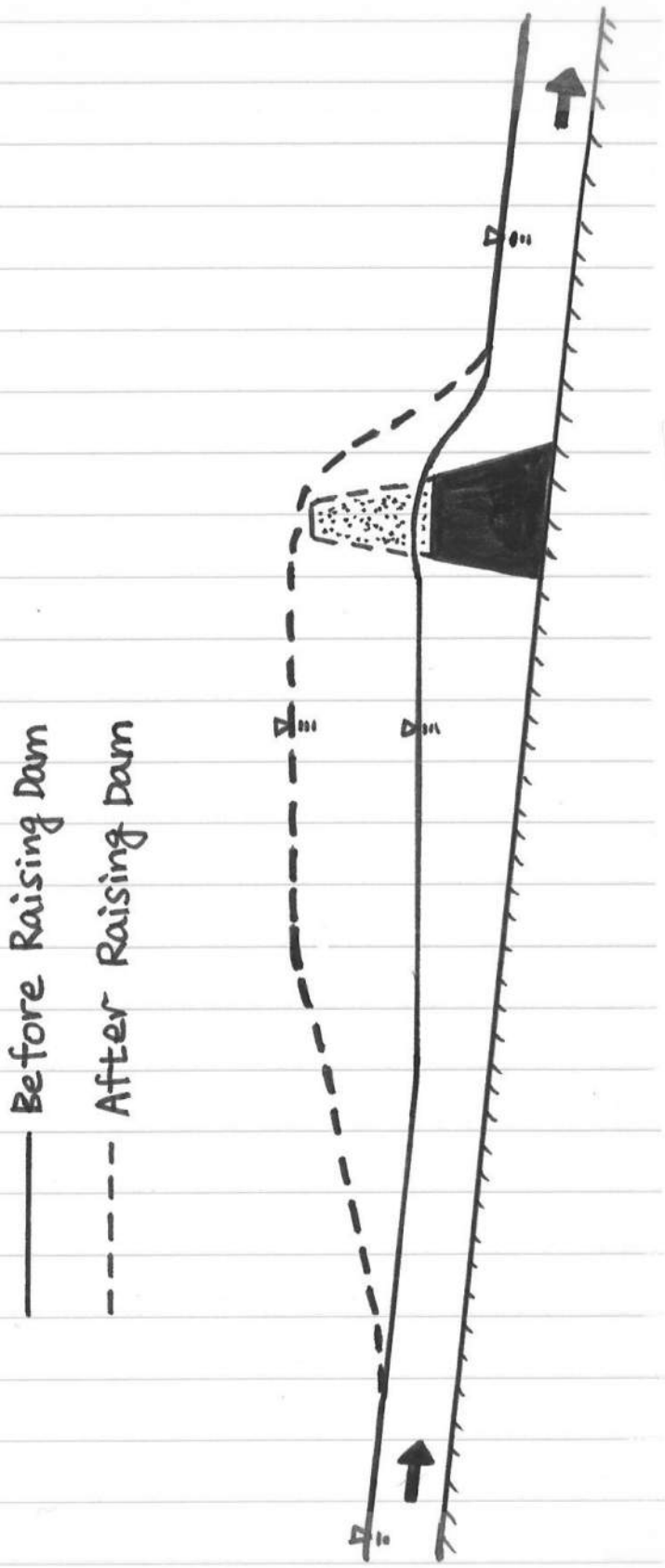

Figure 3: Backwater Effect behind Raised Dam in River

On the other hand, water in the vicinity of the Ditch and the roadway between the two bays is mostly driven by the difference between the hydrostatic pressures below the stillwater elevations on the two bays as explained in relation to Fig. 1. Water flows from one bay with the higher stillwater elevation to the other bay with the lower stillwater elevation. The peak stillwater elevations on both bays have been predicted to be the same as listed in Table 2. It is not certain whether these peak stillwater elevations will occur at the same time. However, the peak stillwater elevations are expected to be essentially horizontal with negligible flow in the area under investigation whose length scale is much smaller than the length scale over which storm surge and astronomical tides vary appreciably. Consequently, the peak stillwater elevations before and after raising the roadway will be essentially the same as depicted in Fig. 4a for a submerged roadway. This will also be the case with a non-submerged roadway. This simple but reasonable assumption could be evaluated by analyzing the time-dependent interaction between the two bays including the overflow over the existing and raised roadway. Such an analysis could quantify the degree of uncertainty associated with the peak stillwater elevations predicted in Table 2 on the basis of no overflow over the existing roadway.

The stillwater elevations on both bays will be different before and after the peak of the storm surge as shown in Fig. 4b. The raised roadway will reduce the water velocity and discharge over the roadway as compared to the existing roadway. The reduction in the water velocity will result in the increase of the stillwater elevation in the vicinity of the roadway even if the stillwater elevations far from the roadway are the same as depicted in Fig. 4b. For the converging sink flow on the side of the roadway where the stillwater elevation is higher, the energy equation per unit water weight expressed by (9) may be used to estimate the increase $\delta\eta$ of the stillwater elevation due to the decrease of δV of the water velocity as follows:

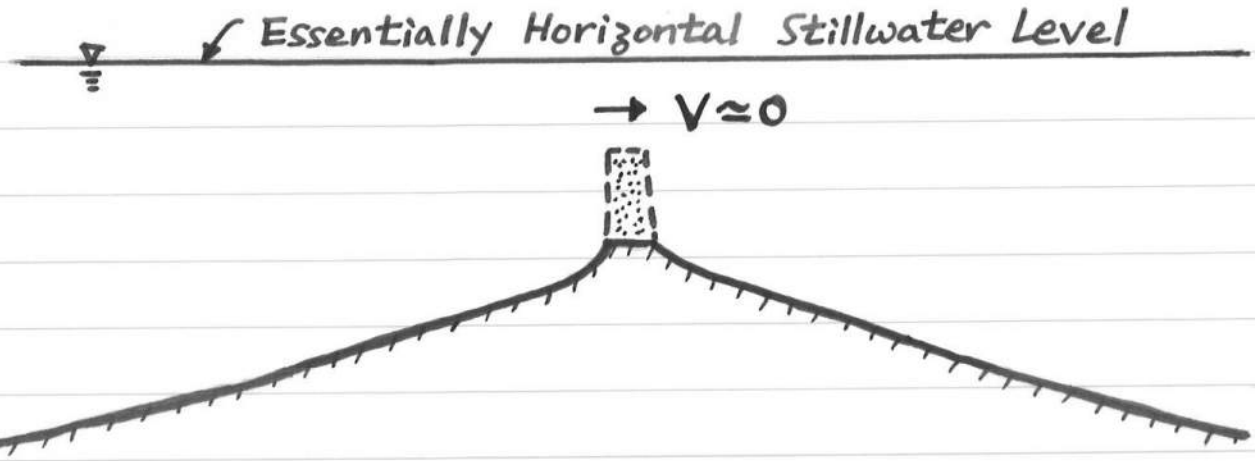

Figure 4: (a)—Peak Stillwater Elevations Before and After Raising Roadway

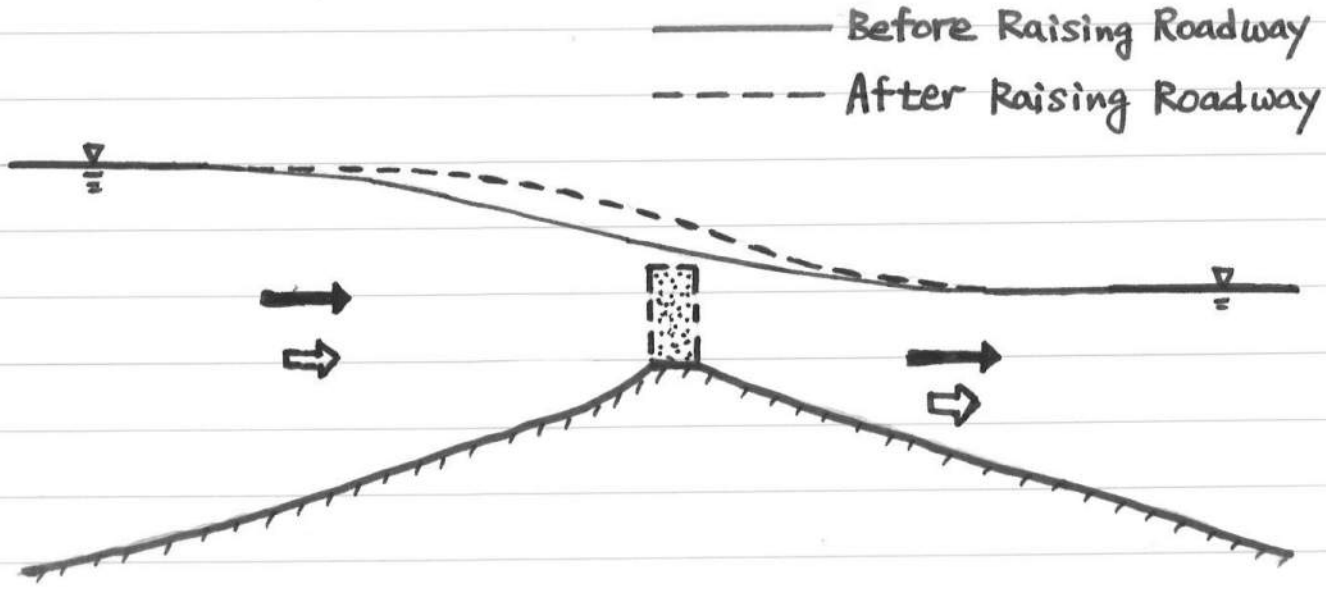

Figure 4: (b)—Increase of Stillwater Elevation due to Reduction of Water Velocity Caused by Raised Roadway

Table 9: Stillwater Elevation Increase $\delta\eta$ in Feet

V	$\delta V/V$			
(ft/s)	0.1	0.4	0.7	1.0
2	0.01	0.04	0.06	0.06
4	0.05	0.16	0.23	0.25
6	0.11	0.36	0.51	0.56
8	0.19	0.64	0.90	0.99

$$(\eta + \delta\eta) + \frac{(V - \delta V)^2}{2g} \simeq \eta + \frac{V^2}{2g} \quad \text{for converging flow} \tag{16}$$

where η and V are the stillwater elevation and water velocity before raising the roadway, whereas $(\eta + \delta\eta)$ and $(V - \delta V)$ are the stillwater elevation and water velocity after raising the roadway. Eq. (16) yields the stillwater elevation increase $\delta\eta$ as a function of V and δV

$$\delta\eta \simeq \frac{\delta V(2V - \delta V)}{2g} \quad \text{for converging flow} \tag{17}$$

$\delta\eta$ at the specified location varies with time during a storm since the corresponding values of V and δV vary with time. Table 9 lists the calculated values of $\delta\eta$ in feet for $V = 2, 4, 6$ and 8 ft/s and $\delta V/V = 0.1, 0.4, 0.7$ and 1.0, corresponding to 10, 40, 70 and 100% reduction in the velocity V. The stillwater elevation increase $\delta\eta$ will be well below 1 ft unless large water velocities are reduced significantly. It should also be noted that the reduction of large water velocities may offset the stillwater level increase as far as the overall damage to structures is concerned.

Finally, the crest elevation of the raised roadway is examined concisely. Since the peak stillwater evelation is essentially horizontal, the crest elevation of the raised roadway should be horizontal to improve the vehicle passage during storms. The roadway crest elevation Z_c above the mean sea level (NGVD) will need to be determined considering all relevant factors

including the hydraulic characteristics on the crest of the raised roadway. The hydraulic analysis procedure developed in Section 4.1 can be used for both existing and raised roadways. As an example, the calculated results for Z_c = 3.5 ft are presented in the following. The most appropriate value of Z_c will need to be determined by comparing the cost, the degree of vehicle passage improvement, and intangibles for different values of Z_c.

Table 10 shows the calculated values of η_c, h_c and V_c for the raised crest elevation Z_c = 3.5 ft where the variables η_s, η_n, η_c, h_c and V_c are defined in Fig. 2. The maximum stillwater depth h_c on the crest of the roadway is assumed to be the difference between the peak stillwater elevation η_s and the crest elevation Z_c. To examine the effects of the difference between the stillwater elevations on the two bays, the cases of $(\eta_s - \eta_n)$ = 0.1, 0.5, 1.0 and 2.0 ft have been considered in Sections 3.2 and 4.2. The stillwater elevation η_c, the stillwater depth h_c, and the water velocity V_c on the crest of the raised roadway listed in Table 10 are compared with those listed in Table 7 for Z_c = 2.1 and 2.5 ft. Talbe 11 shows the stillwater elevation increase $\delta\eta_c$, the stillwater depth decrease δh_c, and the water velocity decrease δV_c caused by the increase of the crest elevation Z_c from 2.1 or 2.5 ft to 3.5 ft. The stillwater elevation increase $\delta\eta_c$ at the crest of the roadway is less than 0.5 ft and consistent with the results given in Table 9. The stillwater depth decrease δh_c is equal to or less than the crest elevation increase δZ_c = 1.4 or 1.0 ft since $(\delta h_c + \delta\eta_c) = \delta Z_c$. This is because the water velocity decrease δV_c results in the stillwater elevation increase $\delta\eta_c$. Consequently, the stillwater depth on the crest of the roadway decreases no more than the increae of the roadway crest elevation. It should be noted that Table 11 is limited to the segments of the existing roadway with Z_c = 2.1 and 2.5 ft. The same calculations are recommended to be made for the entire length of the roadway under investigation.

Table 10: Calculated Values of η_c, h_c and V_c at Crest of Raised Roadway

η_s (ft)	Z_c (ft)	$\max h_c$ (ft)	η_n (ft)	η_c (ft)	h_c (ft)	V_c (ft/s)
3.8	3.5	0.3	3.7	3.7	0.2	2.5
			3.3	3.7	0.2	2.5
			2.8	3.7	0.2	2.5
			1.8	3.7	0.2	2.5
5.4	3.5	1.9	5.3	5.3	1.8	2.5
			4.9	4.9	1.4	5.7
			4.4	4.77	1.27	6.4
			3.4	4.77	1.27	6.4
6.0	3.5	2.5	5.9	5.9	2.4	2.5
			5.5	5.5	2.0	5.7
			5.0	5.17	1.67	7.3
			4.0	5.17	1.67	7.3

Table 11: Changes of η_c, h_c and V_c due to Increase of Roadway Crest Elevation Z_c

		$Z_c = 2.1 \rightarrow 3.5$ ft			$Z_c = 2.5 \rightarrow 3.5$ ft		
η_s (ft)	η_n (ft)	$\delta\eta_c$ (ft)	δh_c (ft)	δV_c (ft/s)	$\delta\eta_c$ (ft)	δh_c (ft)	δV_c (ft/s)
3.8	3.7	0	1.4	0	0	1.0	0
	3.3	0.4	1.0	3.2	0.33	0.67	2.8
	2.8	0.47	0.93	3.6	0.33	0.67	2.8
	1.8	0.47	0.93	3.6	0.33	0.67	2.8
5.4	5.3	0	1.4	0	0	1.0	0
	4.9	0	1.4	0	0	1.0	0
	4.4	0.37	1.03	1.6	0.34	0.66	1.5
	3.4	0.47	0.93	2.0	0.34	0.66	1.5
6.0	5.9	0	1.4	0	0	1.0	0
	5.5	0	1.4	0	0	1.0	0
	5.0	0.17	1.23	0.7	0.17	0.83	0.7
	4.0	0.47	0.93	1.8	0.34	0.66	1.4

6 CONCLUSIONS AND RECOMMENDATIONS

Collected available data on the storm surge on Little Assawoman Bay and the part of Assawoman Bay in Sussex County is limited to the computed peak stillwater elevations for the recurrence intervals of 10, 50, 100 and 500 years. Available field data on peak storm surge appears to be limited to the 1991 Halloween storm. The temporal variations of the stillwater elevations on both bays durnig storms are not available. Simple analysis procedures for the flow through the Ditch and the overflow over the roadway have been proposed. Example calculations have been made for the assumed stillwater elevations on the two bays on the basis of the available data on the peak stillwater elevations. The calculated results have indicated that the water velocity and discharge over the existing roadway and through the Ditch are comparable. Consequently, it is desirable to develop a numerical model to examine the time-dependent interactions betwen the two bays including the overflow over the roadway, which appears to have been neglected in previous studies.

The roadway improvement alternatives considered in this report include bridges, culverts, an elevated permeable roadway and a raised impermeable roadway. A bridge with a dredged channel, which is similar in size to that over the Ditch, would be required to compensate for the overflow over the existing roadway. The discharge through culverts would be much smaller than the discharge through the Ditch and over the roadway. Alternatives based on discharge considerations are not effective in reducing the peak stillwater depth on the entire flooded roadway. An elevated peameable roadway may need to be elevated about 7 ft above the mean sea level to satisfy the FEMA new construction requirements. A raised impermeable roadway is a simple and direct approach to improve vehicle passage during storms. The raised roadway will not increase the peak stillwater elevation as long as the peak stillwater elevations on both bays are the same and occur at the same time during

storms. Before and after the peak of storm surge, the raised roadway will increase the stillwater elevation. However, its increase will be well below 1 ft unless large water velocities are reduced significantly by the raised roadway. An example has been given to show how the proposed analysis procedure may be used to calculate the stillwater depth and water velocity on the crest of the raised roadway.

7 REFERENCES

The references provided by Rummel · Klepper & Kahl have been quoted sufficiently when they have been used. The following references are limited to those added in this report.

ASCE Task Committee on Sea-Level Rise and Its Effects on Bays and Estuaries (1992). "Effects of sea-level rise on bays and estuaries." *J. Hydraulic Engrg.*, ASCE, 118(1), 1–10.

Dean, R.G., et al. (1987). *Responding to changes in sea level: Engineering implications.* Marine Board, Nat. Academy Press, Washington, D.C.

Linsley, R.K., et al. (1992). *Water resources engineering.* 4th Edition, McGraw Hill, New York, N.Y.

Shore Protection Manual (1984). U.S. Army Coastal Engrg. Res. Ctr., Government Printing Office, Washington, D.C.

Titus, J.G., et al. (1987). "Sea level rise and coastal drainage system." *J. Water Resour. Planning and Mgmt.*, ASCE, 113(2), 216–227.